Understanding the genetic basis of phenotype variability in individuals with neurocognitive disorders

Michael H. Duyzend

A dissertation submitted
in partial fulfillment of the
requirements for the degree of

Doctor of Philosophy

University of Washington

2016

Reading Committee:

Evan E. Eichler, Chair
Raphael Bernier
Philip Green

Program Authorized to Offer Degree:
Genome Sciences

University of Washington

Abstract

Understanding the genetic basis of phenotype variability in individuals with neurocognitive disorders

Michael H. Duyzend

Chair of the Supervisory Committee:
Professor Evan E. Eichler
Department of Genome Sciences

Individuals with a diagnosis of a neurocognitive disorder, such as an autism spectrum disorder (ASD), can present with a wide range of phenotypes. Some have severe language and cognitive deficiencies while others are only deficient in social functioning. Sequencing studies have revealed extreme locus heterogeneity underlying the ASDs. Even cases with a known pathogenic variant, such as the 16p11.2 CNV, can be associated with phenotypic heterogeneity. In this thesis, I test the hypothesis that phenotypic heterogeneity observed in populations with a known pathogenic variant, such as the 16p11.2 CNV as well as that associated with the ASDs in general, is due to additional genetic factors. I analyze the phenotypic and genotypic characteristics of over 120 families where at least one individual carries the 16p11.2 CNV, as well as a cohort of over 40 families with high functioning autism and/or intellectual disability. In the 16p11.2 cohort, I assessed variation both internal to and external to the CNV critical region. Among *de novo* cases, I found a strong maternal bias for the origin of deletions (59/66, 89.4% of cases, $p=2.38x10^{-11}$), the strongest such effect so far observed for a CNV associated with a microdeletion syndrome, a significant maternal transmission bias for secondary deletions (32 maternal versus 14 paternal, $p=1.14x10^{-2}$), and nine probands carrying additional CNVs disrupting autism-associated genes. In the same cohort, I assessed genome wide exonic variation, including in the 27 16p11.2 CNV critical region genes and the 3 genes that lie in the flanking

segmental duplications, *BOLA2*, *SLX1A*, and *SULT1A3* with the hypothesis that dosage imbalance in these genes could lead to variable phenotypes. I find an absence of variation across the critical region, compared to similarly sized regions genome-wide by average heterozygosity (2^{nd} percentile) and Tajima's D (3^{rd} percentile) metrics. Among the 27 critical region genes and three duplicated genes, I find no loss of function variants in 16p11.2 CNV carriers. Our genome-wide exome analysis revealed 13 likely-gene disruptive (LGD) variants in 13 probands in autism-associated genes, which is fewer than would be expected by chance ($p<10^{-16}$) and individuals having such variants trend towards being more severely affected on FSIQ (p=0.19). To understand the genetic heterogeneity associated with high-functioning autism and intellectual disability, I assessed genetic variation observed in a cohort of 43 local families of which 29 have a diagnosis of high functioning-autism. I discovered variants in novel autism candidate genes, including *LPHN1* and *NUMBL*, find that the high functioning autism cohort tends to have more inherited loss of function and severe missense variation per individual than low functioning cohorts ($p<2.2*10^{-16}$), but fewer *de novo* LGD variants per individual (p=0.007). I also find that *de novo* variants in high functioning cases lie in a protein-protein interaction network including proteins involved in the NOTCH signaling pathway. Our findings suggest that modifiers external to, as opposed to variants internal to the critical region, may play a role in the observed phenotypic differences observed in individuals with a 16p11.2 CNV and those with ASDs in general.

List of Figures

List of Tables

Acknowledgements

"On the mountains of truth you can never climb in vain: either you will reach a point higher up today, or you will be training your powers so that you will be able to climb higher tomorrow." – F. Nietzche

The scientific journey is one of profound introspection into nature's truths. Like any journey, those surrounding us have tremendous influence on our way forward and the lens through which we see the world. Fortune looked kindly on me, and tremendous individuals from all aspects of life have surrounded me. I am deeply indebted to all who shared their wisdom with me, encouraged me, and were there for me during this voyage of discovery.

I would like to thank my parents and brother, for their constant encouragement, and always enabling me to see the wisdom I would gain from every situation. I learned from them to see the world not as black and white, but rather a multi-layered, multi-faceted set of truths and illusions which is thrilling to navigate. They are always enthusiastic about my scientific interests, and intense motivators and advocates for equality and truth. Perhaps this is a reason that I am the first person in my extended family to pursue a PhD.

I would like to thank my mentors, especially Evan Eichler, Mary-Claire King, and my committee members Raphe Bernier, Phil Green, Debbie Nickerson, and Peter Byers. I admire their passion for discovery, and ability to separate the scientific pursuit from other motivators so prevalent in society. These mentors have allowed me to view the scientific pursuit as an exciting playing field, where each effort, even if leading to negative results, helps pave the path forward. As Dr. Eichler once said, "Let the science speak for itself."

I would like to thank the great many friends and extended family who provided balance and insight during these years. Gordon Griggs and Valerie Stevens served as great "family" when my parents moved away from Seattle. My childhood friend Alan Charnley, whose mother was Chair

of Botany at UW, and passed away from ovarian cancer far too soon, influenced my decision to pursue science and medicine. My close friends, Allen Chen, Joshua Cook, Isabel Huang-Doran, Mathew Plucinski, Alexandre Babeanu, and Dave Young, now spread all over the world for being, in Emerson's words, "masterpieces of nature." My cousins Molly Gross and Emily Gross, both pursing medical careers, offered great advice, support, and fun during the PhD.

I would like to thank the other students, postdocs and staff who were with me in the lab, department, and Medical Scientist Training Program, especially Xander Nuttle and Brad Coe, with whom I collaborated extensively, and who provided great companionship and mentorship both inside and outside of the lab.

The outdoors, art, and travel have provided insightful and balancing reprieve from the rigors of the scientific pursuit. The opportunity to serve on medical school committees and national organizations gave important perspective on the worldwide state of medicine and science. Observing people around the world working hard to make the most of their lives, from the favelas of Brazil to the steppes of Mongolia to the financial district of London, not only gave me hope in humanity but also cemented the necessity of collaboration and selflessness across socioeconomic and cultural bounds. The authors Emerson, Blake, Wollstonecraft, Tolstoy, Neruda, Huxley, and more; composers Bach, Beethoven, Handel, Buxtehude, Enaudi, and more; painters Monet, Lichtenstein, Van Gogh, Vermeer, and more; mathematicians Riemann, Tao, Euler, and Ramanujan, and more. These artists have revealed beauty in the world and enriched my humanity.

I would like to thank the mentors and teachers I have had over the years. Larry Muir, a PhD biochemist come high school teacher, sparked my passion for understanding biologically active molecules (of which DNA is one of the most important). Dave Alberg, professor of Chemistry at

Carleton College, confirmed my love for organic synthesis and biochemical manipulation. Bob Dobrow, professor of Mathematics at Carleton College let me see the power of probability, statistics, and combinatorics. David Liben-Nowell associate professor of Computer Science at Carleton College encouraged me to think big and pursue a computational degree and allowed me to realize the insight one can gain for huge datasets. Martha Bulyk, Professor of Medicine and Biology at Brigham and Women's hospital and Harvard Medical School, incidentally a former benchmate of Jay Shendure, for opening up the world of genomics.

Finally, I would like to thank the Department of Genome Sciences and the Medical Scientist Training Program at the University of Washington as well as the National Institutes of Health (in particular the National Institute of Mental Health), Simons Foundation, and Howard Hughes Medical Institute for providing tremendous resources and support during my PhD years. I cannot think of a better place to have done this program.

1. Introduction:

1.1 Overview

The overarching theme of my thesis is to assess the genetic basis of phenotype variability in individuals with variants strongly associated with the autism phenotype (genotype-first ascertainment) or diagnosed with an autism spectrum disorder (ASD, phenotype-first ascertainment). First, I analyze a cohort of individuals carrying the 16p11.2 CNV to assess the presence of genetic modifiers in individuals already carrying a variant associated with autism (chapters 1 and 2). I divide modifiers into two types. Those *internal* to, that is found in the 16p11.2 critical region and those *external* to or found outside of the 16p11.2 critical region. Second, I assess a cohort of high functioning autism cases to understand the variants associated with the social deficits of ASD in the absence of intellectual disability (ID) (chapter 3). The results of my research have the potential to improve immediately clinical diagnosis, counseling of affected individuals and their families, and management of individuals with the 16p11.2 CNV and ASD. Furthermore, the research community can apply the techniques developed here to the study of other variants associated with ID, ASD, and epilepsy.

1.2 The connection between genotype and phenotype

Identifying the patterns between genotype and phenotype gave rise to modern genetics[1]. The patterns of segregation of traits provided powerful insight into how genetic variation can lead to particular attributes, including disease traits. Researchers initially observed that traits segregate in a dominant or recessive fashion, and later mapped them to particular chromosomal regions. In model organisms, such as mouse, fly, yeast, zebrafish and worm, this has allowed for the genetic

manipulation of particular loci and observation of the resulting phenotype. Such an approach can often provide insight into a disease causing variant discovered in humans.

Humans are not traditional model organisms. For ethical reasons, one cannot keep colonies of humans, perform genetic manipulations, and observe the resulting phenotype. However, the advent of rapid targeted and whole-genome sequencing approaches has allowed assessment of hundreds of thousands of human genomes at relatively low cost. For example, the sequencing of the coding part of the genome "the exome" of over 2,000 families with one affected individual with autism has led to the identification of more than 30 genes involved in the phenotype[2–5]. Through ascertainment, of either a particular phenotype, or a particular genetic variant, we can now survey the variation extant in the over 7 billion humans to understand better the relationship between genotype and phenotype. In this way, we are utilizing nature's laboratory.

There are two possible ways to ascertain a cohort. In human studies, individuals are typically ascertained on the basis of a particular clinical phenotype, for example autism, melanoma, or macular degeneration. Researchers then assess these cohorts for shared genetic variation using a *phenotype-first* approach. The approach taken with model organisms is often the reverse, or a *genotype-first* approach. Researchers generate variants in a particular organism and observe the resulting phenotypic characteristics. For human disorders with a wide heterogeneity of clinical presentations, such as autism, variants in different genes are likely causative for different clinical subtypes of the disorder. Rapid and targeted sequencing approaches allow researchers to ascertain cohorts based on a particular variant, or variants discovered in a particular gene. Such an approach provides a handle to better understand phenotypic heterogeneity associated with a particular variant.

In the assessment of any cohort, it is crucial to have access to comprehensive phenotype and genotype data. Detailed phenotype information allows association of subtle features with particular variants and assessment of the scale of heterogeneity associated with single genetic variants. Most large sequencing studies have focused on the identification of LGD variants, with less emphasis on missense and non-coding variation. Indeed, a recent study showed that both synonymous and non-synonymous exonic variation may be important in determining the phenotype landscape[6]. The availability of comprehensive genetic and phenotypic data allows assessment of all forms of variation and its association with phenotype.

Both genetic and phenotypic data should be assessed in the context of family (if possible) and population. For example, proband 1 may have a full scale IQ (FSIQ) of 80, and proband 2 may have an FSIQ of 100. However, if the mean IQ of the parents of proband 1 is 100, and of proband 2, 120, the difference in FSIQs for both probands when compared to their parents is 20. Hence, calibrating metrics within the family can allow more normalized comparisons between families. From a genetic standpoint, familial information is important to understand inheritance patterns, and as a control population. If an inherited variant is only found in affected individuals, for example, but not unaffected siblings, it has a higher likelihood of pathogenicity.

1.3 The Simons VIP collection

One of the first cohorts ascertained using a "genotype-first" approach was a collection of over 200 individuals with a 16p11.2 CNV and their carrier and non-carrier family members[7]. The discovery of the 16p11.2 deletion in ~1% of autism cases[8,9] highlighted the importance of recurrent CNVs underlying the genetic etiology of autism spectrum disorders[10–12]. Unlike other disorders with a known genetic etiology, such as Prader-Willi or Smith-Magenis syndromes,

detailed study of individuals with the 16p11.2 deletion failed to reveal a set of phenotypic criteria associated with the disorder[13,14]. The factors responsible for the phenotype variability found in individuals with seemingly identical genomic alterations presented challenges for diagnosis, counseling, and management. Collection of larger cohorts of individuals with the 16p11.2 CNV revealed different and sometimes mirror phenotypes associated with the region: deletion is associated with seizures[15], obesity[16], intellectual disability[14], and macrocephaly[13], while duplication is associated with schizophrenia, reduced BMI, and microcephaly[17,18]. While it is clear that the 16p11.2 CNV confers a strong risk for disease [19–21], it alone is not sufficient to define a particular phenotype outcome.

Given the well-established association of the 16p11.2 deletion with autism, the Simons Foundation collected a cohort of over 200 individuals with the 16p11.2 CNV and their family members for study as part of the Simons Variation in Individuals Project (Simons VIP)[7]. Families find out about the study via the internet or their clinician. Individuals and their families travel to one of three centers for comprehensive examination, including a structural brain MRI for participants who can complete the study without the use of sedation. Importantly, both comprehensive phenotype information, including psychiatric evaluation by licensed clinicians for >200 ascertained probands, and whole blood DNA for >120 ascertained probands and >200 family members was collected allowing for comprehensive genotype and phenotype characterization. The phenotypes represented in this set are diverse and include individuals with coordination disorder, enuresis, autism, tremors, and articulation disorder among others. This collection offers an unparalleled resource to study how genetic changes on a background sensitized by a known pathogenic CNV affect phenotype.

1.4 Basis for genotype heterogeneity

Despite the vast advances in identifying variants that are strongly associated or causative for a particular disease phenotype, little is understood about what modulates the severity or penetrance of that phenotype. For example, a recent study screened over 874 genes in 500,000 individuals and led to the identification of 13 adults with variants for 8 severe Mendelian conditions, with no reported clinical manifestation of the indicated disease[22]. At the same time, the majority of identified events leading to severe phenotypes (for example cystic fibrosis) are loss-of-function in nature and involve a single variant, even though a combination of variants could potentially lead to a similar phenotype.

The importance of additional or second hits affecting phenotype severity has been established in several disorders, and a model has been developed to explain the phenotype variability associated with pathogenic CNVs[17,23,24]. This was based initially on the study of a rare 16p12.1 microdeletion[17] that is inherited in 95% of families and where the severity of disease correlates with the presence of additional large CNVs (>400kbp) in individuals with intellectual disability. This study was extended and analysis performed on more than 30 genomic disorders from 2,312 individuals carrying a primary pathogenic CNV variant[24]. Individuals with the same primary pathogenic CNV but variable phenotype outcomes are more likely to have inherited (as opposed to sporadic) primary CNVs and are more likely to carry another CNV, a so-called "second hit." There is a positive correlation (Spearman correlation coefficient, 0.68; $P<0.001$) between the proportion of individuals carrying an additional CNV and the proportion of inherited CNVs (**Figure 1.1a**).

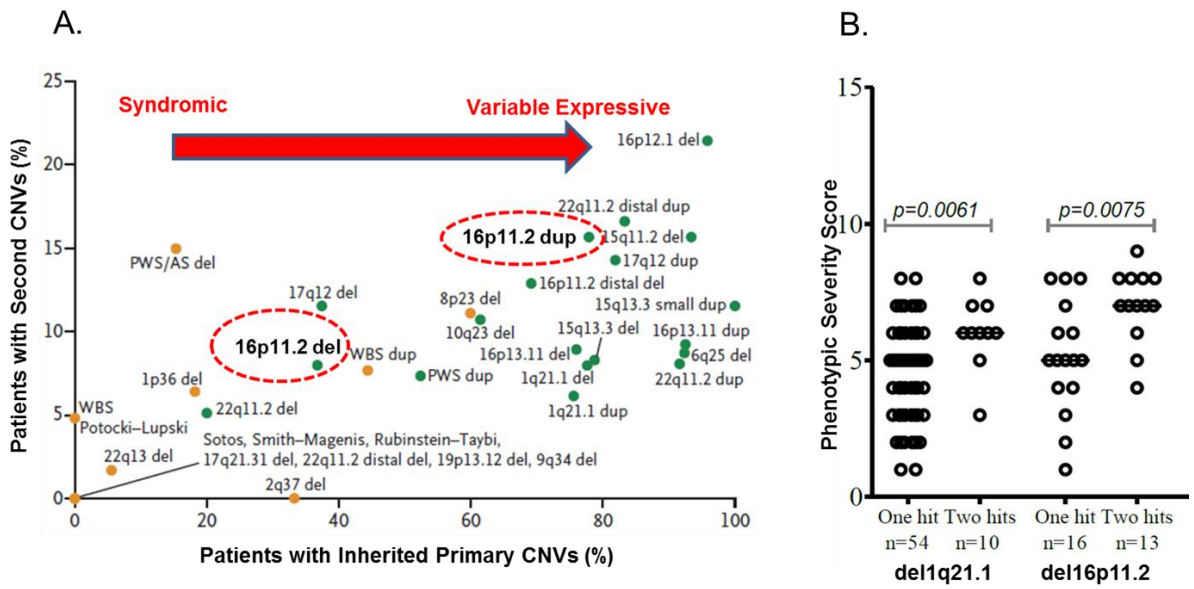

Figure 1.1: Two-hit model and phenotype variability. a) Analysis of over 30 genomic disorders demonstrates that disorders where a preponderance of individuals have an inherited primary CNV along with an additional large CNV are more variably expressive. For each disorder, there is a correlation (Spearman correlation coefficient, 0.68, P<0.001) between the proportion of individuals carrying a second CNV and the proportion of inherited CNVs. b) Individuals carrying an additional CNV>400kbp are more severely affected compared to individuals only carrying the primary CNV for both the 16p11.2 (p=0.0075) and 1q21.1 (p=0.0061) deletions. (Adapted from Girirajan *et al.*, 2012).

One of the more than 30 disorders studied was the 16p11.2 typical deletion. In the study, a phenotype severity score was assigned to 29 individuals with a 16p11.2 deletion which distinguished between 16 individuals with a single hit versus 13 individuals with an additional hit[24] (**Figure 1.1b**). Individuals with 2 hits (n=13) are more severely affected when compared to individuals with a single hit (16 individuals) (p=0.0075). These data, along with clinical reports[25] suggest that additional disruptive variants compounded with the 16p11.2 deletion lead to more severe outcomes and provide a general model for understanding phenotype variability.

There are several examples of known modifier loci in humans and other model organisms[26], for example in humans the phenotype resulting from a variant in the *CFTR* locus depends on genetic background[27] and only double heterozygotes (as opposed to single heterozygotes) for the *RDS*, *ROM1* genes lead to a diagnosis of retinitis pigmentosa[28].

1.5 The 16p11.2 CNV helps to define a subtype of autism

While individuals carrying the 16p11.2 CNV in the Simons VIP show extensive phenotype variability[8,9], the size of the cohort allows quantification of specific aspects of phenotype. While the 16p11.2 deletion was initially ascertained in autism cohorts, an important conclusion is that the 16p11.2 deletion is *not* primarily associated with a clinical diagnosis of autism[13,15,29]. In the Simons VIP, for example, only 20 out of 84 carriers (24%) have a clinical diagnosis of autism and only 15 (18%) meet strict criteria for an autism diagnosis based on the autism diagnostic observation schedule (ADOS) and the autism diagnostic interview (ADI).

However, many of the individuals carrying the deletion have clinical features similar to autism. Of the deletion carriers, for example 71% (60/85 carriers) show a speech or language-related disorder such as expressive/mixed receptive-expressive language deficits or a phonological processing (articulation) disorder. Carriers are also 2.7 times more likely to show restricted or repetitive behavior patterns when compared to controls (88% of deletion carriers vs. 33% of controls showed more than two types of these behaviors). As expected[15], a remarkable decrement in full-scale IQ (FSIQ) of 26.8 points or 1.8 SD was observed when comparing carriers and non-carriers[29]. The decrement was slightly greater for verbal IQ (VIQ), 27.6 points or 1.5 SD, when compared to nonverbal IQ (NVIQ), 23.5 points or 1.6 SD. A population-based study also found a significant decrement in VIQ in carriers vs. controls ($p=5.90x10^{-16}$) as well as a reduction in fecundity ($p=1.6x10^{-12}$)[30].

Despite these unifying features of the 16p11.2 deletion phenotype, the question remains: why is there such great variability in disorder manifestation even within the context of a family (**Figure 1.2a**)? Notwithstanding the limitations of the DSM-IV-TR[31], it is clear that there are a variety of diagnoses associated with the 16p11.2 deletion, with the number of distinct diagnoses

ranging from zero to more than a dozen. There is also wide variance in terms of the FSIQ difference with some cases actually showing an increase in FSIQ when compared to their parents (**Figure 1.2b**). Likely explanations include genetic, stochastic and/or environmental factors. Of these, the former is perhaps the most tractable.

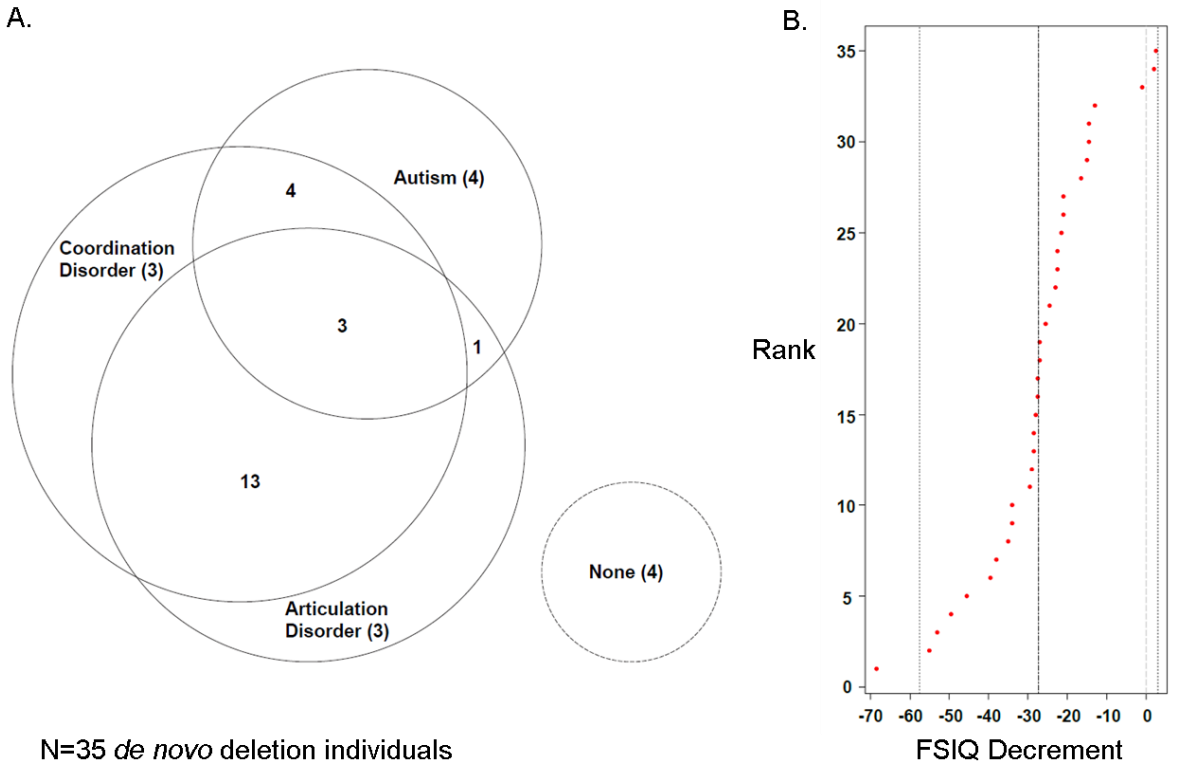

Figure 1.2: Phenotypic heterogeneity of 16p11.2 deletion cases. a) Overlap of three disorders in 35 individuals <3 years old with phenotype information from both parents and a *de novo* deletion (only). Four individuals did not have one of these three diagnoses. No single DSM-IV-TR diagnosis predominates, although >50% carry two or more diagnoses. b) The full-scale IQ (FSIQ) decrement measures the change in FSIQ between parents and child carrying a *de novo* 16p11.2 deletion. We define the FSIQ decrement as the average of the FSIQ of the parents subtracted from the FSIQ of the child. *De novo* deletion carriers show, on average, a 27-point decrement of FSIQ. However, the range is considerable with some individuals being more significantly impaired (five have a >40-point decrement), whereas others show almost no change (three have a decrement or increment within 5 points of zero).

It is clear that the 16p11.2 CNV phenotype eludes simple classification spanning more than 20 different disorders as described by the defunct DSM-IV-TR. Although the majority of individuals would not qualify as autistic by this strict definition, some aspects of the 16p11.2

deletion phenotype are remarkably consistent with a "type of autism" not yet recognized by the DSM. These conclusions highlight the power of the genotype-first-based approach[32] to studying autism and neuropsychiatric disease more generally. Similar to reports for other autism genes[33], the findings presented suggest that "autism" phenotypes conditioned on a common genetic etiology may be superior and more meaningful diagnostically than the strict DSM nosology.

1.6 The 16p11.2 CNV critical region

The typical 16p11.2 CNV deletes or duplicates a unique region of ~550kbp in length as well as ~50kbp of segmental duplications (**Figure 1.3**). The unique part contains 27 genes and the duplicated 3 genes and variation in these genes and their regulatory regions is likely important in determining phenotype outcome. At least 17 of the 27 genes are neuronally expressed[18] and a bioinformatics analysis revealed that at least 12 of the genes are involved in a single interaction network.[9] Evidence from model organisms suggests that particular genes within the critical region are associated with particular phenotypes[34–36]. In an attempt to determine the macrocephaly phenotype associated with the 16p11.2 deletion, for example, a group used a zebrafish model and systematically knocked out all unique genes in the critical region[34] and observed that knockout of the gene *KCTD13* leads to macrocephaly in zebrafish. Despite this result, none of the critical region genes have come to significance in human exome sequencing studies, and only a handful of partial deletions of the region have been discovered, none associated with a particular phenotype. A recent publication showed that compound inheritance of a rare null variant and a hypomorphic allele of *TBX6* accounted for 11% of congenital scoliosis cases[37]. This suggests that a combination of deletion or duplication of critical region genes or non-coding dosage imbalance in this region results in the observed phenotypes.

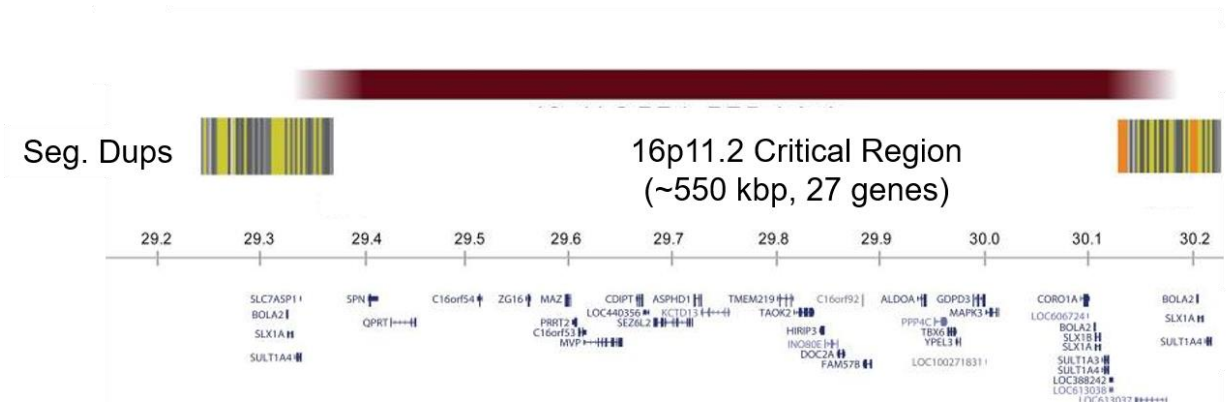

Figure 1.3: 16p11.2 critical region. The 16p11.2 critical region is flanked by segmental duplications which mediate non-allelic homologous recombination. The critical region contains 27 genes, none have which come to significance in exome sequencing studies, focal deletions are not associated with particular phenotypes, and only one gene, *KCTD13*, is associated with a head size phenotype in zebrafish. In the flanking segmental duplications lie three genes, one of which, *BOLA2* is duplicated only in *Homo sapiens* and has a putative role in cytosolic iron regulation. (Image adapted from Zufferey *et al* J. Med Genet, 2014).

Due to the highly identical segmental duplications flanking the critical region, these regions have not been accurately assembled and the breakpoints were not resolved until recently[38]. High identity (>99.5%) blocks of segmental duplications act as substrates for non-allelic homologous recombination (NAHR), predisposing to genomic disorders[39]. Despite most individuals presenting with a typical deletion or duplication, the possibility of distinct breakpoints emphasizes the need to comprehensively assess the extent of the CNV in each individual. Recent work assembling haplotypes using long-read sequencing of bacterial artificial chromosome libraries from 8 humans and 3 non-human primates allowed design of molecular inversion probes (MIPs) enabling refinement of the breakpoint down to a 90 kbp region that includes the genes *BOLA2*, *SLX1A*, and *SULT1A3*. In 96% of the cases, the deletion or duplication fell in a 90 kbp duplicated region specific to *Homo sapiens*, not found in any of the non-human primates or ancient hominins Neanderthal or Denisova. Hence, copy number of the three duplicate genes may be an important determinant in phenotype severity.

1.7 The SAGE cohort

The Study of Autism Genetics Exploration (SAGE) cohort is a cohort collected at the University of Washington of individuals with autism and/or intellectual disability. Families are recruited to the study through (1) the Seattle Children's Hospital Autism Center Clinic Registry; (2) Area listservs for families with ASD, DD or ID (e.g. IAN, Autism Speaks, Parent to Parent, ARC, FEAT, etc.); (3) Providers who work with individuals with ASD or DD. Blood samples are collected from individuals and array CGH analysis is performed to identify large and potentially pathogenic copy number variants. To date, a total of 252 families have been screened for large CNVs, and a set of 42 families (148 samples, 21 trios, 20 quads, 1 quint) were selected for exome sequencing. Families were chosen that were multiplex, to enrich for the possibility of finding Mendelian variants, as well as those with a diagnosis of high functioning autism. No family chosen had a likely pathogenic CNV.

Most variants discovered in the exome sequencing of large autism cohorts are found in individuals with severe phenotypes. No study has decoupled intellectual disability with the other features of autism, including lack of social reciprocity and repetitive behaviors. Through studying these families as well as high functioning families from the Simons Simplex Collection (SSC)[40], I analyze all types of exonic variation to understand what contributes to autism in the absence of intellectual disability.

1.8 Research goals and hypotheses

The overarching theme of my thesis is to assess the genetic basis of phenotype variability in individuals with a variant strongly associated with the autism phenotype (genotype-first ascertainment) or diagnosed with an ASD (phenotype-first ascertainment).

- **Genotype-first assessment of a 16p11.2 CNV cohort.** My goal is to assess the genetic basis of the phenotype variability in individuals with copy number variation at 16p11.2, events which are strongly associated with autism but lead to variable phenotypes. I hypothesize that differences in genetic background or in the CNV itself contribute to phenotype variability and to the severity of disease. I divide my analyses into the assessment and discovery of genetic modifiers *internal* and *external* to the 16p11.2 critical region and correlate these to phenotype.
- **Phenotype-first assessment of an ASD cohort.** My goal is to assess individuals from families with high functioning autism to discover a network of genes associated with the social deficits of the ASDs without intellectual disability.

Stemming from these goals, I have several hypotheses:

1) Analysis of internal and external modifiers in the background of a 16p11.2 CNV will identify genetic features important for phenotype penetrance and hence clinical ascertainment.

2) The analysis of exome sequencing data from individuals with high functioning autism will reveal a network of genes and classes of variants responsible for the social deficits associated with the ASDs.

3) In the majority of cases, several variants or modifiers must be present to lead to as clinically ascertainable phenotype (oligogenic model).

In order to address these hypotheses, my thesis has two broad aims:

Aim 1: Assessment of genetic modifiers in a cohort of individuals with a 16p11.2 CNV and their non-carrier family members.

In this aim, I divide modifiers into those *internal* and *external* to the 16p11.2 critical region. For *internal* modifiers, I assess variation in the 27 unique and 3 duplicated 16p11.2 critical region genes. For *external* modifiers, I assess CNVs discovered in addition to the 16p11.2 CNV, and exonic variants outside of the critical region. I use a large population of individuals with intellectual disability or autism and controls to assess variation in the 3 duplicated 16p11.2 critical region genes, due to low sequencing coverage in variant databases.

Aim 2: Analyze a high functioning autism and intellectual disability cohort to determine genes associated with the social deficits of ASD

In this aim, I assess variants discovered from the exome sequencing of a cohort of 42 locally collected families with a diagnosis of intellectual disability and/or autism, of which 29 have a diagnosis of high functioning autism.

The ultimate goal of my thesis is to understand the genetic modifiers that underlie the phenotype variability associated with the ASDs. First, I analyze a cohort of individuals carrying the 16p11.2 CNV to assess the presence of genetic modifiers in individuals already carrying a variant associated with autism. Second, I assess a cohort of high functioning autism cases to understand the variants associated with the social deficits of ASD in the absence of ID. The results of my research will inform future experiments, allow for correct interpretation of transcriptomic, induced pluripotent stem cell, and other resources, and has the potential to immediately improve clinical diagnosis and counseling of affected individuals and their families.

2. Maternal Modifiers and Parent-of-Origin Bias of the Autism-Associated 16p11.2 CNV

This chapter has been published: Duyzend, MH, Nuttle X, Coe BP, Baker C, Nickerson DA, Bernier R, Eichler EE. *Am. J. Hum. Genet.* **98**, 45-57 (2016).

I designed the study with Evan E. Eichler, performed array CGH experiments with Carl Baker, wrote analysis software, analyzed data, and wrote the paper with Evan E. Eichler.

2.1 Summary

Recurrent deletions and duplications at chromosome 16p11.2 are a major genetic contributor to autism but also associate with a wider range of pediatric diagnoses, including intellectual disability, coordination disorder, and language disorder. In order to investigate the potential genetic basis for phenotype variability, I assessed the parent-of-origin of the 16p11.2 copy number variant (CNV) and the presence of additional CNVs in 126 families where detailed phenotype data were available. Among *de novo* cases, I found a strong maternal bias for the origin of deletions (59/66, 89.4% of cases, $p=2.38 \times 10^{-11}$), the strongest such effect so far observed for a CNV associated with a microdeletion syndrome. In contrast to *de novo* events, I observed no transmission bias for inherited 16p11.2 CNVs, consistent with a female meiotic hotspot of unequal crossover driving this maternal bias. I analyzed this 16p11.2 CNV cohort for the presence of secondary CNVs and found a significant maternal transmission bias (32 maternal vs. 14 paternal, $p=1.14 \times 10^{-2}$). Of the secondary deletions that disrupted a gene, 92% were either maternally inherited or *de novo* ($p=3.4 \times 10^{-3}$). Nine probands carry secondary CNVs that disrupt genes associated with autism and/or intellectual disability risk variants. Our findings demonstrate a strong bias in maternal origin of 16p11.2 *de novo* deletions as well as a maternal transmission bias for secondary deletions that contribute to the clinical outcome on a background sensitized by the 16p11.2 CNV.

2.2 Introduction

Duplication and deletion of an ~550 kbp region on chromosome 16p11.2 accounts for ~1% of autism cases, representing one of the most common contributors to autism spectrum disorder (ASD) in the human population[9,41]. Unlike many other syndromic disorders, such as Smith-Magenis or Prader-Willi syndromes, detailed studies of individuals with the 16p11.2 copy number variant (CNV) have revealed marked phenotypic variability[13–15,42–47]. Phenotypic studies indicate different and sometimes mirror phenotypes associated with the CNV. For example, the deletion has been associated with seizures[15], obesity[16], intellectual disability[14], and macrocephaly[13], while the duplication has been associated with schizophrenia[18], reduced body mass index (BMI)[48], and microcephaly[13]. While it is clear that the 16p11.2 CNV confers a strong risk for neurodevelopmental disease[20,21,49,50], it is likely that other factors, including genetic background, may be key in determining the severity of phenotype outcome[24,37].

Recently, a cohort of over 120 families, with at least one proband carrying a 16p11.2 CNV, was assembled as part of the Simons Variation in Individuals Project (Simons VIP)[51]. This collection is one of the largest cohorts for the 16p11.2 CNV and is distinctive in its comprehensive phenotypic assessment of participants. It offers a useful resource to study genetic differences on a background sensitized by a known pathogenic CNV and how these differences affect phenotype severity. In this analysis, carriers of the 16p11.2 CNV refer to either probands or other family members that are heterozygous for the deletion or duplication irrespective of diagnostic ascertainment or inheritance status. The goal of this study was twofold: 1) to provide genetic detail regarding the extent and transmission characteristics of the CNV in these families and 2) to investigate the presence of CNVs in addition to the 16p11.2 CNV in modifying the severity of the phenotype. For clarity and to distinguish from the ascertained 16p11.2 CNV, we

will refer to the rare additional CNVs (present in <0.1% of controls) as secondary CNVs. In this study, we assess the parent-of-origin and mechanism of unequal crossing over for the 16p11.2 *de novo* CNVs and examine transmission bias for secondary CNVs within these families.

2.3 Subjects and methods

2.3.1 Samples

DNA samples were derived from peripheral blood obtained from 482 individuals from 141 16p11.2 CNV families as part of the Simons VIP. Exclusion criteria included any additional pathogenic CNVs or other neurogenetic or neurological diagnoses unrelated to 16p11.2[51]. Greater than 80% of probands were of full European ancestry (**Table S1**). We utilized the Simons VIP release (9.30.2014) of phenotypic information for these individuals. All procedures for clinical assessment and blood extraction were approved by the institutional review boards (IRBs) of participating institutions, and informed consent was obtained for participation in this research.

2.3.2 Phenotypic assessment

As part of participation in the Simons VIP[51], standardized assessments, including psychiatric, neurocognitive, behavioral, motor, and neurologic evaluation, were conducted at three Simons VIP clinical sites along with collection of a detailed medical history through interview and medical records review for each participant. Psychiatric and neurodevelopmental conditions were diagnosed by experienced, licensed clinicians following DSM-IV-TR criteria[31] using all available information, including clinical observation, caregiver history, and records review. Diagnostic foci included: ASD, attention deficit hyperactivity disorder (ADHD), communication

disorders, anxiety disorders, mood disorders, intellectual disability, tic disorders, elimination disorders, learning disorders, and behavioral disorders, totaling 27 diagnostic codes. Full-scale intelligence quotient (FSIQ) was determined by the developmentally appropriate cognitive measure (Mullen Scales of Early Learning[52]), the Differential Abilities Scale, Second Edition[53], or the Wechsler Abbreviated Scales of Intelligence[54]. For our phenotype analysis, we define the FSIQ decrement as the average of the FSIQ of the parents subtracted from the FSIQ of the proband (**Table 1**).

Table 1. Clinical Characteristics of Screened Probands

	Probands with Deletions (40 F and 50 M)			Probands with Duplications (16 F and 20 M)		
	Median	Range	Number Reported	Median	Range	Number Reported
Age (years)	7.83	0.83–20.75	89/90	5.83	(1.42–23.42)	35/36
FSIQ	86	46–122	87/90	77	(28–114)	33/36
FSIQ decrement	25.5	−9–68.5	49/90	22	(6.5–89)	23/36
Social Responsiveness Scale score	74.5	37–90	78/90	76	(42–90)	25/36
Autism Diagnostic Interview Revised score	11	2–30	60/90	11.5	(2–26)	18/36
Head circumference (cm)	54	45–59.7	86/90	51.05	(44.4–58)	34/36
BMI	19.2	13.35–37.13	86/90	16.17	(13.36–28.37)	34/36
Number of diagnoses[a]	3	1–5	80/90	2	(1–5)	32/36

Abbreviations are as follows: F, female; M, male.
[a]This includes ASD, ADHD, communication disorders, anxiety disorders, mood disorders, intellectual disability, tic disorders, elimination disorders, learning disorders, and behavioral disorders, totaling 27 diagnostic codes. 21/89 deletion-carrying probands and 8/35 duplication-carrying probands for whom data was reported have been diagnosed with clinical autism.

2.3.3 CNV detection

Single-nucleotide polymorphism (SNP) microarray data was generated from the Illumina HumanOmniExpress v1 (104 probands, 280 family members) and v2 (26 probands, 72 family members) microarray platforms. Each microarray contains over 715,000 probes and has the power to detect CNVs >100 kbp with more than 95% sensitivity (**Figure S1**). CNVs were detected using the cnvPartition algorithm (see **Web Resources**). We chose this algorithm because its performance (as determined by the cnvPartition score) had been previously optimized by comparison against CNVs detected by deep whole-genome sequence data[55]. For both array

designs, we generated a cluster definition file from only the individuals that did not carry the 16p11.2 CNV using the Illumina Genome Studio software (see **Web Resources**). Samples in the extremes for call rate and autosomal LogR standard deviation were manually inspected. We assessed one triplication family, which we did not include in the subsequent analysis, and removed families where the proband did not have the expected 16p11.2 CNV identified in the clinic (Simons VIP families 14904 and 14925). Familial relationships were assessed using the program KING[56], and samples that did not match their expected pedigree membership were removed (**Table S1**). The analysis showed that the probands were unrelated with the exception of two probands that have a possible third-degree relationship (14710.x7 and 14877.x7). To ensure accurate comparisons between OmniExpress platforms, we required a minimum of seven probes within unique regions for both platforms and excluded the call if it contained >50% segmental duplication. Calls with the same state in the same individuals within 500 kbp of one another were merged if appropriate following manual inspection and all calls identified as *de novo* were manually inspected. A subset of the calls >100 kbp were validated using an array comparative genomic hybridization (CGH) platform (**Tables S2, S3**). Following this curation, 102 probands and 264 family members were analyzed on the HumanOmniExpress v1 platform and 24 probands and 68 family members were analyzed on the HumanOmniExpress v2 platform. Secondary CNVs intersecting genes associated with autism risk variants were defined using the SFARI gene list (June 2015, see **Web Resources**). We used the two-sided binomial test in this study, unless indicated otherwise.

2.3.4 CNV inheritance and validation

For each CNV call in a proband, we genotyped parents and siblings (if present), computed the median log ratio across these regions, and used this information to genotype across the family. We further validated a subset of large (>100 kbp) CNVs using a custom array CGH platform (Table S3). We utilized a previously designed custom 12-plex NimbleGen array with a total of 135,000 probes targeted to genomic hotspots for CNV detection[57]. The hotspot array consists of a high density of probes (approximately 2.6 kbp apart) targeting 107 genomic hotspot regions and a probe spacing of approximately 36 kbp in the genomic backbone. Array hybridization experiments and analysis were performed as described previously[57]. All signal intensities from the array CGH experiments were loaded onto a UCSC Genome Browser mirror (Santa Cruz, CA, USA) and manually visualized. 26/34 secondary CNVs >100 kbp called by the SNP microarray were validated by array CGH. The eight events that did not validate had insufficient coverage on the array CGH platform (≤5 probes spanning the region).

2.3.5 Control CNV analysis

To assess the population frequency of each secondary CNV, we used two sets of curated control samples. Set I focuses on larger CNVs from 19,584 previously published controls[19] where ethnicity is similar to our cases (79.2% with known ethnicity are of European descent). Set II is a curated set of 4,092 samples from the Welcome Trust Case Control Consortium (WTCCC, see **Web Resources**) analyzed using a custom Illumina 1.2 million SNP microarray. The higher density of probes in Set II increases sensitivity for smaller events compared to Set I. Set II CNVs were recalled using the cnvPartition algorithm in order to improve the comparison with the case calls. We called CNVs on 2920 samples from the WTCCC 58C cohort and 2698

samples from the WTCCC UKBS (UK Blood Service) cohort. The ethnicity of the UKBS cohort is 100% European ancestry. While the ethnicity of the 58C cohort is not available, this is a 1958 British Birth Cohort and therefore likely to contain primarily individuals of European descent. Controls were not ascertained specifically for neurological disorders, but all controls were obtained from adult samples providing informed consent, so severe developmental phenotypes should be exceedingly rare.

Samples with a SNP call rate <0.98 and/or an autosomal LogR standard deviation ≤0.37 were removed[19]. We utilized an outlier detection method for skewed data[58] to identify and remove additional samples with an excess of calls and/or excess of larger calls (>100 or >500 kbp). Finally, we applied this outlier method to exclude CNVs within these size ranges when their mean LogR–median LogR value was greater than 0.2 or less than -0.15—known characteristics of false positive calls. 4092 samples passed quality control (2025 samples from the 58C cohort and 2067 from the UKBS cohort). Similar to our analysis of case CNVs, we required at least seven unique probes for each CNV call. Calls with the same CNV state and mapping within 500 kbp of one another were manually inspected and merged if appropriate. To assess frequency of case CNVs, we computed the number of state-matched events that have a 50% reciprocal overlap with a control event in both Set I and Set II. Because of the probe density, Set II offered greater sensitivity for assessing the frequency of smaller CNVs in cases. In addition, Set II uses the same technology as the case platforms and CNV calls were made using the same algorithm. We only considered secondary CNVs as rare if there were sufficient probes to call the variant in either Set I or Set II and the estimated control frequency was below 0.1% (**Table S3**).

2.3.6 *De novo* 16p11.2 CNV parent-of-origin analysis

We used the signal intensity data (LogR) to confirm the presence of the 16p11.2 CNV and b-allele frequency (BAF) across the critical region to infer the parent-of-origin for 79 families where a *de novo* 16p11.2 CNV had been identified (**Figure 2.1a-b**, **Tables S4, S5**). This included 64 individuals from the Simons VIP (58 deletions, 6 duplications) as well as 15 individuals from the Simons Simplex Collection (SSC) that were previously assessed using SNP microarrays[12,59] (8 deletions, 7 duplications, **Table S6**). In total, 34 quads, 22 trios and 10 probands with single parents were used to assess *de novo* deletion cases (**Table S4**). A total of 8 quads and 5 trios were used to assess *de novo* duplication cases (**Table S5**). We restricted this analysis to probes mapping within the 16p11.2 critical region (112 for the OmniExpress arrays). For deletions, only two genotypes are possible for each probe (A or B) with a corresponding BAF of 0 or 1, while for duplications four genotypes (AAA, AAB, ABB, and BBB) with corresponding BAFs of 0, 1/3, 2/3, and 1, respectively, are possible (see **Supplemental Appendix**). For cases where we had SNP microarray data from both parents (trios), we computed the probability that the unaffected haplotype came from the mother or father using parental SNP genotypes. In the deletion cases where we had only one parent available, but the 16p11.2 deletion was previously confirmed as *de novo*, we estimated the probability of the genotypes for the unobserved parent using the known allele frequencies for particular probes from the 1000 Genomes Project[60]. To test the fidelity of this approach for incomplete deletion families, we estimated the false discovery rate by removing a parent from a subset of the families where we had information from both parents (**Table S7**). Using this approach, 78/88 parent-of-origin estimates matched our inferences for a false discovery rate of 11.4%.

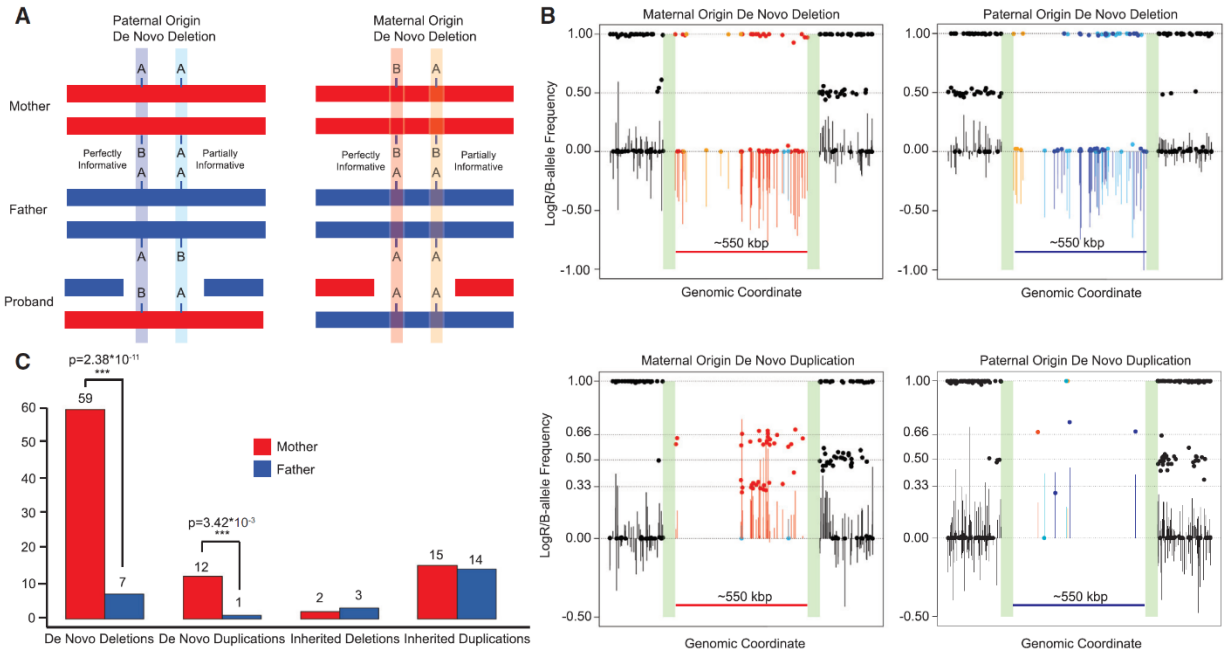

Figure 2.1: Maternal origin of 16p11.2 *de novo* CNVs. a) SNPs on the unaffected critical region haplotype were assigned to either a paternal or maternal haplotype using B-allele frequency (BAF) data. Markers informative or partially informative for parent-of-origin are shown. b) LogR (lines) and BAF (dots) plots for all *de novo* deletion and duplication categories. Colors correspond to the inferred parent-of-origin of the 16p11.2 CNV from each type of SNP marker highlighted in (a). Green bars indicate the location of segmental duplications associated with breakpoints 4 and 5—collapsed here for ease of display. c) Approximately 90% of *de novo* 16p11.2 deletions and duplications originate on the maternal haplotype, a significant maternal bias ($p=2.38 \times 10^{-11}$ deletions, 3.42×10^{-11} duplications, two-sided binomial test). Such a bias was not observed for inherited 16p11.2 CNVs.

2.3.7 Mechanism of unequal crossover and recombination analysis

To determine the mechanism of unequal crossover of *de novo* 16p11.2 CNV events, we phased the haplotypes in the unique regions flanking the 16p11.2 critical region in the proband using the sibling (if present) or dbSNP (if absent) (see **Supplemental Appendix** for details and calculation). An exchange of flanking SNP markers was used to infer an unequal crossover between homologous chromosomes (interchromosomal; nonallelic homologous recombination

(NAHR) during meiosis I); maintenance of haplotype phase (i.e., no exchange) was classified as intrachromosomal or interchromatidal (likely NAHR during meiosis II). Male and female recombination rates for the critical region were obtained from Kong *et al*.[61] The genetic distance between the leftmost and rightmost markers in our analysis is 6.20 centiMorgans for the female versus 0.45 centiMorgans for the male, which corresponds to a probability of crossover of 6.2% for the female and 0.45% for the male, respectively. We also used the recombination rate data to estimate the average difference between male and female recombination rates within the 16p11.2 critical region, and in 550 kbp regions genome-wide, for comparison. We sampled 10,000 regions of 550 kbp (the size of the 16p11.2 critical region), excluding regions containing segmental duplications or gaps and the sex chromosomes, and determined that the region ranks in the 87th percentile for mean difference between male and female recombination rates genome-wide (**Figure S2**).

2.4 Results

2.4.1 Characterization of 16p11.2 CNVs in the Simons VIP cohort

We confirmed the presence or absence of the 16p11.2 deletion or duplication using a SNP microarray (Illumina OmniExpress) in a total of 459 individuals from 126 families where either a duplication (n=36) or deletion proband (n=90) had been identified (**Table 2**). For 81% of the probands (102/126) DNA was available from at least one parent and 60% (76/126) had DNA available from both parents (**Table S1**). We confirmed the presence of the canonical breakpoint 4 to breakpoint 5 (BP4-BP5) deletion or duplication for most (125/126) of the probands, corrected familial transmission status for one Simons VIP family (14784.x15, **Figure S3**), and confirmed the presence of a *de novo* deletion in a set of monozygotic twins (family 14824,

Figure S4). In one severely affected proband (14720.x7), we identified a larger 2 Mbp deletion extending from BP2 to beyond BP5 (**Figure S5**)[15]. In addition to cases screened with available DNA, phenotype information is available for a larger set of 150 probands and their family members. Considering the entire Simons VIP collection, for cases where both parents were also screened for the 16p11.2 CNV (109/150) based on clinical microarray, FISH and/or the present analysis, 90% of deletion cases (65/72) were *de novo* or mosaic in the germline. In contrast, only 24% (9/37) of duplication cases were confirmed as *de novo*.

Table 2. Number of 16p11.2 CNV Carriers and Non-carrier Family Members Analyzed

	Male Probands	Female Probands	Mother	Father	Sibling	Other Family Member[a]	Total	Trios	Quads
16p11.2 Deletion Carriers									
De novo[b]	37	24	0	0	1	0	62	22	27
Inherited	3	6	0	0	4	0	13	1	2
Unknown	10	10	3	4	0	0	27	NA	NA
Total	50	40	3	4	5	0	102	23	29
16p11.2 Duplication Carriers									
De novo	3	5	0	2	0	0	10	3	3
Inherited	16	7	2	4	6	13	48	9	9
Unknown	1	4	9	8	0	4	26	NA	NA
Total	20	16	11	14	6	17	84	12	12
Non-carriers									
Total	NA	NA	94	69	73	27	263	NA	NA

Abbreviation is as follows: NA, not applicable.
[a]Other family members include grandparents, half-siblings, aunts, uncles, and cousins.
[b]Includes one proband with a confirmed deletion resulting from germline mosaicism.

2.4.2 Maternal parent-of-origin of the 16p11.2 CNV

We observe a striking maternal bias for the parent-of-origin of 16p11.2 *de novo* deletions (**Figure 2.1**). 89.4% (59/66) occur on the maternal haplotype, representing a significant departure from expectation ($p=2.38 \times 10^{-11}$) (**Figure 2.1c**). A similar result was observed for duplications (12 maternal vs. 1 paternal, $p=3.42 \times 10^{-11}$). For inherited 16p11.2 CNVs for which we have information from both parents, we observed no significant parental transmission biases for either duplication (15/29 maternal, p=1) or deletion (2/5 maternal, p=1) cases (**Figure 2.1c,**

Table S8). We additionally used the microarray data to assess the relative proportion of interchromosomal (between homologues) and intrachromosomal (within homologue) NAHR events by phasing haplotypes of the unique regions flanking the critical region (see **Methods** and **Supplemental Appendix**). We observed no preference for a particular mechanism of crossover for either maternal events (29 inter vs. 28 intra, p=1) or paternal events (1 inter vs. 4 intra, p=0.375) (**Figure 2.2**). If we restrict the analysis to families where we have high confidence phasing information due to the presence of unaffected siblings, there is a trend toward maternal interchromosomal unequal crossover events for deletions (19 vs. 8, p=0.052) (**Tables S9, S10**).

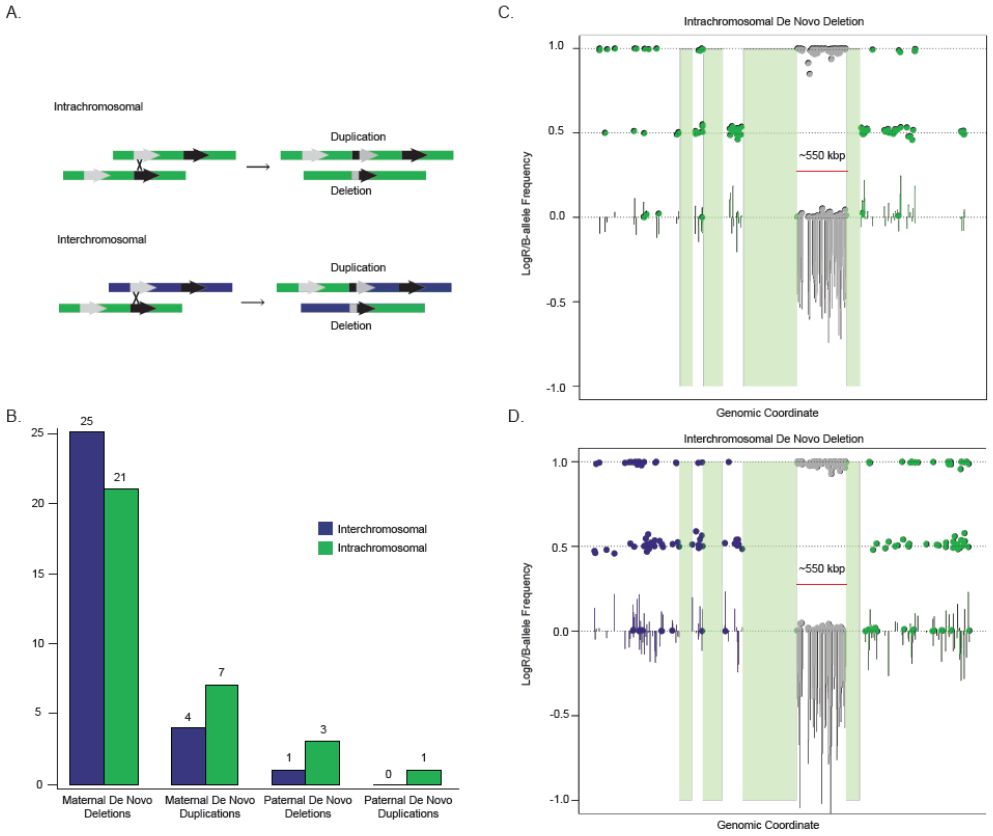

Figure 2.2: Mechanisms of unequal crossing over. a) Schematic shows intrachromosomal and interchromosomal NAHR events and the resulting products. Colors (green and purple) indicate different homologs. b) Counts of interchromosomal and intrachromosomal NAHR events by parent-of-origin and by deletion vs. duplication status. None of the differences are significant based on a two-sided binomial test. c,d) LogR (lines) and BAF (dots) plots are shown for an intrachromosomal (c) and interchromosomal (d) *de novo* deletion across the 16p11.2 region. Green bars indicate the location of segmental duplications associated with breakpoints 1-5.

2.4.3 Secondary CNVs and maternal transmission bias

We considered the presence of secondary rare CNVs (frequency <0.1% of controls) as a potential modifier of phenotype severity within the context of each family. The SNP microarray used in this study to detect CNVs has >95% sensitivity for detecting events >100 kbp throughout the genome, although we note that events as small as 2 kbp can be detected (**Figure S1**). Despite the Simons VIP exclusion criteria for additional pathogenic CNVs, 70% of assessed probands (88/126) carried at least one secondary CNV, with 35% (44/126) of probands having two or more secondary CNVs. The fraction of deletion and duplication probands carrying a secondary CNV is similar (69% and 69.5%, respectively) and no significant differences in secondary CNV presence were observed between males and females (65% and 75%, respectively) (**Tables 3, S11**). Overall, only five of the secondary CNVs were determined to be *de novo* (4 deletions and 1 duplication), although in 40% of the families (50/126) inheritance status could not be determined due to the absence of DNA from both parents. Over a third (50/126) of all probands carried a secondary CNV greater than 100 kbp in size (**Tables 3, S11**). 81 secondary CNVs disrupted an annotated exon of a gene. Eleven of these corresponded to genes associated with autism risk variants (**Table S12**), consistent with their potential contribution to disease etiology in the nine individuals in which they were found.

Among secondary CNVs where inheritance could be unambiguously determined (i.e. both parents screened), maternally inherited events predominate (52 maternal vs. 35 paternal, p=0.086). The maternal bias is strongest for the most likely pathogenic events. If we consider only secondary deletions, 70% are transmitted maternally (32 maternal vs. 14 paternal, $p=1.14 \times 10^{-2}$). This is significant both in terms of the number of events as well as the number of probands inheriting an event from a particular parent (29 maternal vs. 10 paternal, $p=3.38 \times 10^{-3}$). This

effect remains significant if we restrict our analysis to secondary deletions intersecting an exon (13 maternal vs. 4 paternal secondary CNVs, $p=4.9x10^{-2}$). These trends also hold for secondary deletions above 100 kbp in length although this finding does not reach significance due to sample size limitations. This maternal bias for deletions is observed for both 16p11.2 deletion and duplication individuals irrespective of gender of the proband (**Table S11**).

Table 3. Secondary CNVs

	Secondary Deletions[a]		No. of Probands						
	Total	Maternal	Secondary CNVs	>1 Secondary CNVs	>1 Secondary Deletion	>1 Secondary Duplication	Secondary Deletion > 100 kbp	Secondary Duplication > 100 kbp	>1 Secondary CNV > 100 kbp
Probands with a 16p11.2 Deletion									
Total (90)	31	19 (61.3%)	62	28	10	11	19	19	6
Males (50)	21	14 (66.7%)	32	13	4	6	11	10	5
Females (40)	10	5 (50%)	30	15	6	5	8	9	1
Probands with a 16p11.2 Duplication									
Total (36)	19	13 (68.4%)	25	16	6	6	9	8	5
Males (20)	13	7 (53.8%)	13	8	5	3	4	4	4
Females (16)	6	6 (100%)	12	8	1	3	5	4	1

[a]Number of events in probands with inheritance information available from both the mother and father.

2.4.4 Phenotypic features

Carriers and non-carriers of the 16p11.2 CNV within the same family vary dramatically in their phenotypic presentation (e.g., FSIQ difference[15,42], **Figure 2.3, Tables 1, S13**). We observe statistically significant differences between the FSIQ distributions of parents carrying the 16p11.2 deletion and probands with the deletion ($p=6x10^{-3}$, t-test). Similarly, the FSIQ between parents and probands carrying the duplication are significantly different ($p=3.89x10^{-6}$, t-test). Such differences between parents and children carrying the 16p11.2 CNV suggest that other genetic and non-genetic factors are contributing to the phenotype. We investigated the relationship between additional CNV burden and severity of phenotype using the FSIQ, Social Responsiveness Scale (SRS), Autism Diagnostic Interview Revised (ADI R), head circumference, and BMI as phenotypic metrics. We find a modest negative correlation between

FSIQ and the number of secondary CNVs (R^2=0.04, p=0.03, **Figure S6**). This signal is driven primarily by secondary deletions and is consistent with previous findings on the overall burden of CNV deletions and reduced IQ[24]. Although no other significant correlations are observed with other quantitative measurements, an examination of the clinical details for individuals carrying these secondary CNVs showed evidence of clinodactyly, scoliosis, hypopigmentation and craniofacial abnormalities consistent with a more severe phenotypic outcome.

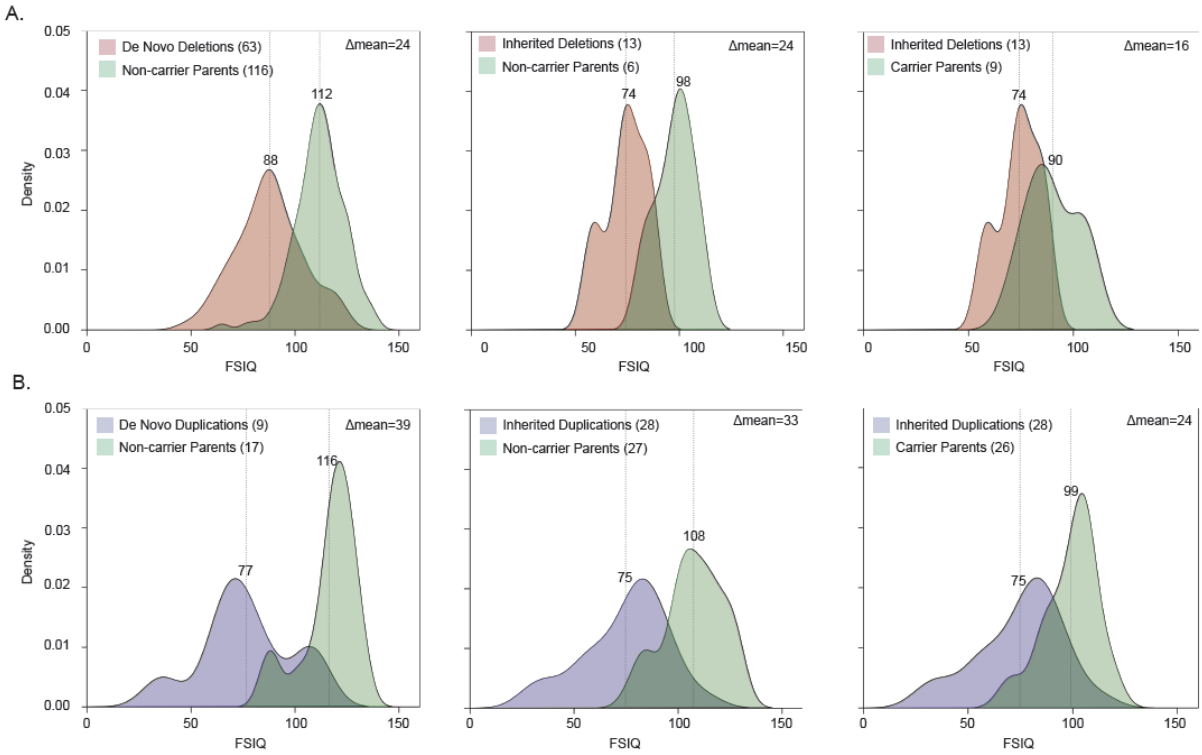

Figure 2.3: Familial IQ decrement in 16p11.2 deletion and duplication families. a) Density plots of FSIQ for deletion families (a) and duplication families (b) from the entire Simons VIP cohort. The significant decrement between parents carrying a 16p11.2 deletion and inherited deletion probands ($p=6x10^{-3}$, t-test) and between parents carrying a 16p11.2 duplication and inherited duplication probands ($p=3.89x10^{-6}$, t-test), shown in the third panel of a and b suggest factors other than the 16p11.2 CNV contribute to FSIQ decrement.

Among the secondary CNVs were several deletions and duplications corresponding to genes strongly implicated in synaptic function and/or risk of autism. Nine individuals, for example, had rare deletions or duplications in genes implicated in autism as defined by a curated list of genes

associated with autism risk (see **Web Resources**), including *CACNA2D3* [MIM 606399], *TRIO* [MIM 601893], and *KATNAL2* [MIM 614697] (**Table S12**). In a proband with a 16p11.2 deletion we validated an additional private ~400 kbp deletion that affects six genes, including *RAB10* [MIM 612672]—a gene important in vesicular transport and membrane trafficking in neurons[33]. This proband is among the most severely affected females in our cohort. She exhibits autism (SRS=90), intellectual disability (FSIQ=54), pediatric seizures, anxiety, obsessive compulsive disorder (OCD) and phobia along with structural defects of the brain, including enlarged ventricles and abnormal cerebellar vermis and corpus callosum (**Figure 2.4a**). As DNA is not available for either parent, inheritance status for both deletions is unknown. The severity of this proband is similar to the male proband with severe intellectual disability (NVIQ=29) who carried an atypical deletion of 16p11.2 encompassing more than 50 genes (**Figure S5**). We also discovered a secondary duplication disrupting *DNAH5* [MIM 603335] and *TRIO* that was transmitted from grandmother, to daughter, to son. Transmission of this CNV was associated with a characteristic facies. While the mother and son both carry the 16p11.2 deletion, the severity of the phenotype based on FSIQ increased from generation to generation (**Figure 2.4b**) with the son manifesting other features such as gynecomastia, clinodactyly and scoliosis.

In a high-functioning female autism proband carrying a 16p11.2 deletion, a ~250 kbp additional deletion of *TOP3B* [MIM 603582] was validated (**Figure 2.4c**). *TOP3B* has been strongly implicated in neurodevelopmental disorders and is thought to be important in the co-recruitment of FMRP to mRNPs[62]. While this event is found in 24 of 19,584 controls (0.123%), this same deletion in the homozygous state was found to be segregating with schizophrenia or intellectual disability in three Northern Finnish families[63]. We discovered an 840 kbp duplication harboring the autism risk locus, contactin-6 (*CNTN6* [MIM 607220]), transmitted from a mother

(Broader Autism Phenotype Questionnaire (BAPQ) 124) to her daughter (**Figure 2.4d**). In this particular case, the autistic daughter inherited the 16p11.2 deletion from her father. Hence, this is a case where a 16p11.2 deletion is transmitted from the father, and a secondary event from the mother. We also observe in this proband a smaller ~50 kbp *de novo* deletion disrupting *BIRC6* [MIM 605638]. BIRC6 inhibits apoptosis through facilitating the degradation of apoptotic proteins by ubiquitination[64], and previous studies have identified three *de novo* variants in this gene in individuals with an ASD diagnosis[65,66]. In this family, it is highly unlikely that the decrement in IQ can be solely attributed to the 16p11.2 deletion event since the FSIQ of the father carrying the 16p11.2 deletion and his proband daughter who also carries the 16p11.2 deletion differ by more than 28 points. In addition to these autism candidates, we note that two 16p11.2 duplication carriers have rare independent deletions in *CTNNA3* [MIM 607667] (**Figure S7**)—a locus previously associated with autism[67,68] and for which rare deletions have been reported in ASD individuals[3].

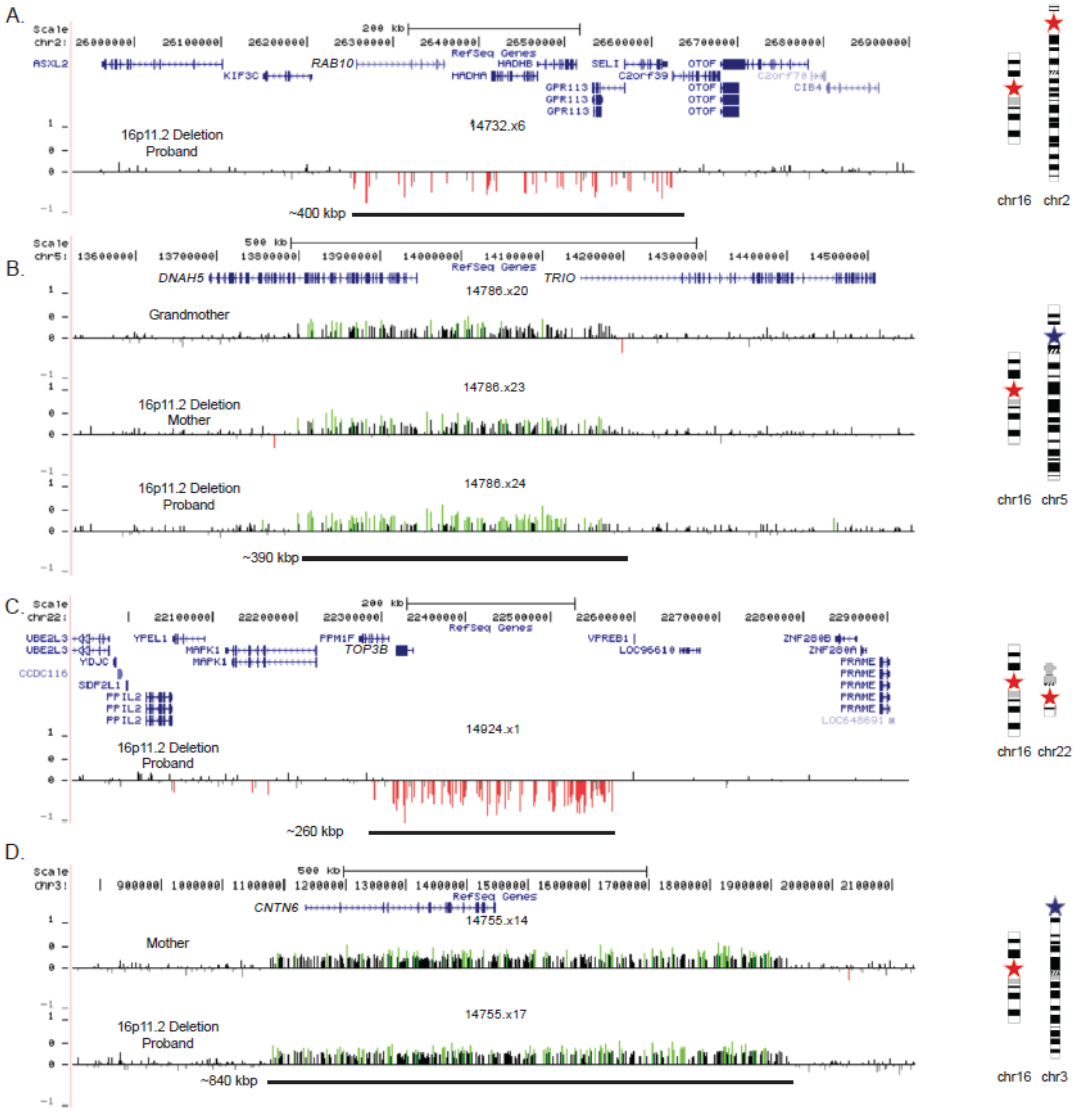

Figure 2.4: Examples of secondary large CNVs. Microarray signal intensity data shown for: a) 400 kbp gene-rich deletion of *RAB10* in 16p11.2 deletion female proband (14732.x6) with FSIQ=54, SRS=90, autism, intellectual disability, pediatric seizures, anxiety, OCD, and phobia. The CNV was private and not observed in 19,584 population controls; parental DNA was not available for analysis. b) 390 kbp duplication disrupting *DNAH5* and *TRIO* in a grandmother (14786.x20), mother (14786.x23) and male proband (14786.x24). The mother and proband also carry the 16p11.2 deletion. From grandmother, to daughter, to grandson, the FSIQ decreases from 99 to 89 to 63, respectively. This CNV was private and not observed 4,092 population controls. c) 260 kbp deletion of *TOP3B* in a 16p11.2 deletion female (14924.x1) with non-verbal IQ (NVIQ)=109, SRS=80, autism, language, learning and articulation disorder and ADHD. The CNV was observed in 24 of 19,584 population controls; parental DNA was not available for analysis. d) Maternally inherited 840 kbp duplication of *CNTN6* in 16p11.2 deletion female (14755.x17) with FSIQ=75, SRS=90, intellectual disability and enuresis. The CNV was observed in only 1 of 4,092 population controls. Stars on chromosome ideograms designate the presence and approximate position of the deletion (red) or duplication (blue).

2.5 Discussion

Our results show that most recurrent rearrangements between breakpoints 4 and 5 in chromosome 16p11.2 originate maternally. Specifically, nearly 90% of *de novo* deletions and duplications arise on maternal haplotypes, with an approximately equal proportion of inter and intrachromosomal rearrangements consistent with unequal crossover events during meiosis I and II, respectively. This observation stands in stark contrast to 75-80% of *de novo* CNVs identified in other studies that originate paternally[69,70]. Excluding genomic disorders associated with imprinted loci, a maternal parent-of-origin bias has been reported for two genomic disorders to date: the *NF1* region on 17q11.2 and the 22q11.2 microdeletion associated with velocardiofacial and DiGeorge syndromes[71,72]. Neither of these regions, however, demonstrates such a high level of female bias as what we have observed for the 16p11.2 CNV. For 16p11.2, we observe no correlation with advanced maternal age (p=0.43, t-test) (**Tables S4, S5**) and there is no compelling evidence of imprinted genes within the critical region[73,74]. Importantly, no bias is observed in maternal or paternal transmission for inherited events arguing against selection at the level of the germline or early embryogenesis.

The most likely explanation for this maternal bias is different recombination rates at 16p11.2 between males and females. Examining data from published recombination maps[61,75], there is a clear hotspot of female recombination within the critical region (**Figure S8**). Females have a significantly higher mean recombination rate within this region than do males (0.82 vs. 0.083, p=0.01, t-test) with this particular region ranking in the 87th percentile for mean difference between male and female recombination genome-wide (**Figure S2**). The maximum recombination rate for females for the 16p11.2 critical region is 13.24, whereas for males it is 1.27, a more than tenfold difference. A much milder excess of female recombination is also

noted for the 22q11.2 microdeletion (1.2- to 2.8-fold) commensurate with a more subtle maternal bias for this genomic disorder (56% maternal)[71]. The 16p11.2, 22q11.2, and 17q11.2 CNVs all lie close to the centromere of their respective chromosomes, consistent with higher female recombination rates in pericentromeric regions[61]. Thus, it is likely that gender-specific recombination hotspots may be a much more general predictor of female and male biases for NAHR.

We observe not only a maternal parent-of-origin bias for *de novo* 16p11.2 deletions, but also that mothers transmit a significantly greater number of secondary deletions to probands than do fathers. Such a transmission disequilibrium has been observed for small CNVs and single-nucleotide variants (SNVs) in individuals with ASD[76,77], and this effect may result from a higher female tolerance towards additional variants. We extend this putative female protective effect to secondary CNVs with 16p11.2 families. It is striking that of the nine probands with a secondary CNV disrupting a gene from a curated list associated with autism risk (**Web Resources**) six are female, including two with multiple events, suggesting that females may be more tolerant of severe variants[77]. We do not observe this bias for secondary duplications likely because duplications are generally less deleterious than deletions.

Our results suggest that genetic background plays a role in the observed phenotypic heterogeneity and that dosage imbalances at other loci contribute, especially in the case of 16p11.2 duplication carriers. It is interesting that the FSIQ decrement for probands with an inherited 16p11.2 duplication compared to their parents who also carry the 16p11.2 CNV is greater than the difference observed for transmission of the deletion (**Figure 2.3**). Such a difference, along with the statistically significant differences between the mean FSIQ of parents carrying the 16p11.2 CNV and probands, suggests that additional factors are contributing to the

severity of the phenotype. Our finding of a modest negative correlation between FSIQ and secondary CNVs as well as the increased phenotypic severity of such individuals argues in favor of additional rare gene disruptive variants. These findings are consistent with studies focused on different genomic disorders which have shown that individuals with more than one large CNV tend to have lower IQ when compared to individuals with only a single CNV[24]. Similarly, a recent study of an Estonian population cohort reported that a greater proportion of individuals carrying large CNVs (>250 kbp) failed to graduate high school when compared to individuals without such events. When CNVs exceeded 1 Mbp in size, there was a significant risk for intellectual disability.[78]

There are some clear limitations of this study. The number of complete families with a *de novo* variant and parental phenotypic information is insufficient, especially for duplications. Investigation of a larger sample of 16p11.2 CNVs in conjunction with more detailed phenotypic data is necessary in order to confirm the observed trends. The Simons VIP is not a population cohort, but rather was clinically ascertained and subject to inclusion and exclusion criteria. Importantly, the Simons VIP was screened for large, likely pathogenic CNVs, thus depleting the number of individuals with large secondary CNVs. A population-based cohort of sufficient size would prove most valuable if large-scale genetic screening were followed by detailed phenotypic assessment of individuals with particular genotypes[32]. Because we focused on CNVs (typically >50 kbp), we did not assess other potentially deleterious variants (e.g., SNVs or small CNVs).

The importance of secondary hits at other loci affecting phenotype severity has been established in several disorders, and a model has been developed to explain the phenotype variability associated with pathogenic CNVs[17,23,24]. Importantly, 11 of the secondary CNVs have already been implicated as risk factors for autism and developmental delay (e.g., 240 kbp

deletion of the *TOP3B* locus on chromosome 22q11.22)[63]. Our results extend observations of secondary variantal hits to the 16p11.2 CNV and suggest that full-genome sequencing of individuals carrying the 16p11.2 CNV will ultimately be required to more precisely predict the severity of disease within the context of families. This is an important consideration because once the 16p11.2 CNV is discovered such individuals are routinely excluded from further exome and genome sequencing analyses[2,21,79]. The presence of additional risk factors discovered by either sequencing or diagnostic microarray will be important for projecting the disease trajectory and the diverse outcomes associated with this pathogenic CNV.

2.6 Notes

Description of Supplemental Data
Supplemental Data include Eight Figures, and Fifteen Tables.

Acknowledgements
We thank F. Hormozdiari, K. Steinman, and T. Brown for useful discussion and edits to the manuscript. We thank all of the families at the participating Simons Variation in Individuals Project (VIP) sites, as well as the Simons VIP Consortium. We appreciate obtaining access to phenotypic data on SFARI Base. Approved researchers can obtain the Simons VIP population dataset described in this study by contacting the Simons Foundation Autism Research Initiative. A full list of the investigators who contributed to the generation of the WTCCC data is available from http://www.wtccc.org.uk/. M.H.D. is supported by U.S. National Institute of Mental Health grant no. 1F30MH105055-01 and by the Simons Foundation and X.N. was supported by a U.S. National Science Foundation Graduate Research Fellowship (Grant No. DGE-1256082). This work was supported by the Simons Foundation Autism Research Initiative Grant No. 294112 (E.E.E.), National Institutes of Health Grant No. R01MH101221 (E.E.E.), and National Institutes of Health Fellowship Grant No. 1F30MH105055-01 (M.H.D.). E.E.E. is an investigator of the Howard Hughes Medical Institute.

Competing Financial Interests
E.E.E. is on the scientific advisory board (SAB) of DNAnexus, Inc., is a consultant for the Kunming University of Science and Technology (KUST) as part of the 1000 China Talent Program.
Web Resources
cnvPartition Algorithm: http://www.illumina.com/content/dam/illumina-marketing/documents/products/technotes/technote_cnv_plug_ins.pdf
Illumina Genome Studio Software: http://www.illumina.com/techniques/microarrays/array-data-analysis-experimental-design/genomestudio.html

OMIM [Online Mendelian Inheritance in Man]: http://www.omim.org
SFARI List: https://gene.sfari.org/autdb/
Simons VIP: https://simonsvipconnect.org/
Wellcome Trust Case Control Consortium 2: http://www.wtccc.org.uk/ccc2/

Accession Numbers
Underlying SNP microarray data are available from NDAR under accession number [accession in progress].
Underlying calls for the recalled WTCCC set ("Set II") is available in dbVar under accession number [accession in progress].
CNV calls for the 19,584 ("Set I") controls are available in dbVar under accession nstd100.

3. Exonic variation and population genetic analysis of the Autism-Associated 16p11.2 CNV

This chapter has not been published. Evan Eichler and I designed the study. I designed the MIP assays and performed MIP capture. Kendra Hoekzma and Holly Stessman performed sequencing experiments. Xander Nuttle designed the 206 copy number MIPs. I performed all analyses and wrote this section.

3.1 Summary

Recurrent deletion and duplication at chromosome 16p11.2 is one of the largest genetic contributors to autism and autism-like phenotypes. Despite carrying the seemingly identical CNV, affected individuals present with a wide range of phenotypes ranging from severely affected to relatively unaffected. In order to explore the genetic underpinnings of this heterogeneity we resequenced the coding regions of the 27 unique and 3 duplicated genes in the 16p11.2 critical region in a cohort of over 100 individuals with a 16p11.2 CNV and their families. Strikingly, we find a relative lack of diversity across the critical region, with no proband carrying an LGD event in any of the 30 critical regions genes. We find that the critical region lies below the 3rd percentile for both Tajima's D and average heterozygosity metrics genome-wide, suggesting that the critical region is under selection. In order to understand natural variation in the 3 duplicated genes that are missed by exome sequencing, we resequenced the exons of these genes in >10,000 individuals and find fewer than 50 likely gene disruptive events. Our resequencing data also identified an individual with a 16p11.2 triplication and quadruplication, demonstrating that higher copy number states of the critical region are viable. Reanalysis of exome sequencing data from the 16p11.2 cohort reveals 13 probands with LGD or severe missense variants in autism-associated genes. Our results elucidate properties of the critical region and modifiers of the phenotype associated with the 16p11.2 CNV.

3.2 Introduction

In addition to secondary CNVs, deleterious variants in the 27 genes within the 16p11.2 critical region could affect the phenotype as shown for the *TBX6* gene and scoliosis[37]. For example, a 16p11.2 deletion individual with an LGD variant on the remaining haplotype might be expected to have a more severe phenotype due to the "unmasking" of a recessive allele. We hypothesize that dosage imbalance of rare variation in the critical region genes could contribute to the observed phenotype heterogeneity. In order to test this hypothesis, we resequenced the exons of the 27 unique genes within the 16p11.2 critical region.

Along with the 27 unique genes in the 16p11.2 critical region, 3 genes are present in the segmental duplications flanking the critical region: *BOLA2*, *SLX1A*, and *SULT1A3*[15]. Analysis of whole-genome sequencing data from humans, ancient hominins, and great apes has revealed that *BOLA2* is duplicated only in *Homo sapiens*[38] and no ortholog of the duplicated gene *SULT1A3* (also called *SULT1A4*) has been identified in non-primate species[80]. Evidence suggests that human specific duplicated genes are important for neural development as in the case of the *SRGAP2* gene family[81]. We hypothesize that rare nucleotide variation or copy number variation in these genes could contribute to the observed phenotype. In order to test this hypothesis, we resequenced the exons of the 3 duplicated genes in the Simons VIP cohort. Since these genes are not well covered in exome sequencing data, we additionally resequenced the exons of these genes in thousands of cases with autism and controls. Finally, to assess copy number variation in these duplicated genes, we designed probes to distinct markers that allow determination of genic copy number.

3.3 Methods

3.3.1 SNV detection and validation in 16p11.2 critical region genes

We designed and optimized 526 MIPs corresponding to the exons of 27 unique genes covering a total of 58,912 base pairs (34,879 coding exons) in addition to 37 MIPs corresponding to three duplicated genes covering a total of 4,144 base pairs (2,175 coding exons) (**Tables S1, S2**). After rebalancing, 480 unique and 33 duplicated gene MIPs remained. We successfully captured >90% of exonic base pairs with a median average coverage of 337 per base per unique gene and 1,865 per base[1] per duplicated gene among 120 probands (85 deletions, 35 duplications), 57 carrier family members (13 deletions, 44 duplications) and 264 family members with no event (**Table S3**). Included in this set were 71 families where complete trios or quads were present. While most genes capture well, we note that some genes such as *MAZ* had low median coverage (**Table S4**). All libraries were initially tested on the Illumina MiSeq for performance and sequenced on an Illumina HiSeq 2000 and/or Illumina MiSeq.

For the 16p11.2 exon targeting MIPs, overlapping sequence reads were merged using PEAR v0.9.2[82], mapped using BWA-MEM version 0.0.7[83] to the hg19 chromosome 16 reference genome with the telomeric most segmental duplications hard-masked, and SNV/indel variants called using FreeBayes v0.9.14 across the critical region chr16:29649996-30199854 (hg19). Variants were called adjusting for the copy number of the 16p11.2 region in individual carriers and allowing a minimum of 5% alternate allele reads. We considered all variants QUAL >20 and read depth >10, removed dbSNP sites excluding sites after build 129, removed Mills and 1000 Genomes gold standard indels, and removed SNPs present with frequency >1% in dbSNP144. Variants were annotated using the program Alamut Batch version 1.4.4[84], which provides

[1] Interestingly, the median copy number of these genes is 6 and 1865/6=310.8, almost exactly the median coverage for the unique genes.

functional predictions for RefSeq isoforms of each gene. We additionally annotated the called set for the non-psychiatric cases in Exac (ftp://ftp.broadinstitute.org/pub/ExAC_release/release0.3/subsets/ExAC.r0.3.nonpsych.sites.vcf.gz), and for the version 1.3 CADD scores[85]. For our analyses, we selected the transcript with the most severe variant at each position in each gene. We selected 35 sites in the unique genes for validation (**Table S5**).

3.3.2 Case and control resequencing

In order to assess the variation of the three duplicated genes, we designed a total of 7 *BOLA2*, 15 *SLX1A*, and 15 *SULT1A* MIPs targeting the exons of these genes and spiked into a pool of 2,642 MIPs (**Table S6**). After rebalancing, 3 *SULT1A* MIPs were removed. Samples were prepared and sequenced as previously described[2,86]. Briefly, sequence reads were indexed by barcode, the reads merged using PEAR v0.9.2, trimmed, and mapped using bwa version 0.7.3a to a hg19 chromosome 16 contig with the centromeric copies of *BOLA2*, *SLX1A*, and *SULT1A* hard masked in order to provide a single mapping location for each correctly targeted MIP. Sequencing data were generated on the Illumina MiSeq (151 PE) and HiSeq2000 (101PE) instruments.

We sequenced and analyzed a total of 11,100 cases with autism or intellectual disability and 2,782 controls (**Table S7**). We performed quality control on a per MIP and per sample basis. First, we removed MIPs with median coverage per sample <30x across all samples with the result that three MIPs were removed from subsequent analysis. Second, we removed samples with >8 MIPs (out of 22 analyzed for *BOLA2* and *SLX1A*) with per sample coverage less than 30 (**Table S8**). After quality control, a total of 8,440 cases and 2,139 controls remained.

We additionally resequenced the third duplicated gene *SULT1A3* in our analysis. Due to the high identity of *SULT1A3* with the family of *SULT* genes throughout the genome, we performed a similar but separate quality control analysis. In particular, we first removed MIPs with median coverage per sample <30x across all samples. No additional MIPs were removed. Second, we removed samples with >5 MIPs (out of 12 analyzed for *SULT1A3*) with per sample coverage less than 30. After quality control, a total of 8,124 cases and 2,113 controls remained.

Variants were called using freebayes v0.9.21 over the region chr16:29,460,712-29,483,159 of GRCh37 (hg19), which contains the genes *BOLA2*, *SLX1A*, and *SULT1A*. The copy number of *BOLA2, SLX1A* and *SULT1A3* ranges from 3-8 in humans, with a median of copy number of 6[38]. In order to call variants in individuals with up to 8 copies of *BOLA2* or *SLX1A*, we first set the minimum alternate fraction of observations supporting an alternate allele in a single individual (–min-alternate-fraction flag) to 0.07. This means that at least 7 in 100 observations must be of the alternate allele. Second, we kept the default minimum alternate count (–min-alternate-count flag) at 2, which means that at least 2 reads must support an alternate allele in each individual. Across all individuals, our average coverage per MIP for *BOLA2* and *SLX1A* was 179.5 (range 49 to 828, excluding MIPs removed during quality control). We calculated the probability of detecting an alternate variant in the extreme case assuming a high copy number state of 8 of *BOLA2* and *SLX1A* and a total coverage of 32x across these genes. If an alternate variant is present in only one of the copies, 1 in 8 reads (12.5%), 4 reads in total should have the alternate allele in a sample with 32x coverage. Our parameters for calling allow detection of such a variant. We used the same parameters to call *SULT1A*. Our average coverage per MIP for *SULT1A* was 187 (range 31 to 668, excluding MIPs removed during quality control).

We applied several filters to achieve a final call set using the vcflib suite of programs[87]. We required a variant quality of at least 20 and per-sample read depth of at least 30 (vcffilter –g "DP>20" –f "QUAL>20" vcf.file), removed homopolymer repeats (grep -v 'AAAAAAAA\|TTTTTTTT\|ATATATATATATATATATAT'), and broke multi-allelic records into single records (vcfbreakmulti). We annotated called variants using AlamutBatch v.1.4.3 (database version 1.4-2015.11.02) for two transcripts of *BOLA2* (NM_001031827.1 and the 10kDa transcript discussed in Nuttle and Giannuzi *et al.*) and two transcripts of *SLX1A* (NM_001014999.2 and NM_001015000.2). We used AlamutVisual v2.7.1, which uses the same databases as AlamutBatch to annotate the single transcript of *SULT1A3* (NM_177552.3). We considered a variant a splice site variant if it was in intronic sequence and located within 1 basepair of the nearest annotated splice site. For each site we computed the Combined Annotation Dependent Depletion (CADD) v1.3 scores[85].

3.3.3 Copy number genotyping

We designed 206 MIPs to identifiers in the segmental duplications flanking the critical region as well as in the critical region that allow assessment of copy number of the *BOLA2*, *SLX1A*, and *SULT1A3* and the critical region proper (**Table S9**). MIPs were designed and analyzed according to a previously described method[88].

3.3.4 Exome sequencing and analysis

In order to assess genome-wide exonic variation and its potential contribution to phenotypic heterogeneity, we analyzed exome sequencing data from the Simons Variation in Individuals Project (Simons VIP, https://sfari.org/resources/autism-cohorts/simons-vip). We analyzed a total

of 431 exomes from the VIP including 85 deletion probands and 34 duplication probands (**Tables 1 and S3**). We applied several filters to the variants present in the exome VCF available through SFARI base using the VCFlib[87] and VCFtools[89] software suites. For filtering we selected only variants with a PASS flag, depth>10, QUAL>20, removed dbSNP sites excluding sites after build 129, removed Mills and 1000 genomes gold standard indels, removed segmental duplications and tandem repeats, removed variants found at >1% frequency in dbSnp144, and removed sex chromosomes. We annotated using SeattleSeq build 138, selected the transcript with the most severe annotation for the variant, and retained only non-synonymous and splice variants. We additionally annotated each variant with the CADD v1.3 score[85], the allele frequency from the Exac database containing non-psychiatric cases (ftp://ftp.broadinstitute.org/pub/ExAC_release/release0.3/subsets/ExAC.r0.3.nonpsych.sites.vcf.gz), and the Residual Variation Intolerance Score[90] (version 3_12_Mar16, columns all 0.1% and %All 0.1%.)

Table 1: VIP exomes analyzed.

	De novo Deletion	Inherited Deletion	Unknown Deletion	*De Novo* Duplication	Inherited Duplication	Unknown Duplication	Triplication
Quads	23	1	0	1	8	0	1
Trios	21	2	0	4	6	0	0
Mother Only	9	2	6	1	3	0	0
Father Only	2	1	0	2	2	0	0
Proband Only	4	2	12	0	2	5	0
Total	59	8	18	8	21	5	1

In order to compare the critical region variants called by exome with those called by MIPs, we extracted variants corresponding to the critical region genes. Variants were annotated using the program Alamut Batch version 1.4.4[84], which provides functional predictions for RefSeq isoforms of each gene, and uses the same databases used for annotating the MIP resequencing data of the critical region genes. We additionally annotated the called set for the allele frequency

of non-psychiatric cases in Exac, and for the version 1.3 CADD scores[85]. For our analyses, we selected the transcript with the most severe variant at each position in each gene (**Table S10**).

3.3.5 Diversity and selection across the critical region

In order to see if the critical region had any special population genetic characteristics, we utilized the haplotype phased 1000 genomes phase 3 release (ftp://ftp.1000genomes.ebi.ac.uk/vol1/ftp/release/20130502/) in order to determine if there is selection over the critical region using average heterozygosity as well as Tajima's D metrics. In order to calculate the observed and expected heterozygosity we used the VCFlib suite of tools; in order to calculate Tajima's D, we used the VCFtools software suite. Given that there are different methods to calculate Tajima's D, and the estimates will depend on sample filtering, it is crucial to compare the region of interest with a genome-wide distribution of similarly sized regions. To do so, we calculated the genome-wide distribution of average heterozygosity for 550kbp regions from 2,500 individuals from the 1000 Genomes Phase 3 release sampled 100,000 times across autosomal regions not containing gaps or segmental duplications and performed the same analysis across chromosome 16 sampling 30,000 times. In order to get better resolution across the critical region, we reduced our window size to 10kbp with a 5kbp step across the critical region and calculated thresholds for significance based on the chromosome 16 and the genome-wide distribution of 10kbp windows of average heterozygosity. We performed the same analyses for Tajima's D, though calculated the statistic for non-overlapping 550kbp regions genome-wide. Again, to assess selection in the critical region, we calculated Tajima's D for 10kbp non-overlapping windows across the critical region and calculated thresholds for

significance based on the chromosome 16 and genome wide distributions of 10kbp windows of Tajima's D.

3.4 Results

3.4.1 Unique critical region genes

We designed and optimized 527 MIPs spanning 90.8% of the exons of the critical region genes (**Table S2**). We sequenced these exons to a median sequence coverage of 337-fold per sample per gene (**Figure S1**). We examined 85 deletion probands, 35 duplication probands, and 253 non-carrier family members (**Table S3**). In this analysis, we specifically searched for severe variants, defined here as non-synonymous events with a CADD[85] v.1.3 score >20.

Among the 16p11.2 deletion and duplication probands, we observe a trend towards a lower SNV burden between probands and non-carrier parents after we corrected for allelic abundance (**Table S11**). In particular, when we require the observed variants to be present at <0.1% Exac frequency and with a CADD>20, we notice statistically significant differences in burden for both deletions and duplications. However, this observation does not hold at other frequencies or CADD score cutoffs. Based on our haplotype assessment of the individuals carrying a 16p11.2 duplication and a rare protein-altering variant (private in cohort families, <1% frequency Exac), we observe a bias for the protein-altering variants to occur in a single copy (allele balance ~0.33, (36/36 alleles among 12 individuals map to a single copy, $p=2.91x10^{-11}$ two-sided binomial, **Table S12**).

Of the 70 families for which we have inheritance information, we identified one *de novo* protein-altering event in *de novo* deletion proband 14701.x7, a missense variant in the gene *QPRT*, quinolinate phosphoribosyltransferase (**Table 2**). Two private loss-of-function variants

were found in non-carrier mothers of 16p11.2 deletion probands (a nonsense variant in *KIF22*, 14809.x3, a kinesin-like binding protein (Chr16:g.29802150G>T)), and a frameshift variant of the gene *GPD3*, glyceraldehyde 3-phosphate dehydrogenase, 14779.x6, (Chr16(GRCh37):g.30123709_30123724del). Neither of these were transmitted to probands. We identified eight severe private (CADD>20, <0.1% frequency Exac, private in cohort) missense variants in eight probands. An examination of clinical records of probands with additional severe variants did not show that these individuals were either more affected with respect to FSIQ or have a greater number of diagnoses than other probands (**Table 2**). It is notable that three of these individuals have FSIQ<70, and three have 3 or more diagnoses.

Table 2: Probands with a rare severe coding SNV (<0.1% Exac, private in cohort) CADD>20, from MIP resequencing data.

Sample	Chrom	Pos	Ref	Alt	Gene	Type	FSIQ	Diagnoses	16p Type	16p Status	Sex	Parent of Origin	CADD	Protein Change	Inheritance
14700.x7	16	30004623	G	A	*HIRIP3*	missense	54	3	duplication	inherited	female	Maternal	23.6	p.Arg526Trp	paternal
14701.x7	16	29708571	G	A	*QPRT*	missense	71	2	deletion	de-novo	male	Maternal	25.6	p.Val245Met	*de novo*
14710.x7	16	30133311	C	T	*MAPK3*	missense	86	1	deletion	inherited	male	Paternal	23.6	p.Val63Met	maternal
14724.x5	16	29884717	C	T	*SEZ6L2*	missense	66	2	duplication	de-novo	male	Maternal	24	p.Glu708Lys	paternal
14744.x5	16	29998669	C	G	*TAOK2*	missense	91	3	deletion	de-novo	male	Paternal	23.9	p.Leu913Val	maternal
14761.x14	16	29820873	C	T	*MAZ*	missense	103	2	deletion	germline-mosaicism	male	NA	22.6	p.Ala431Val	NA
14796.x3	16	29808222	C	T	*KIF22*	missense	59	6	deletion	de-novo	male	Maternal	27.4	p.Arg27Cys	paternal
14799.x1	16	30012264	C	T	*INO80E*	missense	122	2	deletion	de-novo	male	Maternal	23.5	p.Pro100Leu	paternal

3.4.2 Duplicated critical region genes

We designed MIPs to the exons of the three duplicated genes *BOLA2*, *SLX1*, and *SULT1A3* and resequenced these exons in the Simons VIP cohort. In these three duplicated genes, we observe two LGD events, both in *SLX1*. The first is a splice site variant, present in two mothers and a non-carrier sibling (two total families) and the second is a frameshift variant in a mother carrying the 16p11.2 deletion (**Table S5**). Of the missense variants in *BOLA2*, one duplication proband inherits a missense variant with CADD>25. In *SLX1* four probands (all deletion) have missense variants with CADD>25. In *SULT1A* three probands (all deletion) have missense variants with CADD>25 (**Table 3**). We did not observe a trend towards these individuals lying at the fringes of the diagnoses and FSQI severity plot (**Figure S2**). In this analysis, we excluded

variants present in more than 50% of families because such variants likely represent sequencing errors or paralog specific variants (PSVs).

We determined if high or low copy number of *BOLA2* correlated to a particular phenotype. Restricting to deletion individuals, and separating into copy number 3 and 3> groups, we found that the individuals with *BOLA2* copy number 3 are enriched for anemia (p=0.00124, Fisher's Exact).

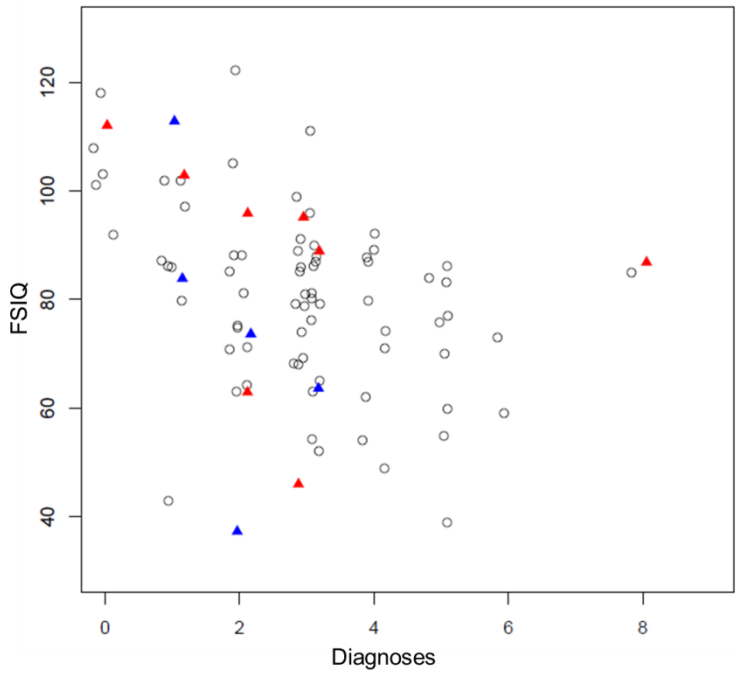

Figure 3.1: Severity plot for 16p11.2 CNV probands. Jittered plot of full scale IQ (FSIQ) and number of additional diagnoses for deletion and duplication probands. Red triangles indicate probands with *BOLA2* copy number of 3 and blue a copy number of 8 or 9. Extremes of copy number do not appear to associate with a more or less severe phenotype based on these metrics.

We utilized MIP copy number estimates in conjunction with the exon resequencing data of the duplicated genes for two purposes. First, we explored the relationship of copy number of the three duplicated genes with severity of disorder, as defined by number of diagnoses and FSIQ (**Figure 3.1**). We observe no correlation between copy number of these genes and severity. Second, in those probands with a severe variant in the duplicated genes, we used the allele

balance of the variant multiplied by the copy number predicted by MIP to determine in how many copies the variant is found (**Table 3)**. In all cases, the number rounds to 1, suggesting that the variant is present on a single copy in these individuals.

Since variation over these genes is not well-understood, we mapped each discovered variant (excluding variants present in >50% of families) to the protein models of these genes (**Figure 3.2**).

Table 3: Severe variants in duplicated genes in probands from the VIP from MIP resequencing.

Chrom	Pos	Ref	Alt	Gene	Effect	Sample	FSIQ	Diagnoses	16p Status	Inherited Status	Sex	CADD	pNomen	AB	BOLA2 CN	Variant present in x Copies	Inheritance
16	29465053	C	G	*BOLA2*	missense	14832.x7	108	5	duplication	de-novo	female	25.8	p.Arg120Ser	0.15	NA	NA	NA
16	29466157	G	C	*SLX1A*	missense	14753.x5	79	3	deletion	de-novo	female	25.8	p.Val32Leu	0.29	5	1.43	NA
16	29466157	G	C	*SLX1A*	missense	14823.x14	90	3	deletion	de-novo	female	25.8	p.Val32Leu	0.25	4	1	Mother
16	29466741	G	A	*SLX1A*	missense	14863.x7	112	0	deletion	de-novo	male	26.5	p.Gly71Ser	0.24	3	0.71	Father
16	29466979	C	T	*SLX1A*	missense	14863.x7	112	0	deletion	de-novo	male	23.8	p.Arg119Cys	0.31	3	0.92	Father
16	29473201	C	T	*SULT1A4*	missense	14785.x5	76	5	deletion	unknown	male	22.5	p.Pro101Leu	0.18	5	0.9	NA
16	29474900	C	T	*SULT1A4*	missense	14728.x10	108	0	duplication	de-novo	female	27.3	p.Ser171Phe	0.12	6	0.69	Mother
16	29474900	C	T	*SULT1A4*	missense	14773.x3	65	3	duplication	inherited	male	27.3	p.Ser171Phe	0.11	7	0.75	Mother
16	29475524	G	A	*SULT1A4*	missense	14731.x8	74	4	deletion	de-novo	male	23.1	p.Arg213His	0.23	4	0.92	NoPass
16	29475566	C	T	*SULT1A4*	missense	14795.x17	87	4	deletion	de-novo	male	23.3	p.Thr227Met	0.06	4	0.24	DeNovo?
16	29475596	T	G	*SULT1A4*	missense	14723.x17	114	1	duplication	inherited	male	23.4	p.Met237Arg	0.1	8	0.82	Father

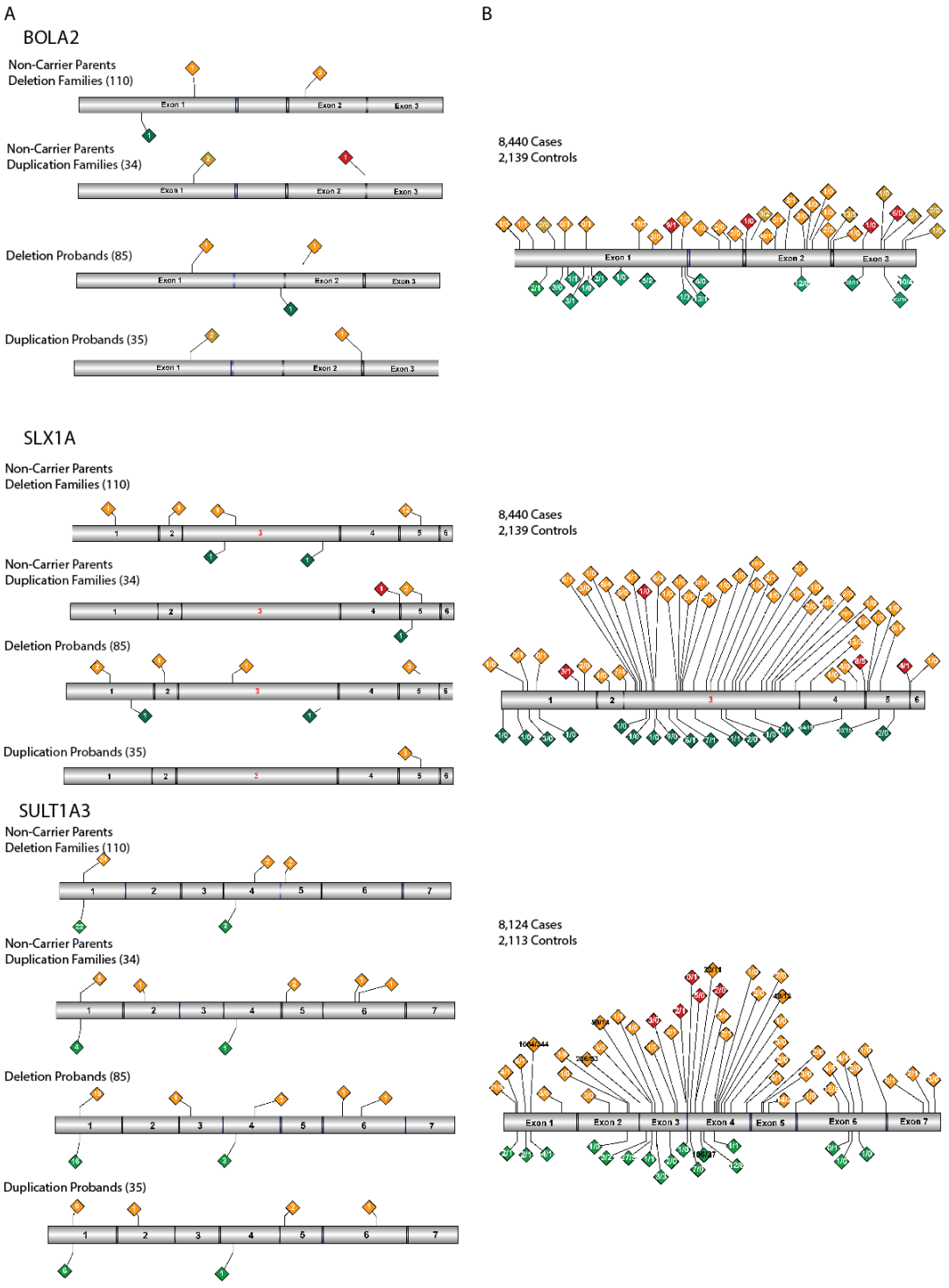

Figure 3.2: Protein models and variation of *BOLA2, SLX1A,* and *SULT1A3*. Variant counts for three duplicated genes in 16p11.2 probands (a) and over 8,000 cases with autism or intellectual disability and over 2,000 controls (b). Red indicated likely gene disruptive (LGD) variant, yellow missense, and green synonymous. Numbers in diamonds indicate the total number of variants (a) and total numbers of variants in cases and controls (case/control) (b).

3.4.3 Resequencing critical region genes in cases and controls

Since *BOLA2*, *SLX1*, and *SULT1A* are not well-covered in exome sequencing studies, variation in case and control populations is not well-understood. In the Exac database (exac.broadinstitute.org), which contains the exomes of over 60,000 individuals, *BOLA2* has 0 mean coverage, *SLX1* mean coverage 7.737, and *SULT1A* mean coverage 4.068. Given that the median copy number of these genes in humans is 6[38], *SLX1A*, the duplicated gene with the best coverage, has mean effective coverage per copy of 7.737/6=1.29, insufficient to call variation. In order to better understand variation in these duplicated genes at a population level, we resequenced the exons of these genes in 11,100 cases with autism or intellectual disability and 2,782 controls. After quality control assuring sufficient coverage to allow comparison between cases and controls, we had remaining a total of 8,440 cases and 2,139 controls to assess *BOLA2* and *SLX1* and a total of 8,124 cases and 2,113 controls to assess *SULT1A*.

We assessed both common and rare exonic variants in two transcripts of *BOLA2* (NM_001031827.1 and the shorter and more common 10kDa transcript discussed in Nuttle and Giannuzi *et al.*), two transcripts of *SLX1A* (NM_001014999.2 and NM_001015000.2) and the single transcript of *SULT1A3* (NM_177552). In total, we discovered 8 LGD variants for the more common 10kDa transcript of *BOLA2* of which 2 were private. The LGD events were discovered only in cases (p=0.3719, Fisher's Exact). In the canonical transcript of *SLX1A* (NM_001014999.1), we discovered 23 LGD variants (16 cases, 7 controls, p=0.29 Fisher's Exact) of which 1 was private and found only in a case. In *SULT1A3*, we observed 14 LGD variants (12 cases, 2 controls, p=0.75 Fisher's Exact) of which 2 are private and found only in controls. We did not observe any statistically significant differences between cases and controls, even when restricting to private or likely damaging events based on CADD score (**Table S13**).

Since each gene exists in a multiple copy state ranging from 3-8 copies, with median copy number 6, we assessed the allele balance of each variant in *BOLA2* and *SLX1A* to determine in how many copies discovered variants were found (**Table S14**). We excluded *SULT1A3* from this analysis due to its high identity with the SULT family of genes elsewhere in the genome. For each low frequency variant (<100 samples with the variant in the sequenced population), we plotted the allele balance density between cases and controls (**Figure 3.3**). The median copy number of *BOLA2* and *SLX1A* in each individual is 6, and assuming this copy number across all individuals, we would expect an allele balance of 1/6=0.2 if all individuals had the variant present in a single copy. The mean allele balance is just below 0.2 in both *BOLA2* and *SLX1A* suggesting that the vast majority of variants are present in a single copy. Furthermore, none of the likely gene disruptive variants in cases had an allele balance >0.3.

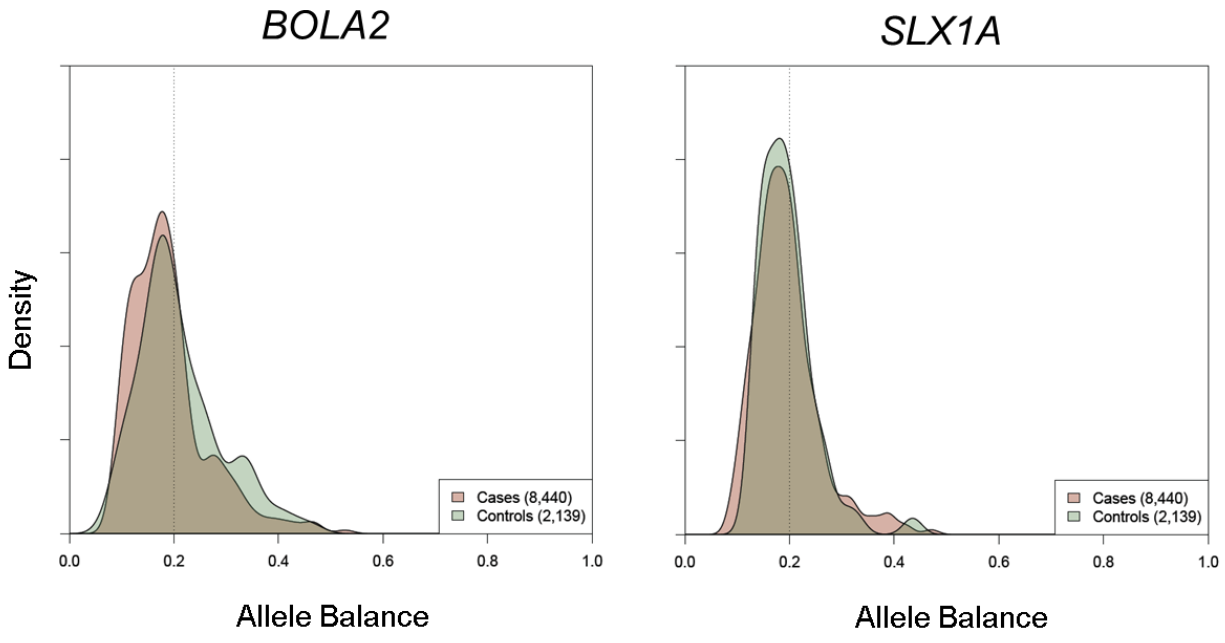

Figure 3.3: Allele balance across discovered variants in *BOLA2* and *SLX1A*. The distribution of allele balance for these duplicated genes shows a mean allele balance just below 0.2. The average copy number of these genes is 6, and if a variant is present in one copy, we expect and allele balance of 1/6=1.67, which is what we observe for the majority of variants.

Since there is a high identity between the SULT family of genes we performed a multiple sequence alignment on the coding sequence (CDS) of all 14 members of the SULT family using the program clustal v2.1 and visualized the results in Jalview v2.9.0b2. We used a custom script to determine the percent identity of *SULT1A3* coding sequence when compared with the coding sequences of all 13 other members of the family (**Table S15**). *SULT1A3* shares greater than 95% identity with both *SULT1A1* and *SULT1A2* whereas it shares a range of 43% to 68% identity with other members of the SULT family of genes. We also used a custom script to determine differences in the coding sequences of the SULT genes that allow us to differentiate *SULT1A3* from all other (a) members of the SULT family of genes (**Table S16**), (b) members of the SULT family of genes excluding *SULT1A1* and *SULT1A2* (**Table S16**) and (c) from *SULT1A1* and *SULT1A2* (**Table S17**). This information allows determination of variants unique to the SULT1A subfamily.

3.4.4 Copy number genotyping

We used MIPs targeting markers in the segmental duplications flanking the 16p11.2 critical region to assess the copy number of the block of genes *BOLA2*, *SLX1A*, and *SULT1A3* as well as MIPs targeting markers in the critical region to allow inference of the critical region copy number. We observed no correlation between those individuals with the lowest copy number (3) or highest copy number (8 or 9) and severity of phenotype as defined by FSIQ and number of diagnoses (**Figure 3.1**).

We confirmed the assessed copy number of the critical region in screened individuals and found that it was consistent in terms of copy number state (deletion or duplication) with a recent SNP microarray analysis of this same cohort[91]. However, upon analysis of the MIP copy number

results, we noticed signatures in three individuals inconsistent with the stated critical region copy number. In particular, in triplication family 14752, the mother (14752.x6) and aunt (14752.x7) were annotated as having a triplication (four total copies of the critical region), however the MIP and microarray data suggests that they have a duplication (**Figure 3.4, Figure S3**). In mother 14742.x3 annotated as having a duplication, and transmitting that duplication to her son, the MIP data suggests a quadruplication (five total copies of the critical region) (**Figure S4**).

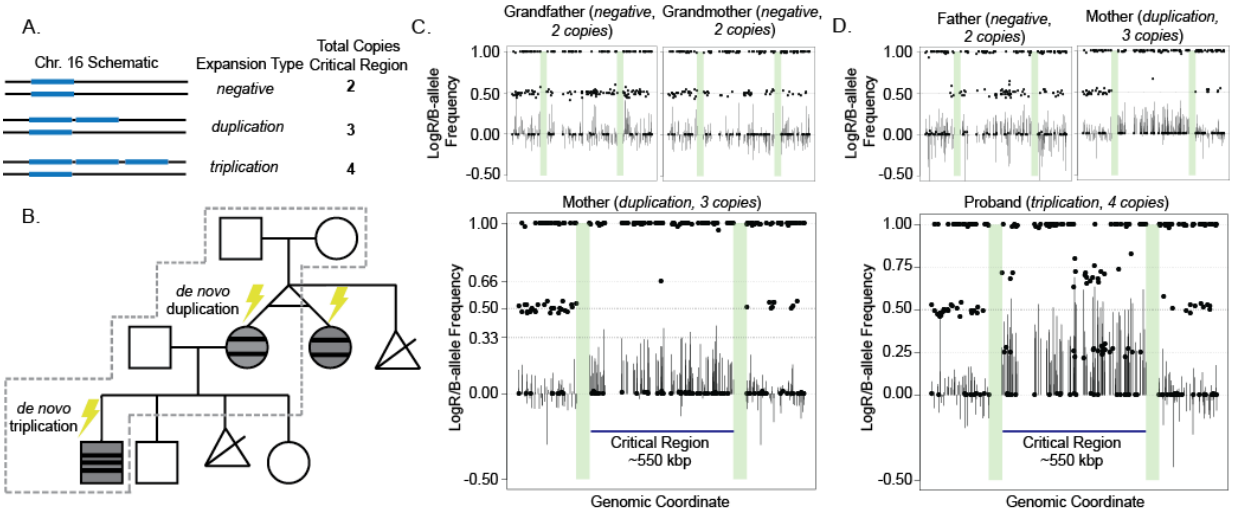

Figure 3.4: Expansion of the 16p11.2 critical region. In triplication family 14752, a *de novo* duplication in a mother expands to a triplication in proband (a). The mother has an identical twin who shares the *de novo* duplication (b). LogR and B-allele frequency plots from microarray demonstrate the duplication (c) and triplication (d). The ratio of raw intensity values between the proband and mother is 1.3=4 copies /3 copies on average.

In order to confirm this assessment, we analyzed previously generated SNP microarray data from the triplication family using the Illumina Human OmniExpress platform (112 probes over the critical region)[91] (**Figure 3.4**). In the triplication proband (four total critical region copies, 14752.x10), we see B-allele/paralog specific read count frequencies at 0, 0.25, 0.75, and 1, corresponding to the A/B allele states (AAAA, AAAB, ABBB, BBBB). This is in contrast to duplications (three total critical region copies) where we would see B-allele/paralog specific read

count frequencies at 0, 0.33, 0.66, and 1, corresponding to states (AAA, AAB, ABB, BBB). For the individuals not carrying an event (two total critical region copies), we would see ratios of 0, 0.5, and 1, corresponding to states (AA, AB, and BB).

The mother of the triplication proband (14752.x6) and her identical twin (14752.x7) are homozygous across the critical region, with the exception of one probe found at a B-allele frequency of 0.66 (as expected for the ABB, a state found in an individual with a duplication). The mother and aunt have B-allele states of AAA and BBB across the critical region assuming duplication or AAAA and BBBB assuming triplication. This homozygosity is the reason we don't see the AABB state in the triplication proband (band at ratio 0.5).

Because the B-allele frequency/ratio data alone in the critical region in family 14752 cannot definitively distinguish the copy number state of the mother and aunt, we used the MIP and microarray data in two additional ways. First, we looked at the paralog specific read count frequencies at targeted loci within the segmentally duplicated sequence where telomeric and centromeric copies are distinguishable by SNV markers. Normally an individual has 4 total copies of this region, 2 that are centromeric and 2 that are telomeric[38]. Individuals with a 16p11.2 duplication have 5 total copies (3 telomeric + 2 centromeric based on analysis of where breakpoint nearly always maps), while individuals with a triplication have 6 total copies (4 telomeric + 2 centromeric). Individuals with a duplication have 3 telomeric out of 5 total copies of the region, and 2 centromeric out of 5 total copies of the region, giving paralog specific count frequencies at 3/5=0.6 and 2/5=0.4. Similarly, for the triplication, we expect paralog specific count frequencies at 4/6 = 0.66 and 2/6=0.33. Here the mother of family 14752 (14752.x6) and her identical twin (14752x7) show the duplication signature where the proband (14752.x10) shows the triplication signature. Second, we looked at the signal intensity data over the critical

region from the microarray. The ratio of the raw intensity data (2^logR) between the proband and the mother is 1.3=4/3 on average, as expected if the proband has a triplication (four total copies) and the mother a duplication (three total copies).

Since we have SNP microarray data from the grandmother (14752.x1) and grandfather (14752.x4), we can assign the parent of origin of the *de novo* 16p11.2 duplication present in the mother and aunt. In particular, since the grandmother and grandfather are not homozygous over the critical region, we can use the haplotype of the mother and aunt across the critical region to phase the parents. Since all three copies over the critical region in mother and aunt are homozygous but the parents are not homozygous over this region, the mechanism of unequal crossing over must be intrachromosomal. Not assuming any phase information, we compute the number of markers that partially or perfectly support a maternal or paternal parent of origin and inter or intrachromosomal mechanism of crossing over (**Table S18**). Out of the 112 markers, we observe 27 supporting a maternal parent of origin, 5 supporting a paternal of origin; and 58 markers supporting an intrachromosomal mechanism and 0 supporting an interchromosomal mechanism. This evidence strongly suggests that the *de novo* duplication occurred on a grandmaternal haplotype by means of an intrachromosomal mechanism of unequal crossover.

Based on the haplotype of the proband (three identical copies and one distinct copy of the critical region), we can phase the father and using the father the two non-carrier siblings of the proband (14752.x11 and 14752.x12). Since there is no exchange of markers flanking the 16p11.2 critical region, we infer that the expansion from duplication to triplication also occurred by an intrachromosomal mechanism (**Table S19**).

Using a similar approach, we observe a contraction from five to three total copies, from a mother (14742.x3) to a proband (14742.x6). In particular, allele read count frequencies as well as

B-allele frequencies in the mother (14742.x3) cluster around 0, 1/5, 2/5, 3/5, 4/5, and 1 (corresponding to AAAAA, AAAAB, AAABB, AABBB, ABBBB, BBBBB) and suggest five total copies of the critical region whereas the proband has allele read count frequencies as well as B-allele frequencies (14742.x6) that cluster around 0, 1/3, 2/3, 1 (corresponding to AAA, AAB, ABB, and BBB) suggesting three total copies (**Figure S4**).

3.4.5 Exome analysis

In order to understand the effect of exonic single nucleotide and indel variation outside of the critical region, as well as to compare our MIP resequencing results with another dataset, we analyzed exome sequencing data available for the Simons VIP (**Table S3**).

For the 66 trio and quad families, we have inheritance information from both mother and father, and can determine whether or not a variant is *de novo*. In order to call a variant as *de novo*, we required no alternate allele reads in mother and father, the variant had to be private in the cohort, not found in the Exac database, not have a dbSNP variant at the same site, and have at least 5 alternate allele supporting reads (**Table S20**). In total, we found 12 unique *de novo* non-synonymous variants (6 in probands). None are associated with autism or intellectual disability. We find a *de novo* frameshift variant in a female non-carrier sibling in *FBXO15*, an F-box protein associated with autism[92].

In deletion and duplication probands, we assessed the total numbers of deleterious variants compared to non-carrier parents and non-carrier siblings. In particular, we selected variants with RVIS<50, CADD>25, Exac <0.01% frequency, and private in the cohort. These filters resulted in 203 unique variants across 101 families, including 179 variants found in 92 probands. Of these families, family 14702 had significantly more variants than the other families, suggesting a

quality issue with this sample and it was removed from further analysis. We divided the remaining samples into 16p11.2 CNV class (deletion, duplication, non-carrier) and family member (mother, father, proband, sibling) and compared the groups (**Table S21**). We tested if the distribution of the number of variants per individual were different amongst the groups and found no significant differences using both the Kolmogorov-Smirnov test with continuity correction as well as the Mann-Whitney U test, and observed no statistically significant differences between groups (**Table S22**).

Among this group, we filtered for those genes already associated with autism from a list of compiled variants (SFARI list). A total of 13 inherited deleterious variants intersected with SFARI list genes (7 deletion, 6 duplication probands; **Table 4**). We plotted the positions of these individuals on the plot of diagnoses vs. FSIQ and noted that several fall in the extremes (**Figure S5**). In particular, three of these genes that have particularly strong evidence for involvement in autism and these individuals have amongst the lowest FSIQs and highest number of diagnoses in the cohort. We additionally subsampled 120 non-affected siblings from the Simons Simplex Collection (SSC) 10,000 times, and found that 16p11.2 probands had fewer autism associated genes hit in every simulation. As a group the individuals with an additional hit in a SFARI gene trend towards being more severely affected on the basis of FSIQ (p=0.19, Mann Whitney-U).

Table 4: SFARI genes hit in probands from exome data.

Sample	Chrom	Pos	Ref	Alt	Sex	Gene	functionGVS	16p Status	16p Inheritance	Diagnoses	FSIQ	Exac AF	CADD	RVIS
14840.x22	3	97198170	CAGAAG	C	male	*EPHA6*	frameshift	deletion	de novo	6	67	0.0000111	35	13.15
14796.x3	3	121341713	CA	C	male	*FBXO40*	frameshift	deletion	de novo	6	59	0	33	12.57
14893.x7	5	112487005	C	A	male	*MCC*	splice-donor	deletion	de novo	3	86	0	25.4	4.04
14863.x7	7	117351832	A	AC	male	*CTTNBP2*	frameshift	deletion	de novo	0	112	0.00004408	35	3.9
14913.x1	9	131708380	ACT	A	male	*DOLK*	frameshift	deletion	de novo	5	82	0	34	11.18
14710.x7	18	19353656	TA	T	male	*MIB1*	frameshift	deletion	inherited	1	86	0	35	4.1
14755.x17	18	19429348	A	AG	female	*MIB1*	frameshift-near-splice	deletion	inherited	2	75	0	35	4.1
14787.x4	7	100282160	GC	G	male	*GIGYF1*	frameshift	duplication	inherited	3	52	0	25.2	2.75
14922.x3	10	116880023	T	C	male	*ATRNL1*	coding-unknown	duplication	inherited	2	86	0	26.8	3.07
14788.x5	15	81571214	GC	G	male	*IL16*	frameshift	duplication	inherited	5	39	0.00001108	35	47.8
14705.x16	16	76389356	T	C	female	*CNTNAP4*	coding-unknown	duplication	inherited	2	35	0.00003306	27.4	36.37
14723.x17	22	21349212	GA	G	male	*LZTR1*	frameshift	duplication	inherited	1	114	0	35	0.73
14967.x25	22	50900874	TCC	T	male	*SBF1*	frameshift	duplication	inherited	4	28	0	33	0.17

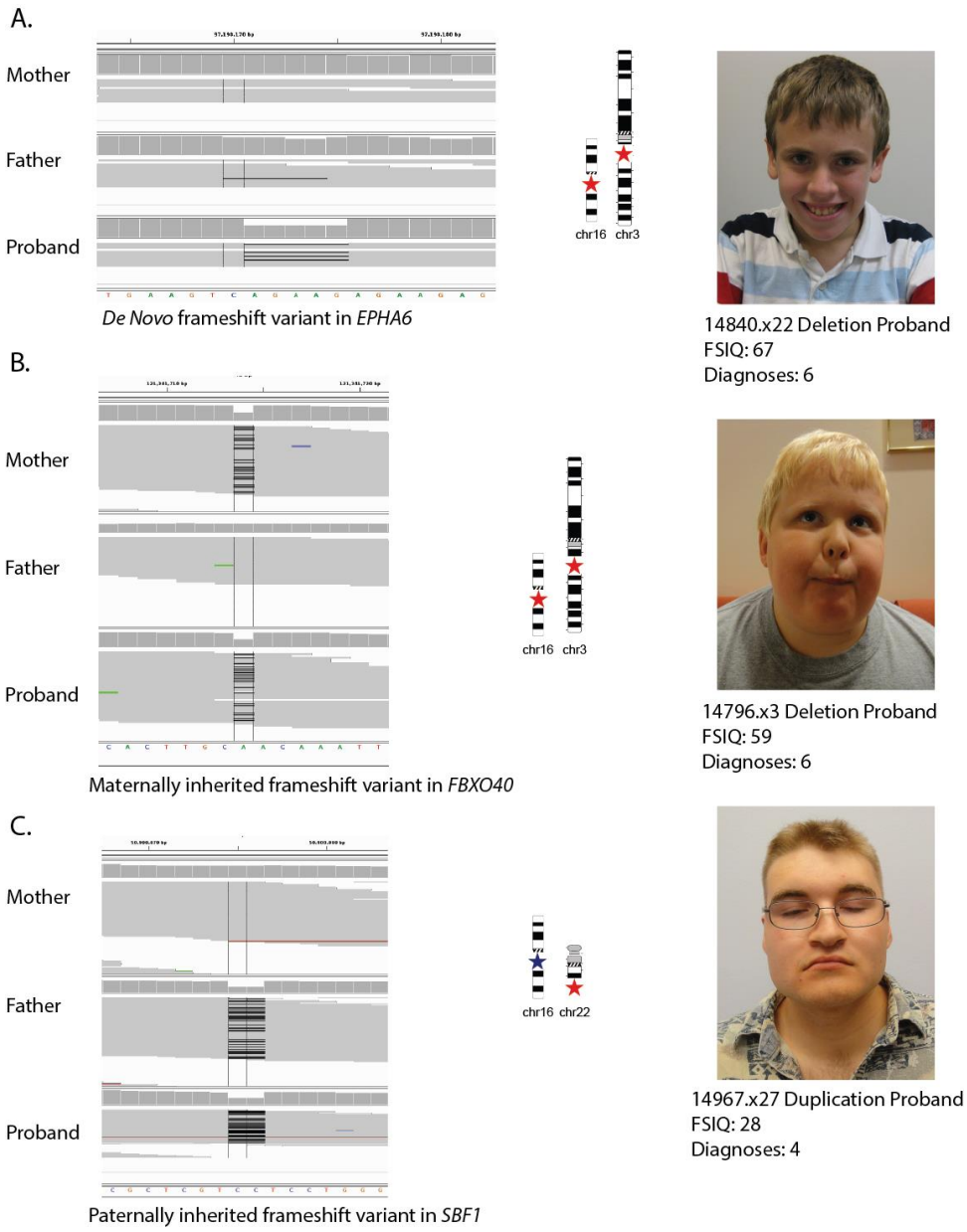

Figure 3.5: Likely gene disruptive variants in autism associated genes. a. This *de novo* 16p11.2 deletion proband with an FSIQ of 67 and 6 additional diagnoses including anxiety OCD phobia, behavior disorder, clinical ASD, coordination disorder, and enuresis disorder has a rare frameshift variant in the ephrin receptor gene *EPHA6*. b. This *de novo* 16p11.2 deletion proband has an FSIQ of 59 and 6 additional diagnoses including attention deficit hyperactivity disorder (ADHD), articulation disorder, clinical ASD, coordination disorder, intellectual disability, and Tourette's disorder as well as a private maternally inherited frameshift variant in the gene *FBXO40*. c. This maternally inherited duplication proband has an FSIQ of 28 and 4 additional diagnoses including clinical ASD, coordination disorder, intellectual disability, and anxiety, OCD, and phobia as well as a paternally inherited frameshift variant in the *SBF1* gene. These individuals have some of the most severe phenotypes in the cohort.

De novo male deletion proband 14840.x22, for example, has an FSIQ of 67 and 6 additional diagnosis including anxiety OCD phobia, behavior disorder, clinical ASD, coordination disorder, and enuresis disorder as well as a frameshift variant in the ephrin receptor gene *EPHA6* (**Figure 3.5a**). This variant is rare, found in less than 2 in 45,000 individuals ascertained from the Exac database. While this variant is not found in the father, the mother did not have sufficient coverage to make a variant call, but the variant appears *de novo*. Rare copy number variants in this gene have been found in individuals with autism[93,94], the gene is a candidate for susceptibility to schizophrenia[95], the gene is differentially expressed in Angelman syndrome mice[96], and genetic inhibition of the gene in mice produce behavioral deficits in learning and memory[97]. Interestingly, this individual also has a paternally inherited duplication affecting the gene *CACNA2D3* which has been previously associated with autism[91].

De novo male deletion proband 14796.x3 has an FSIQ of 59 and 6 additional diagnoses including attention deficit hyperactivity disorder (ADHD), articulation disorder, clinical ASD, coordination disorder, intellectual disability, and Tourette's disorder as well as a maternally inherited frameshift variant in the gene *FBXO40* private in the cohort and not found in the Exac database (**Figure 3.5b**). In autism individuals, CNVs were statistically enriched in this gene that were not observed in controls[98], and a rare variant in this gene has been identified in two individuals with ASD[99]. This individual did not have any additional rare CNVs disrupting genes associated with neurogenic disorders.

Maternally inherited male duplication proband 14967.x25 has an FSIQ of 28 and 4 additional diagnoses including clinical ASD, coordination disorder, intellectual disability, and anxiety, OCD, and phobia as well as a paternally inherited frameshift variant in the Set-Binding Factor 1 gene, *SBF1* that is private both in the cohort and not found in over 45,000 individuals from the

Exac database (**Figure 3.5c**). *De novo* and rare inherited missense variants in this gene have been found in exome sequencing studies of autism individuals and individuals with neurogenic disorders[3,66,100,101]. Homozygous variants in this gene are also associated with Charcot-Marie-Tooth disease, type 4B3[102,103] (Omim 615284). This individual did not have any additional rare CNVs disrupting genes associated with neurogenic disorders.

We additionally used the exome data, annotated using the same methods as for the MIP resequencing data, in order to validate and compare our MIP resequencing results for the critical region genes (**Table S23**). In particular, we compared variants found in probands in <0.1% frequency in Exac, and private in the cohort. In samples assessed by both exome and MIP resequencing (111 probands), we called 24 variants from the exome and 22 from the MIP resequencing study. Of the 46 total variants called, 34 were shared, 7 were called only from the exome, and 5 only from resequencing. In order to determine where the 12 variants called using only one method came from, we assessed the raw read data. In 11/12 cases, the variant had been filtered, typically for low coverage.

3.4.6 Selection analysis

Based on the heterozygosity and Tajima's D analysis we find that the critical region shows signatures of selection. In particular, the critical region lies in the lowest 2% of 550kbp regions for average heterozygosity genome-wide (**Figure S6**) and in the lowest 3% of Tajima's D windows genome-wide (**Figure S7**). This is in contrast to the flanking 550kbp telomeric flanking region which lies in the 50th percentile for Tajima's D and 61st percentile for observed average heterozygosity, respectively.

Using smaller 10kbp windows across the critical region itself for both Tajima's D and average heterozygosity (**Figure 3.6**), we notice that a cluster of windows containing the genes *KIF22*, *MAZ*, *PRRT2*, *MVP*, *CDIPT*, and *SEZ6l2* all are in windows of genome-wide significant. Another cluster of windows reaches significance, though is less striking, containing the gene *ALDOA*.

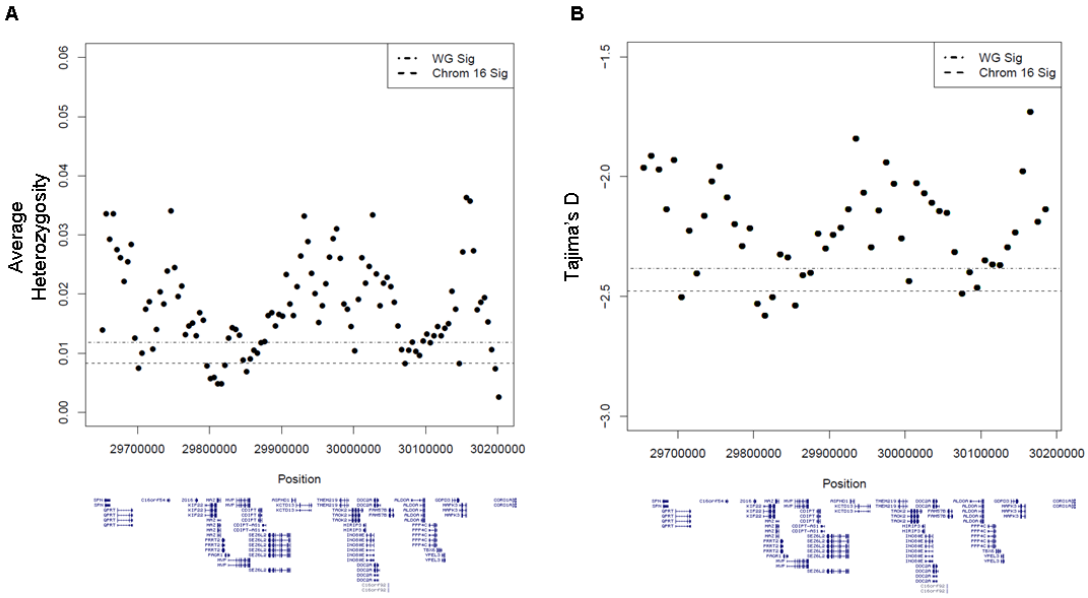

Figure 3.6. Signatures of selection across the 16p11.2 critical region. (a) The average heterozygosity in 10kbp windows (5kbp step) and (b) Tajima's D in 10kbp windows (10kbp step) across the critical region. Dashed lines indicate the levels below which windows fall in the lowest 5th percentile of similarly sized windows genome-wide or on chromosome 16 only. There appear to be two distinct regions of conservation.

3.5 Discussion

Our results demonstrate a trend towards lower SNV burden in probands when compared to non-carrier parents. Such a reduction in variation could result from a lower *in utero* survivability of individuals with a 16p11.2 CNV and additional deleterious variants in the critical region. A diagnostic study screening 194 individuals with ASDs for CNVs and candidate genes located in inherited deletions found that most CNVs contribute to ASDs in association with other CNVs or point variants located elsewhere in the genome, not in the hemizygous region[104], supporting this

hypothesis. From population estimates, the 16p11.2 CNV occurs in ~0.05% of the population[30], a rate high enough that the CNV itself may act as a sieve for genetic variation in this region. The concept of a "monoploid" sieve has been developed in plants, where the presence of lethal or deleterious alleles in the monoploid region prevents regeneration[105].

Analysis of 2,500 individuals from the 1000 Genomes Project suggests that the 16p11.2 critical region is under selection, as its Tajima's D and average heterozygosity values lie in the lowest 3% of similarly sized regions genome-wide (**Figures S6 and S7**). A refined analysis of 10kbp windows across the critical region revealed two clusters of genes which lie in the lowest 5% of such windows for both Tajima's D and average heterozygosity (**Figure 3.6**) including *KIF22, MAZ, PRRT2, MVP, CDIPT, SEZ6L2* and *ALDOA*. Of these *KIF22* is associated with skeletal dysplasia and joint laxity[106], *PRRT2* is a key component of calcium neurotransmitter machinery[107], and has been associated with epilepsy[108] and paroxysmal diseases[109], and *MVP* potentially play a role in autism[110] and higher copy number has been linked to chemotherapy resistant cancers[111]. As no one critical region gene has come to significance in exome sequencing studies of large numbers of individuals with autism[3,3–5], and no focal deletions have been found to associate with particular phenotypes it is likely that dosage imbalance of the 27 critical region genes, or a subset thereof, leads to the observed clinical phenotype.

We found no loss of function variants in probands in critical region genes and the probands with a severe (CADD>20) missense variant did not have a more severe phenotype as assessed by FSIQ and number of diagnoses. One explanation is that a LGD variant on the background of a 16p11.2 CNV is non-viable. Of the severe variants discovered among probands with a 16p11.2 duplication, all occurred in a single copy. It remains to be seen if deleterious variants existing on multiple copies exist and what phenotype impact they have.

Analysis of exome resequencing data from the Simons VIP identifies 13 probands with a LGD variant in a gene that has a prior for involvement in autism and/or intellectual disability. Of these 13 individuals, 8 have 3 or more diagnoses and/or an FSIQ less than 70, suggesting that additional rare, exonic variation outside of the critical region contributes to the severity of phenotype (**Figure S5**). These individuals trend towards being more severely affected on the basis of FSIQ compared to the population of probands. Interestingly, 16p11.2 carriers tend to have fewer variants in autism associated genes than controls, suggesting that such variation is particularly damaging in the background of a 16p11.2 CNV. A comparison of critical region MIP resequencing data and critical region exome sequencing data showed good agreement, with the variants missed using either approach over 90% of the time due to low coverage.

The three genes lying in segmental duplications flanking the critical region, *BOLA2*, *SLX1A*, and *SULT1A3* are not well-covered by exome sequencing and hence diversity in these genes has not been assessed. In the 16p11.2 cohort, we observe no likely gene-disruptive events in probands and those probands carrying a severe missense variant (CADD>25) do not have more severe phenotypes on the basis of FSIQ and number of diagnoses (**Figure S2**) suggesting that severe variation in these genes has the potential to affect phenotype. We observe no correlation between copy number of these genes and phenotype severity, however, it is possible that a deleterious variant present in an individual with low copy number of these genes may have a more severe clinical presentation than an individual with a higher copy number. The severe variants that we discovered almost always exist on a single copy, suggesting a recent origin.

To gain a sense of natural variation in the three duplicated genes, we resequenced the exons of these genes in over 8,000 autism and intellectual disability cases and over 2,000 controls. The presence of LGD variants suggests that loss of a single genic copy is not lethal. While we do not

observe a statistically significant difference in the number of LGD variants between cases and controls in *BOLA2*, a bonafide *Homo sapiens* specific duplicated gene, it is interesting that LGD variants only are found in cases.

BOLA2, *SLX1A* and *SULT1A3* lie in a region of high diversity in the human and great ape lineages. Of particular interest, *BOLA2* and putatively *SLX1A* exist in a higher copy number state than all other great apes as well as the ancient hominins Neanderthal and Denisova. Moreover, these genes lie in sequence that is specifically duplicated in *Homo sapiens*.[38] While the function of *BOLA2* is not specifically known, there is evidence that it plays a role in cell cycle signaling and in the formation of iron-sulfur complexes,[112] helping to control the redox state of the cell.[113] The higher copy number state of *BOLA2* could potentially be important in the developing human brain, as the human brain experiences greater oxidative stress during development than does chimpanzee.[114] Strikingly, we find that 16p11.2 deletion individuals with the lowest copy number (copy number 3) are enriched for anemia, suggesting that *BOLA2* has an effect in a hematological pathway. If replicated, low *BOLA2* copy number is a definite modifier of the 16p11.2 phenotype, and one of the only genetic variants known that increases susceptibility to anemia.

The function of *SLX1A* is better known. Through interaction with the protein SLX4, SLX1 functions as an important regulator of genome stability, acting as an endonuclease against replication forks, 5' loops and resolving Holliday junctions into linear duplex products.[115–120] Furthermore, there is evidence that SLX1 catalyzes nucleolytic resolution of telomere DNA structures, suggesting a role in telomere homeostasis and may contribute to genome stability in humans.[121–123]

Interestingly, the 5-prime UTR of *BOLA2* and the 5-prime UTR and first translated exon of *SLX1A* overlap, as the two genes are transcribed from opposing strands and they presumably share a promoter (**Figure S8**). Hence, even if the complete *SLX1A* gene is not specifically duplicated in *Homo sapiens*, the first exon which contains the first 64 amino acids and the active site of the GIY-YIG nuclease domain[124] is. Given that maintenance of telomeres as well as oxidative stress are important in the aging process, *BOLA2* and *SLX1A* may contribute to the longer lifespan of humans compared to great apes. There is also evidence that oxidative stress may be important in the pathogenesis of certain subtypes of autism.[125]

Based on our analysis of allele balance in the population, we infer that most variants are present in a single copy of *BOLA2* or *SLX1A* (**Figure 3.3**). However, we do observe variants in some transcripts that are frequent in the population. This is particularly the case with *SLX1A*, where a subset of events is found in nearly all individuals, suggesting the presence of paralogous sequence variants. Interestingly there is a relative dearth of private synonymous variation when compared to missense and LGD variants (**Table S11**). Also, the majority of the sites of variation in *SLX1A* lie in exon 3, which is not present in the shorter transcript NM_001015000.2.

While *SULT1A3* lies in the region of segmental duplication and shares its copy number with *BOLA2* and *SLX1A*, the gene itself is not part of a *Homo sapiens* specific duplication. Furthermore, the cytosolic sulfotransferases, of which *SULT1A3* is a member, share a high degree of identity, which can render mapping variation to the correct gene challenging. There are 14 genes in the family of cytosolic sulfotransferases (**Table S15**). The identity of the genes in this family is high; for example there is >93% identity between the SULT1A paralogs[126]. The 4 SULT1A genes lie at 16p a subfamily of the cytosolic sulfotransferases which likely originated as a result of duplication and recombination.

SULT1A3, a cytosolic sulfotransferase, catalyzes the sulfation of dopamine, other catecholamines, and structurally related drugs which is significant in that over 95% of the circulating dopamine and approximately 70% of the surface norepinephrine is sulfate-conjugated[126,127]. Within the SULT1A subfamily, SULT1A1 favors simple phenolic substrates like p-nitrophenol where SULT1A3 prefers monoamine substrates like dopamine[128]. Despite >93% sequence identity, these enzymes have remarkable substrate specificity. Structural studies have shown that residues 84-89 and 143-148 play important roles in stereoselectivity and sulfating activity[129]. In particular residue Glu146 in SULT1A3 can form electrostatic interaction with dopamine and could play a role in stereoseletivity and sulfating activity[128,130] and Asp86 appears to be critical to the Mn^{2+}-stimulation of the Dopa/tyrosine-sulfating activity[130]. In SULT1A3, three residues are acidic instead of hydrophobic as in SULT1A1, which results in a more negatively charged binding pocket that can better interact with the amino group of catecholamines. In the entire family of sulfotransferases, SULT1A3 is the only one that can efficiently bind dopamine[129].

While the role of SULT1A3 in the gut is in the pre-systemic elimination of dietary catecholamines[131] the identification of SULT1A3 in the brain, including the dopaminergic regions of the midbrain[132] suggests that it has a role in eliminating dopamine in the brain as well. To better understand the specific function of SULT1A3 in neuron-like cells, Sidharthan *et al.* performed a series of assays and showed that (1) dopamine induces SULT1A3 via a dopamine D1-NMDA receptor-coupled mechanism and (2) that induction of SULT1A3 significantly protects cells from dopamine neurotoxicity[133]. Furthermore, the genotype-tissue expression dataset (GTEx), shows that *SULT1A3* is preferentially expressed in the brain (cerebellar hemisphere, and cerebellum) and in the small intestine (terminal illium) (**Figure S9**). Through

SULT1A3, dopamine can induce its own metabolism and protect neuron-like cells from damage, suggesting that reduced SULT1A3 activity could be a risk factor for dopamine-dependent neurodegenerative disease and other dopamine influence disorders such as ADHD and schizophrenia.

Strikingly, SULT1A3 appears specific to primates as no ortholog has been identified in nonprimate species. Furthermore, several researchers have speculated that evolutionary pressure from a greater catecholamine demand in primates may be responsible for its emergence[80,134–136]. We can hypothesize that *SULT1A3* copy number might be a risk factor in catecholamine-induced neurodegenerative disease as enhanced extracellular dopamine can lead to increased cytosolic oxidative stress that can lead to long-lasting neuronal damage.

Our sequence analysis indicates a >95% sequence identity between *SULT1A3* and *SULT1A1* and *SULT1A2* and a >42% sequence identity between the other members of the gene family (**Table S15**). Six sites corresponding to four residues (44, 84, 89, 144), uniquely distinguish *SULT1A3* from all other members of the SULT family (**Tables S15, S24**). Three of these residues (84, 89, 144) have been implicated in determining the substrate specificity of *SULT1A3*. If we compare SULT1A3 to SULT1A1 and SULT1A2, we identify 19 codons that distinguish SULT1A3 (**Table S24**). Unsurprisingly, these include 4 out of the 6 residues from region 84-89 and 4 out of the 6 residues from region 143-148, which are known to be important in determining the substrate specificity of *SULT1A3*.

In *SULT1A3*, we observe 14 LGD variants of which 2 are private and only found in controls. Furthermore, we did not observe any statistically significant differences between cases and controls, even when restricting to private or likely damaging events based on CADD score (**Table S13 and Figure S2**).

Overall, variation does exist across the genes *BOLA2*, *SLX1A*, and *SULT1A3* and the majority of such variation is rare (<0.1% of samples) or private and exists in only one copy of the locus. Future studies must incorporate a method to assess the absolute copy number in each individual in order to better assess variant rates and more sophisticated variant models.

Our results demonstrate that critical region copy number is viable in numbers greater than 3 (duplication) and that critical region copy number can both expand and contract. In triplication family 14752, for example, the grandmother has two copies of the critical region, the mother three copies (duplication) and the proband four copies (triplication) (**Figure 3.4**). That both these expansions occurred via an intrachromosomal mechanism and a shared critical region haplotype between grandparents suggests that duplication may occur preferentially by intrachromosomal mechanism on select haplotypes. Similarly, we observe a contraction from a mother with copy number 5 (quadruplication) to a proband with copy number 3 (duplication) (**Figure S4**). Such heterogeneity in copy number of the critical region shows that this region is dynamic and susceptible to change.

There are several limitations of our work. First, targeted resequencing using MIPs is not perfect, and not all bases are adequately captured. However, this technique allows sequencing of regions, including regions not targeted by traditional exome capture that have eluded sequencing. Second, assigning variants is challenging in duplicated space. For *BOLA2* and *SLX1A* we know variants map to these genes, however we do not know to which copy. We can use allele balance and copy number estimates to determine in how many copies a variant exists. The SULT genes, however, are highly identical. Hence variants that we discovered in *SULT1A3* may map to another member of this family. Third, we did not recall the publically available exome sequencing data, relying on the original researcher's calls. We could lose variants in this way.

Our results show a relative dearth of variation across the 16p11.2 critical region unique and duplicated genes. The duplicated genes had not been assessed and we provide a resource to understand variation across these genes and provide a model for how, moving forward, variation should be assessed in such genes. We find loss of function variants in genes with a prior for autism outside of the critical region, suggesting that such variation is important in determining phenotype outcome. The presence of additional risk factors discovered by either sequencing or diagnostic microarray will be important for projecting the disease trajectory and the diverse outcomes associated with this pathogenic CNV.

4. Exome sequencing of a local cohort reveals genes implicated in neurocognitive disorders and high-functioning autism

This chapter has not been published. Evan Eichler and I designed the study. Raphe Bernier and I selected the samples. The Northwest Genomics Center and Center for Mendelian Genetics performed library preparation and sequencing experiments and provided unfiltered GATK variant calls. Carl Baker and I performed PCR validations. I performed all analyses and wrote this section.

4.1 Summary

Autism spectrum disorders are characterized by phenotypic heterogeneity and genetic locus heterogeneity. We assess a locally collected cohort of 42 families with an autism spectrum disorder (ASD) of which 29 have an individual with high functioning autism. We find *de novo* and rare inherited variants in novel autism candidate genes, including *LPHN1* and *NUMBL* as well as variants in autism associated genes, such as *CLSTN3* and *POGZ*. The presence of multiplex families allows inference of variants, such as an LGD variant transmitted from affected father to son in *DNM1L*, as responsible for a high functioning ASD phenotype. In high functioning families, we observe a higher rare inherited variant burden ($p<0.007$) when compared with individuals who have autism with intellectual disability. We also find evidence for enrichment in the actin genes in high functioning autism families ($p=2.51x10^{-2}$). Our results confirm the extreme locus heterogeneity associated with the ASDs, and show progress towards defining genetic characteristics of autism in the absence of intellectual disability.

4.2 Introduction

The autism spectrum disorders (ASDs) are among the most common mental health disorders, affecting an approximate 1 in 68 school-aged children[137] and are characterized by persistent difficulties in social communication and interaction and restricted and repetitive patterns of behavior, interests, or activities[138]. The ASDs have a large heterogeneity in clinical presentation

and additional diagnoses can include intellectual disability, seizures, and attention deficit hyperactivity disorder (ADHD). Despite this phenotypic heterogeneity twin studies have estimated a genetic contribution to the disorder of 40-90%[139,140]. Array and exome sequencing studies of thousands of autism families have revealed extreme locus heterogeneity of the disorder[5,59,66,141–143] and more than 30 genes are now implicated in the etiology of autism[144]. Analysis of individuals with variants in the same gene has revealed clinical presentations and co-morbidities more consistent with one another, than with the autism population as a whole[33].

Despite the discovery of recurrent likely gene disruptive (LGD) variants in autism cases, much of the etiology of the ASDs remains unknown. Studies have shown the importance of inherited and missense variation[145] and multiple variants may be necessary to lead to a clinically ascertainable phenotype[24]. The majority of LGD variants are associated with severe phenotypes, and the genetic factors leading to autism without intellectual disability are largely unknown.

Over the past six years, a collection of over 400 families with autism, ID, and other communication disorders was assembled at the University of Washington, with clinical data and DNA samples available. The goal of this study was two-fold: (1) To assess rare *de novo* and inherited variation in multiplex and high functioning autism (HFA) families; (2) To determine if there are particular genes involved in autism without intellectual disability.

4.3 Subjects and methods

4.3.1 Samples

DNA samples were derived from peripheral blood obtained from 148 individuals from 42 families as part of the Serial Analysis of Gene Expression (SAGE) project at the University of Washington. Diagnoses included autism spectrum disorder (ASD), developmental delay (DD),

and intellectual disability (ID). Of the families assessed, 26 were multiplex, 29 had at least one high functioning individual as defined by a DSM-IV-TR diagnosis of Asperger's or autism with no diagnosis of intellectual disability, and all were of European Ancestry (**Table S1**). Study participants were ascertained in three ways: (1) The Seattle Children's Hospital Autism Center Clinic Registry, which consists of families who expressed interest in participating in research, (2) Seattle area listservs for families with ASD, DD, or ID, including listservs pertaining to Autism Speaks, Parent to Parent (P2P), The Arc, FEAT, and others. (3) Providers who work with individuals with ASD, DD or ID.

We additionally assessed four subsets of high functioning individuals from the Simons Simplex Collection (SSC)[40]. *Subset 1* consists of individual who have a diagnosis of high functioning autism (HFA) as defined by any one of the following: (1) A collaborative programs of excellence in autism (CPEA) diagnosis of Asperger's Syndrome[146] (**Table S2)**; (2) A clinician assessment of high functioning autism or Asperger's syndrome, with a certainty score of 4 or 5 (on a scale of 1 to 5, where 1 is highly certain and 5 is completely certain), even if the proband did not meet strict DSM-IV criteria. *Subset 2* are probands with a full scale intelligence quotient (FSIQ) > 100 (**Table S3**). *Subset 3* are probands with FSIQ<70. *Subset 4* consists of all sequenced siblings. For the first two subsets we filtered out any individuals with an FSIQ<80 or with an additional DSM-IV axis I or axis II diagnosis or diagnosis reported with an International Statistical Classification of Diseases and Related Health Problems 9th revision (ICD-9) code.

All procedures for clinical assessment and blood extraction were approved by the institutional review boards (IRBs) of participating institutions, and informed consent was obtained for participation in this research.

4.3.2 Phenotypic assessment

For the SAGE cohort, psychiatric and neurodevelopmental conditions were diagnosed by experienced, licensed clinicians following DSM-IV-TR criteria[31] using all available information, including clinical observation, caregiver history, and records review. Pedigrees were obtained from family interview and formal diagnosis was assessed after a clinical visit. An individual was determined to have high functioning autism by review of clinical information, if available, and/or pedigree review from a clinical visit.

As part of participation in the Simons SSC[40], standardized assessments, including psychiatric, neurocognitive, behavioral, motor, and neurologic evaluation, were conducted at 12 Simons SSC clinical sites along with collection of a detailed medical history through interview and medical records review for each participant. Psychiatric and neurodevelopmental conditions were diagnosed by experienced, licensed clinicians following DSM-IV-TR criteria[31] using all available information, including clinical observation, caregiver history, and records review. Diagnostic foci included: ASD, attention deficit hyperactivity disorder (ADHD), communication disorders, anxiety disorders, mood disorders, intellectual disability, tic disorders, elimination disorders, learning disorders, and behavioral disorders, totaling 27 diagnostic codes. Full-scale intelligence quotient (FSIQ) was determined by the developmentally appropriate cognitive measure (Mullen Scales of Early Learning[52]), the Differential Abilities Scale, Second Edition[53], or the Wechsler Abbreviated Scales of Intelligence[54]. We used the version 15 release of the SSC phenotype data.

4.3.3 Variant detection from exome sequencing

SAGE:

We selected 42 families from the SAGE cohort on which to perform exome sequencing (**Table S1**). These families were: (1) multiplex or had an individual with high functioning autism (HFA) and; (2) did not contain a >100 kbp rare CNV (present in <0.1% of controls). Genomic DNA was derived from whole blood and exomes for the 42 families (148 individuals) were captured with NimbleGen EZ Exome V2.0. Reads were mapped to human genome reference assembly GRCh37 (hg19) with decoy sequence using bwa-mem version 1.46, and variants were called on all samples together using GATK 3.2 haplotype caller (multisample calling). We required the following filters: (1) Passing records only; (2) depth<10; (3) QUAL<10; (4) dbSNP excluding sites after release 129; (5) Mills and 1000 genomes gold standard indels; (6) Variants lying in segmental duplications or tandem repeats; (7) SNPs >1% frequency in dbSNP 144; (8) homopolymer repeats. We assessed only the autosomes of these individuals. After filtration we broke multiallelic records into single entries and annotated discovered variants with Seattle Seq 137. If multiple transcripts were present, we chose the most severe annotation. We annotated each variant with v1.3 of the CADD score[85] and with a frequency from the Exac database (%ExAC_0.05%, ftp://ftp.broadinstitute.org/pub/ExAC_release/release0.3/subsets/ExAC.r0.3.nonpsych.sites.vcf.gz)., and each gene for presence in a list of genes associated with autism (SFARI gene list, https://gene.sfari.org/, Accessed 1 April 2016), and the Residual Variation Intolerance Score (RVIS, release v3_12Mar16).[90] We determined putative inheritance for each variant using the called genotype and performed Sanger sequencing on a subset of variants called *de novo* and a subset of potentially impactful variants (**Tables S4 and S5**). We utilized the exome sequencing

read-depth data in order to call putative CNVs as previously described with the program CoNIFER[147].

SSC:

For the Simons Simplex Collection (SSC) samples, we used the SNV and indel call sets from a complete reanalysis of the Simons Simplex Collection[148]. We annotated this dataset with the v1.3 CADD scores, Exac allele frequency, RVIS scores, and the SFARI gene list.

4.3.4 Network and enrichment analysis

We used the Panther database[149] to perform pathway analyses and statistical overrepresentation tests. We used stringdb[150] to visualize gene networks.

4.4 Results

We focused on severe private inherited and *de novo* variation in the SAGE cohort; variants that were private to a family, not found in the Exac database, and had a RVIS Score of <50. For missense variants we also required a CADD score>30 (**Table S6**). We used the same filters for the SSC cohort subsets analyzed. In total we identified 138 variants in probands and 59 variants in siblings meeting these criteria. These included 6 variants in probands and 4 in siblings hitting genes with a prior for autism based on the SFARI gene list. There were 131 variants in probands for +59hich perfect inheritance information was available which included 4 *de novo* (3%), 59 paternal (45%) and 68 maternal (52%) events. In siblings, there were 55 variants for which perfect inheritance information was available which included 5 *de novo* (9%), 24 paternal (44%), and 26 maternal (47%) events.

Among the 86 variants in probands with high functioning autism with perfect inheritance information, we observe 1 *de novo* (1%), 40 paternal (47%), and 45 maternal (52%) events. Among the 10 variants in siblings with high functioning autism, we observe 4 maternal, 5 paternal, and 1 *de novo* event.

For the 215 variants for which we have inheritance information (even if only from one parent), we observe a median of 3 severe variants per individual and observe the same for the high functioning individuals (**Table S7**).

4.4.1 *De novo* variation

We observe a total of 26 coding *de novo* variants in probands (8 LGD, 18 missense) with one missense variant with CADD>30. Among the high functioning individuals, we observe a total of 12 *de novo* variants (2 LGD, 10 missense), and none of the missense variants have a CADD score >30. We attempted validation of 32 *de novo* events. Of these, we validated 30 and invalidated 2 private *de novo* LGD variants (**Table S5**). Among the *de novo* variants discovered were several with a prior for involvement in neuropsychiatric disorders, including variants in *THBS1, LACTB, NSUN2, LPHN1, POGZ, NUMBL,* and *CLSTN3* (**Figure 4.1**).

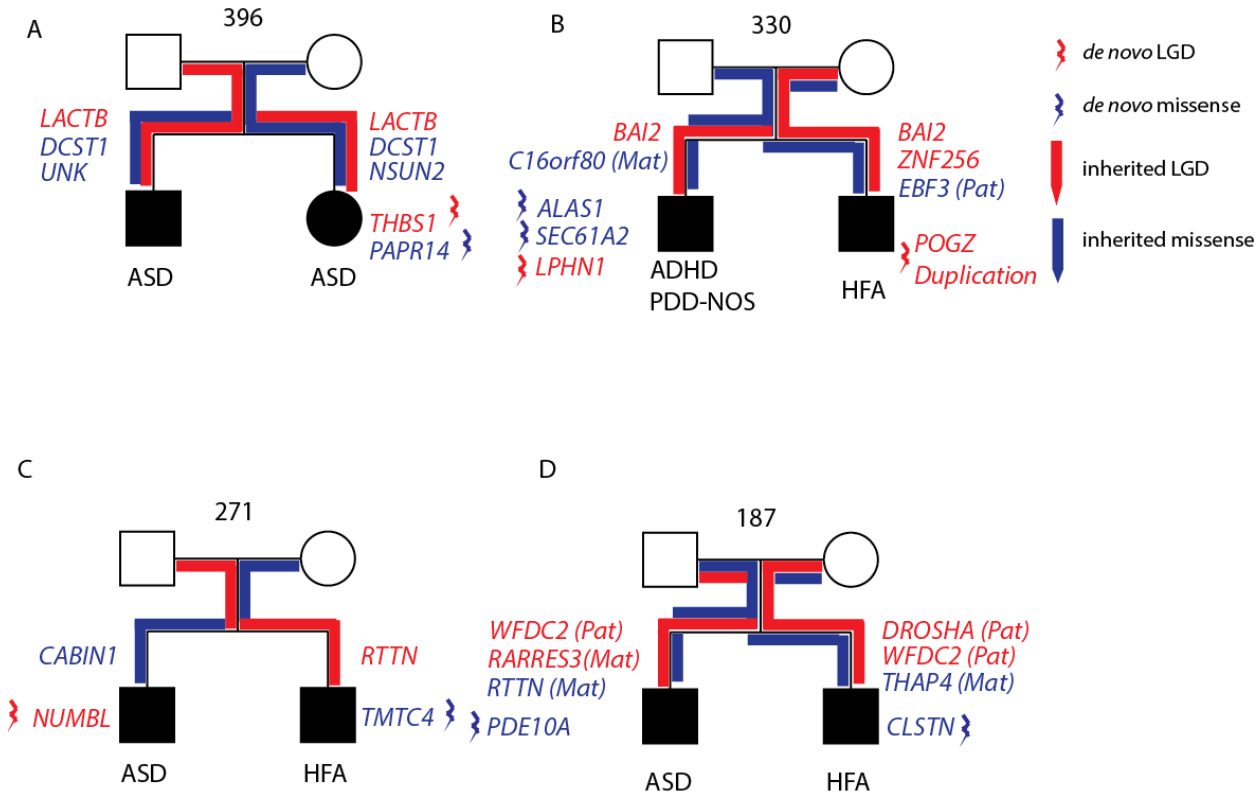

Figure 4.1: Families with *de novo* severe variants in autism and neurocognitive associated genes. a. We validated a *de novo* stop-gain variant in exon 18 of 22 of the thrombospondin I gene (*THBS1*) in female sibling of family 396 who has a diagnosis of autism with a mixed receptive-expressive disorder. Thrombospondin I is an adhesive glycoprotein that mediates cell-to-cell and cell-to-matrix interactions and has a role in synaptogenesis in the developing brain. b. We validated a *de novo* stop-gain variant in exon 2 of 24 of the Latrophillin-1 (*ADGRL1/LPHN1*) gene found in a male proband with a diagnosis of ADHD and PDD-NOS. Latrophillin-1 is a neuronal receptor of α-latrotoxin, that is implicated in neurotransmitter release and control of presynaptic Ca^{2+}. c. We validated a *de novo* stop-gain variant in exon 7 of 10 of the numb homolog (Drosophil)-like (*NUMBL*) found in the proband of family 271with autism and slow to develop language skills. NUMBL, the numb homolog (Drosophil)-like, can directly bind and inhibit the Notch1 intracellular domain, and hence plays an essential role in neural cell fate determination. d. We discovered and validated a private *de novo* missense variant ILE -> THR in exon 5 of 18 of the calsyntenin-3 gene (*CLSTN3*) in cadherin domain of the male high functioning autism sibling of family 187. Calsyntenin-3, is an autism candidate gene and promotes excitatory and inhibitory synapse development. While the identified variant is likely pathogenic, other rare variants shown could also contribute to the pathogenicity.

4.4.2 Variants shared between siblings

Because the quads and quint in this study have at least two affected offspring, shared variants have a higher prior probability of contributing to the observed disorder. Because we are not focusing on somatic variants, we removed monozygotic twins from this analysis. Among the 21

families, we observe 35 private severe variants that are shared between two or more offspring in the same family. This includes 0 *de novo* (as expected), 14 LGD, and 21 severe missense variants (**Table S7**). Among the private LGD and severe missense variants there are several that have been implicated in autism or neurodegeneration as defined as being on the SFARI list of autism genes, having an OMIM ID related to a neurocognitive process, or have functional literature relating to neuronal processes. These include *LEMD3, LACTB, BBS5*, and *JMJD1C*.

4.4.3 Inherited cases

For several of the families, there is a history of neuropsychiatric disease on the maternal or paternal side. In some cases, the parent is diagnosed with a neuropsychiatric disorder, for example in family 258 an LGD variant in *DNM1L* is transmitted from affected father (father has high-functioning autism), in family 329 a missense variant in *NCOR* is transmitted from affected mother (mother has anxiety issues, father has social challenges), and in family 406 a LGD variant in *NGDN* is transmitted from the mother (mother has ADHD) (**Figure 4.2**).

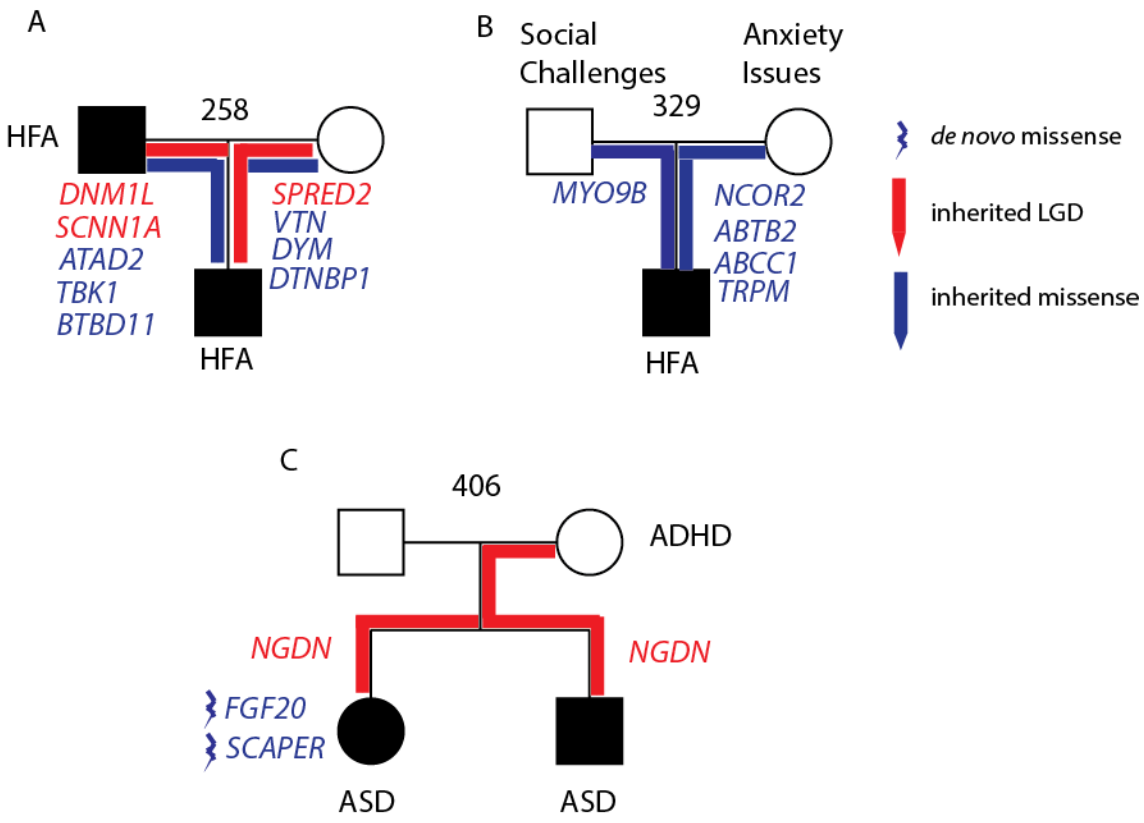

Figure 4.2: Mendelian candidates for pathogenicity. In three families, a likely pathogenic variant segregates with phenotype from parent to child. In family 258 (a) we validated a LGD variant in *DMN1L* that segregates from the father with high functioning autism to the son with the same diagnosis. *DNM1L* codes for the dynamin-like protein 1, is associated with autosomal dominant encephalopathy, plays an important role in the division of the growing mitochondria and peroxisomes, and is associated with autism. In family 329 (b), there is a severe maternally transmitted missense variant in *NCOR*, the nuclear receptor corepressor. Genes associated with the NCOR/HDAC3 complex have been implicated in autism. In family 406 (c) the proband and the sibling *both* have ASD diagnoses and the mother has an ADHD diagnosis, we discovered a frameshift variant transmitted to both sequenced offspring in the gene neuroguidin (*NGDN)*. Neuroguidin is a eukaryotic initiation factor 4E binding protein and associated with the fragile X mental retardation protein (FMRP).

4.4.4 SAGE high functioning autism cases

We next restricted our analysis to look specifically at the 29 families in our cohort with a diagnosis of high functioning autism. Several variants in this cohort are associated with neurocognitive disorders. For example, among the *de novo* variants, we discovered a stop-gain variant in exon 5 of 10 of the matrix metalloproteinase 13 gene (*MMP13*). Variants in *MMP13* (OMIM 602111) have been associated with autosomal dominant metaphyseal anadysplaia. A *de*

novo variant in *CLSTN3* was found and is strongly associated with an ASD diagnosis. Of the private inherited variants, we notice several that overlap with the SFARI list of genes, including *RELN*, *DNM1L*, *NAA15*, *JMJD1C*, *UBE3B*, and *ALDH1A* (**Table 1**). We also find three recurrently hit genes, which include *CEP128*, *RIOK3*, and *RTTN*. Of these Rotatin (RTTN) is associated with autosomal recessive microcephaly, short stature, and polymicrogyria with seizures.

Table 1: SFARI Genes Hit

Sample	HFA?	Multiplex?	Chrom	Pos	Ref	Alt	Exac_AF	RVIS	CADD	Function	Gene	aminoAcids	proteinPosition	Inheritance
306.s1	N	Y	5	112676242	C	A	0	30.51	36	stop-gained	*MCC*	GLY,stop	201/1020	Mother
396.s1	N	Y	15	39885308	C	T	0	23.56	40	stop-gained	*THBS1*	ARG,stop	959/1171	*De Novo*
411.p1	Y	Y	7	103136312	T	TA	0	4.33	36	frameshift	*RELN*	NA	NA	Father
258.p1	Y	Y	12	32861133	CAG	C	0	8.6	35	frameshift	*DNM1L*	NA	NA	Father
494.s1	N	Y	3	78988065	C	T	0	4.93	34	missense	*ROBO1*	ARG,HIS	23/1552	Father
146.p1	Y	Y	4	140262155	G	A	0	9.72	33	missense	*NAA15*	ASP,ASN	112/867	Mother
411.p1	Y	Y	10	64975398	A	T	0	1.92	30	missense	*JMJD1C*	VAL,ASP	27/2304	Mother
411.s1	Y	Y	10	64975398	A	T	0	1.92	30	missense	*JMJD1C*	VAL,ASP	27/2304	Mother
411.p1	Y	Y	12	109921396	G	T	0	1.16	32	missense	*UBE3B*	ASP,TYR	14/245	Father
277.p1	Y	N	15	101427859	G	A	0	11.68	32	missense	*ALDH1A3*	ARG,HIS	96/513	Mother
146.p1	Y	Y	8	3256937	T	G	0	0.17	24.3	missense	*CSMD1*	HIS,PRO	794/3565	*De Novo*
277.p1	Y	Y	9	130425614	C	T	0	14.9	26.6	missense	*STXBP1*	PRO,LEU	187/595	*De Novo*
187.s1	Y	Y	12	7288406	T	C	0	23.06	25.6	missense	*CLSTN3*	ILE,THR	200/957	*De Novo*
531.s1	Y	N	22	40800416	G	A	0	3.7	23.2	missense	*SGSM3*	ARG,HIS	108/750	*De Novo*
475.s1	Y	N	2	179592993	C	CT	0	99.5	36	frameshift	*TTN*	NA	NA	*De Novo*

In order to determine if the high functioning cases were different from cases with intellectual disability or controls, we compared the distribution of variants to the SSC. In particular, we divided the SSC into four groups: high functioning autism; FSIQ>100, FSIQ<70, and unaffected siblings and assessed four classes of variant: *de novo* LGD, *de novo* missense, inherited LGD, and inherited missense. We assessed the total number of variants in each category, the number of individuals carrying a variant type, and also compared distributions (**Table S9**)[151,152].

We find that the SAGE high functioning, SSC high functioning, and SSC FSIQ>100 groups all show significant differences in the numbers of individuals carrying an inherited LGD variant, when compared to the SSC ID<70 group (**Table S9, Figure 4.3**). This effect holds for severe

rare inherited missense variation amongst the SSC high functioning and SSC FSIQ>100 groups as well. We notice a similar effect when we compare the median number of variants in each individual between groups using the Mann-Whitney U test.

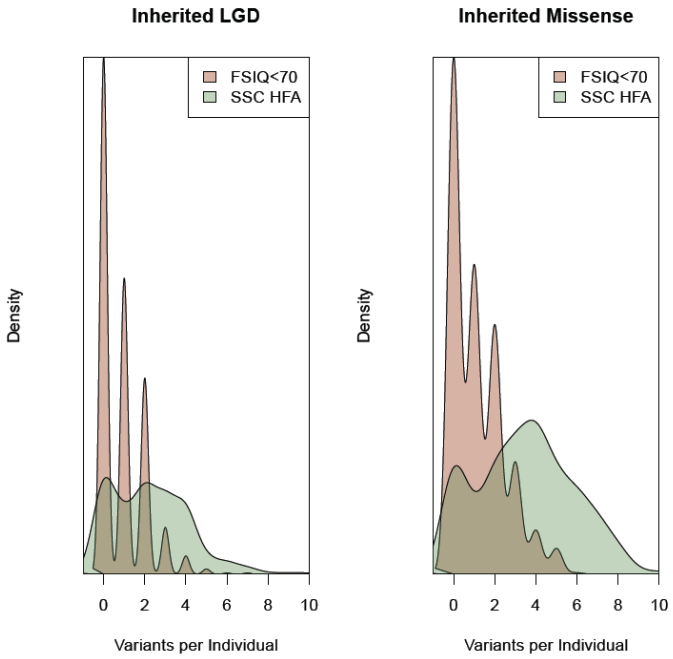

Figure 4.3: Variants per individual in two SSC cohorts. We assessed the number of private inherited LGD and private inherited severe missense variants per individual in the SSC individuals with FSIQ<70 and those with high functioning autism. We notice that those with high functioing autism tend to have more severe inherited variants per individuals that low functioning cases.

Leveraging the *de novo* variants discovered in the SSC high functioning group, we find a protein-protein interaction network underlying several of the *de novo* variants (**Figure 4.4**). This network appears to be associated with the NOTCH signaling pathway. Finally, we found that severe variants in the SAGE high functioning samples are enriched in the actin-binding pathway (Panther-Go Slim molecular function, 7.63 fold enrichment, $p=2.51x10^{-2}$).

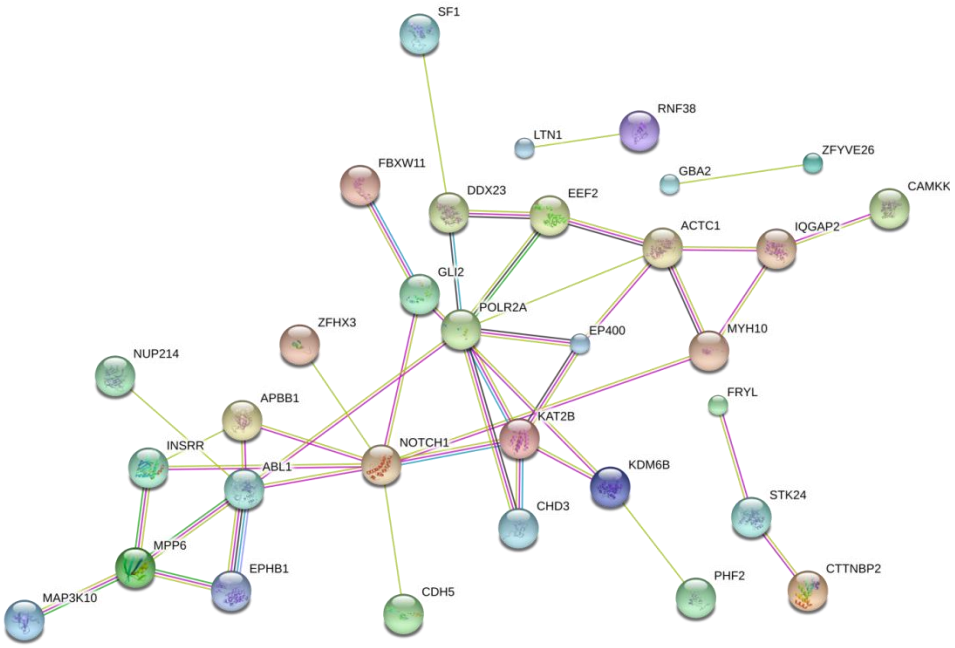

Figure 4.4: Network of connected proteins from *de novo* LGD and severe missense variants from SSC high functioning cases. A protein-protein interaction network for *de novo* variants from the high functioning autism individuals from the SSC shows an importance of the NOTCH pathway.

4.5 Discussion

Our results demonstrate the presence of rare likely gene disruptive and severe missense variants that contribute to the pathogenesis of the ASDs. We observe that mothers transmit more variants than fathers , both in all families (p=0.727) and when restricting to high functioning families (p=0.746), potentially corroborating previous evidence that mothers tend to transmit more deleterious variants to their affected offspring[77,139,148]. Of the families assessed, 26 are multiplex, several with diagnoses from the father's side which might dampen the observed transmission bias.

We observe the presence of *de novo* variants with strong evidence for involvement in neurocognitive function and neuronal development. The available case reports show specific

phenotypes associated with these variants. For example, we discovered and validated a *de novo* stop-gain variant in exon 18 of 22 of the thrombospondin I gene (*THBS1*) in female sibling 396.s1 who has a diagnosis of autism with a mixed receptive-expressive disorder. According to the clinical record, this individual has a normal head size and there were no concerns until regression at age 3 including loss of language and interactions with others. She was administered the WISC-IV and was notable for a verbal comprehension in the 0.5th percentile and a working memory in the 18th percentile.

Thrombospondin I is an adhesive glycoprotein that mediates cell-to-cell and cell-to-matrix interactions and has a role in synaptogenesis in the developing brain[153] and has been implicated in autism[154]. This individual also has a validated paternally inherited private frameshift variant in the *LACTB* gene, which codes for the mitochondrial ribosomal protein L56 which is also shared by her sibling who has an autism diagnosis[155] as well as two private inherited severe missense variants (**Figure 4.1a**). One of these genes, *NSUN2* (maternal) is associated with autosomal recessive intellectual disability[156,157].

We discovered and validated a *de novo* stop-gain variant in exon 2 of 24 of the Latrophillin-1 (*ADGRL1/LPHN1*) gene found in a male proband with a diagnosis of ADHD and PDD-NOS (330.p1) as well as a validated *de novo* private missense variant in the delta-aminolevulinate synthase 1 gene (*ALAS1*, CADD=18.6). The family history is significant for high functioning autism and dyslexia on the mother's side, and notable in that all inherited severe missense variants were maternal in origin (**Figure 4.1b)**. The proband has a WISC-IV intelligence quotient (IQ) of 96.

Latrophillin-1 is a neuronal receptor of α-latrotoxin, that is implicated in neurotransmitter release and control of presynaptic Ca(2+)[158,159]. As an adhesion G-protein-coupled receptor,

LPH1 can convert cell surface interactions into intracellular signaling[160]. ALAS1 is a nuclear encoded mitochondrial housekeeping gene that catalyzes the condensation of glycine with succinyl-coA to form delta-aminolevulinic acid[161]. This proband also had one additional inherited stop-gain variant and one inherited severe missense variant. The sibling in this family with a diagnosis of high functioning autism has a duplication disrupting the gene *POGZ*, which has already been strongly implicated in autism[162,163].

We discovered and validated a *de novo* stop-gain variant in exon 7 of 10 of the numb homolog (Drosophil)-like (*NUMBL*) found in the proband of family 271with autism. This proband was slow to develop language skills with phrase speech only emerging at 27 months. In clinical visits, the family's concerns were related to challenges with language skills, oppositional behavior and poor impulse control including grimacing, rhythmic humming, and hand flapping when excited. These concerns were reflected on the PKS 2nd edition which revealed a low score for social skills (58) and a high score for problem behavior (136) with main problem behaviors including tantrums and being overly sensitive to criticism or scolding. The proband's brother has high functioning autism, and there is a history of epilepsy, bipolar, and depression on the mother's side (**Figure 4.1c**). NUMBL, the numb homolog (Drosophil)-like, can directly bind and inhibit the Notch1 intracellular domain, and hence plays an essential role in neural cell fate determination[164–166]. We discovered an additional maternal severe missense variant in this individual.

We discovered and validated a private *de novo* missense variant ILE -> THR in exon 5 of 18 of the calsyntenin-3 gene (*CLSTN3*) in cadherin domain of the male high functioning autism sibling of family 187 (**Figure 4.1d**). There is a history of fragile X, ASDs, and developmental delays on the mother's side and this individual has a brother with autism. This *de novo* variant

has a CADD score of 25.6. The protein, calsyntenin-3, promotes excitatory and inhibitory synapse development and is an autism candidate gene[167]. In addition, the sibling has 2 inherited LGD and one severe missense variant.

NUMBL has not yet been implicated in a neurological phenotype, but plays a role in neuronal cell differentiation and is hence a strong candidate for a developmental disorder. In these cases, even though there are strong candidates for genetic etiology of the disorder, the probands also inherit variants in genes associated with neurocognitive disorders suggesting that multiple hits may be necessary to lead to a penetrant phenotype.

In three families (258, 329, and 406), we observe disruptive variants that segregate with a diagnosis from the parent (**Figure 4.2**). In family 258, we observe an LGD variant in *DNM1L* that segregates from the father with high functioning autism to the son who has the same diagnosis (**Figure 4.2a**). This variant is found in exon 5 of 22 and the gene is associated with autism[168]. *DNM1L* codes for the dynamin-like protein 1, is associated with autosomal dominant encephalopathy, and plays an important role in the division of the growing mitochondria and peroxisomes[169]. Additional variants could be playing a role in this case, as the proband also has a maternally inherited frameshift variant in *SPRED2* which has some evidence for involvement in childhood speech apraxia[170] as well as 8 other rare inherited variants.

In family 329, where the proband has a high functioning autism diagnosis, the mother has anxiety issues and the father has social challenges, there is a severe maternally transmitted missense variant in *NCOR*, the nuclear receptor corepressor 1 (**Figure 4.2b**). In a recent network analysis of *de novo* variants in autism, genes associated with the NCOR/HDAC3 complex have been implicated in autism[171]. The mother also transmits a missense variant in *TRPM* (CADD 29.1), the transient receptor potential cation channel, subfamily M, member 1, in which an

excess of rare deletions in autism cases was found[94]. The father with social challenges transmits a severe missense variant in the *MYO9B* gene (CADD 29.5), which codes for Myosin IXB, and was identified as a gene strongly enriched for variants likely to affect ASD risk[66]. In family 406, where the proband and the sibling *both* have ASD diagnoses and the mother has an ADHD diagnosis (**Figure 4.2c**), we discovered a frameshift variant transmitted to both sequenced offspring in the gene neuroguidin (*NGDN*). Neuroguidin is a eukaryotic initiation factor 4E binding protein and associated with the fragile X mental retardation protein (FMRP)[172,173]. The first and second examples demonstrate the variable expressivity of disruptive variants, while the third demonstrates the extreme heterogeneity and points towards missing heritability of the ASDs.

We observe likely impactful *de novo* and inherited variation in both simplex and multiplex families. In multiplex family 330, for example, we observe a phenomenon whereby there are two *de novo* variants, one in the proband and one in the sibling, likely contributing to the diagnosis. The proband has a stop-gain variant in the *LPHN1* gene, the product of which is implicated in neurotransmitter release[158,159] while the sibling has a <100kbp duplication disrupting the gene *POGZ*, already implicated in the etiology of ASD[162,163]. We observe variants transmitted to both affected proband and sibling in several families, including those with a prior for involvement in a neuropsychiatric disorder, such as *LEMD3*, *LACTB*, *BBS5*, and *JMJD1C*. Phenotypic categorization into multiplex and simplex families is useful, however our results demonstrate that both *de novo* and inherited variation can play a role in such families.

A major focus of this study was to assess variation in individuals with autism in the absence of intellectual disability. Despite the fact that over half of our families have a diagnosis of high functioning autism, we find few impactful *de novo* variants and we find only a single LGD variant

in the gene *CHRM4*. We do find two private inherited LGD and five severe missense variants in genes strongly associated with autism from the SFARI list as well as two families with a hit in the Rotatin gene, associated with microcephaly and polymicrogyria[151,152]. Using high functioning and >100 FSIQ cases from the SSC allowed us to statistically assess variant burden. While our cohort of high functioning cases is restricted, due to its size, we observe trends towards differences in inherited LGD and missense variant burden when compared to SSC control siblings and <70 FSIQ individuals. Both the SSC high functioning autism, and FSIQ>100 cohorts show statistically significant differences in *de novo* LGD, inherited LGD, and inherited missense burden when compared to the <70 FSIQ individuals. Somewhat surprisingly, the data suggest that low functioning samples are closer to controls in terms of inherited variant burden when compared to high functioning samples (**Figure 4.3**). Interestingly, the burden for inherited variants is greater per individual in high functioning than low functioning cases.

Curiously, we notice a difference in *de novo* LGD variant burden between the SSC high functioning cases and unaffected siblings, but not between the FSIQ>100 group and unaffected siblings. Individuals can have high functioning autism with an FSIQ as low as 80, suggesting that LGD *de novo* variants decrease FSIQ in addition to contributing to an autism diagnoses.

The fact that *de novo* severe variants from the SSC high functioning group form a protein-protein interaction network involving the NOTCH pathway (**Figure 4.4**), suggests that similar genes, but likely different types of variants in those genes, are associated with high functioning autism. The role of actin is important for remodeling of neurons[174,175], and enrichment for these genes in the SAGE high functioning cohort suggest this class of protein may also be important in autism without intellectual disability. *Shank3*, a known autism gene, has been shown to interact

with actin regulators and *Shank3* deficient mice can be rescued by manipulation of actin regulators[176].

Our results confirm the massive locus and phenotype heterogeneity observed in the ASDs. Breaking autism cohorts into distinct phenotypic groups allows assessment of genetic differences associated with subtypes of autism. While our sample size for this study is relatively small, we discovered several novel autism candidate genes and rediscovered several more. Our results point to the importance of both inherited and *de novo* variation, and suggest that inherited variation may be a driving factor in the etiology of high functioning ASDs.

5. Summary and Future Directions

Our work on the heterogeneity of neuropsychiatric disorders sets the stage for future studies. Individuals with a known pathogenic variant, such as a large CNV, are often excluded from exome sequencing and genome sequencing studies. However, insight into the additional variation discovered in these individuals will provide better understanding of the modifiers that lead to phenotype heterogeneity in individuals with a known pathogenic variant.

My study of genetic modifiers in the Simons VIP 16p11.2 cohort led us to discover several features of variation that could account for the observed phenotype heterogeneity. I discovered a maternal inheritance bias of rare (<0.1% in controls) additional deletions in addition to the 16p11.2 CNV and that the number of additional rare deletions negatively correlated with FSIQ. Despite the cohort being screened for additional large, likely pathogenic CNVs, I discovered 9 additional CNVs that disrupt genes already implicated in autism and neuropsychiatric disorders. Many individuals with such events had distinct (more severe) phenotypes, including facial dysmorphologies, and tended to be female.

A distinct advantage of the Simons VIP is the presence of parents and additional family members that allowed us not only to determine the inheritance status of the 16p11.2 CNV, but also of additional CNVs and exonic variants. The SNP microarray data allowed us to assess the parent-of-origin of the 16p11.2 *de novo* events and led us to examine genome-wide recombination rate data. Over 90% of *de novo* 16p11.2 CNVs (deletions and duplications) occur on the maternal haplotype, likely as a result of heterochiasmy (difference in recombination rates between male and female) at the 16p11.2 locus. Data from a large Icelandic cohort shows that the fecundity of the 16p11.2 deletion is lower in males than in females, suggesting that an additional mechanism could also contribute[30]. The SNP microarray data also allowed us to

determine no apparent difference in the mechanism of unequal crossing over for *de novo* 16p11.2 deletions or duplications.

Analysis of exonic variation internal and external to the critical region revealed a relative lack of variation across the 16p11.2 critical region and there was a trend for less variation in probands than non-carrier family members. Population genetics analysis using the 2,500 individuals from the 1000 Genomes Phase III project demonstrates that the 16p11.2 critical region lies in the lower 3rd percentile for both the average heterozygosity and Tajima's D statistics, when compared to the distribution of similarly sized regions genome-wide. These data suggest that the critical region, despite being predisposed to recurrent deletion and duplication, is under selection.

Genes lying in duplicated sequence are not well-captured through targeted sequencing approaches, such as exome sequencing. My analysis of the three duplicated critical region genes revealed, for the first time, natural variation in *BOLA2*, *SLX1A*, and *SULT1A3*. I determined that variants typically occur in a single copy of these genes (median copy number 6 in human populations). In *BOLA2*, a gene with little known function and under intense study because it is part of a *Homo sapiens* specific duplication, I found only 8 individuals with an LGD variant in a population of over 8,000 cases with autism of intellectual disability. Furthermore, no individual in the Simons VIP cohort had an LGD variant in *BOLA2*. From our reanalysis of exome sequencing data from the Simons VIP cohort, I find 13 likely gene disruptive variants in probands in genes with a prior for autism or intellectual disability and these probands were among those most severely affected. That deletion individuals with the lowest *BOLA2* copy number (CN=3) were enriched in anemia gives evidence of *BOLA2* copy number as a phenotype modifier, and one of the only known genetic variants leading to an anemia phenotype.

Our analysis of a locally collected cohort of individuals with autism and intellectual disability revealed several previously uncharacterized variants likely contributing to the diagnosis. Leveraging the Simons Simplex Collection for additional high functioning cases I find that *de novo* variants amongst this group are enriched for genes in the Notch signaling pathway. Our results show that high functioning cases are less similar to controls in terms of burden of rare inherited variants compared to individuals with FSIQ<70, suggesting this is an important form of variation in high functioning cases. I find some evidence that actin binding proteins may be important in the etiology of high functioning autism.

These results support the conclusions from other studies and pave the way for future research. For example, in the 16p11.2 cohort as well as the SAGE cohort, I see a bias toward maternal transmission of deleterious variants. These data support the hypothesis that females have a "buffering capacity" against deleterious variation. The striking maternal parent-of-origin bias and relative lack of diversity across the critical region warrants parent-of-origin, recombination rate, and population genetic studies of other microdeletion and duplication regions. In my study, I observe several trends: the number of rare deletions in 16p cases is negatively correlated with FSIQ; there is lower variation in 16p11.2 probands than non-carrier family members; and *de novo* duplications tend to occur by an intrachromosomal mechanism of crossing over. In order to confirm or refute these trends, a large sample size is needed.

Both the Simons VIP and SAGE study designs provide an important blueprint for going forward on a much larger scale. The rapid recruitment of such a large number of participants was achieved from a network of local providers (for SAGE) and from the Simons VIP Connect (https://simonsvipconnect.org/). The Simons VIP Connect specifically leverages the internet and serves as a portal for clinicians, genetic counselors and families with a 16p11.2 copy number

variant (CNV) diagnosis to network and become involved in specific research studies. While website recruitment introduces a level of ascertainment bias, the fact that participants were flown (at no expense to the family) to a site where standardized testing could be performed, provided not only sufficient numbers but a more rigorous phenotypic assessment. Efforts to network families with specific variants and researchers/clinicians are also occurring in Europe often for the same genes or CNVs (http://www.rarechromo.org/, www.humandiseasegenes.com). The Simons 16p11.2 CNV and SAGE projects provide a powerful roadmap on how to balance the interests of affected individuals, researchers and clinicians.

With exome and genome sequencing becoming routine clinical practice, the genotype-first approach will likely soon spread beyond autism and developmental delay to include genes and CNVs associated with other psychiatric disorders. Routine sequencing will increase numbers to discover additional cases of rare, likely gene-disruptive variants, such as those discussed in the SAGE cohort.

A fundamental goal of my research is to elucidate understanding of genetic variation for use in a clinical context. In the case of 16p11.2 carriers, we found that CNVs and SNVs disrupting autism associated genes may be more important modifiers than those local to the critical region. While sample size is small, and larger cohorts will confirm or refute these trends, the results of this research outline a clinical approach. As therapies are tested for particular autism associated genes, individuals with an additional hit in such genes may benefit from individualized treatments. Trends towards greater global burden of SNVs and CNVs can give families some explanation of their child's case. In terms of prenatal diagnosis, individuals with additional rare variants have a prior for being more severely affected.

Moving forward, experimental techniques need to capture all variation. Our experimental methods did not capture copy number variation between 50bp-50kbp, nor single nucleotide and indel variation genome-wide. It is possible that regulatory variation internal or external to the critical region may play a crucial role as a phenotype modifier as is suggested from recent whole-genome studies[177]. Whole-genome sequencing of affected individuals is a logical way forward to assess all types of variation and refute or confirm observed trends in the data. An understanding of the complete repertoire of variation will provide further insight into phenotype modifiers.

Genome sequencing will allow study of all forms of variation, including non-coding regulatory variation. There are three immediate benefits: 1) establishing or rejecting phenotype–genotype correlations with statistical rigor; 2) networking families with other families in order to provide real-life solutions to often idiosyncratic problems associated with a specific genetic disorder; and 3) linking affected individuals and their families with clinical and basic researchers specifically focused on understanding the biology of a gene or gene network. The latter will ultimately lead to the design of clinical trials and the large number of affected individuals assembled will speed their implementation. The pioneering families recruited through these networks will likely be the most informed by research advances and have the benefit of being at the head of the line when such clinical trials are implemented for their specific genetic subtype of neurocognitive disorder.

In the near future, we will have the ability to analyze over 100,000 individuals with comprehensive whole genome sequencing and phenotype data. This sort of dataset will allow us to ask new questions, and better understand phenotype modifiers in particular, and genetic variation in general.

Researchers will continue to utilize the genotype- and phenotype-first methodologies, however one might not have to plan a study as such. As sequencing moves into the clinic, and whole populations are sequenced, we will have access to a trove of genotype and phenotype data for a variety affected and unaffected individuals. Since the data to answer questions will already be present, there can be productive interplay between the phenotype- and genotype-first approaches. Take, for example, autism spectrum disorder. One could look at the genetic data from 100,000 individuals with ASD and their unaffected family members for recurrent variation. Say researchers identify 300 genes and 100 regulatory regions that contain recurrent severe variants. We could look again at variants in a particular gene identified in a population database, and ask what phenotypes are associated. Is it always autism? What are the comorbidities? Is it syndromic? This approach will not only elucidate the variants associated with particular disorders but also the disorders associated with particular variants.

The comprehensive analysis of phenotype is crucial in two ways. First, we must have a relatively small number of phenotype metrics that help explain the heterogeneity associated with a particular disorder or variant (if such heterogeneity exists) and variables should be minimally correlated with one another. Several examples of such scores have been proposed[24,178]. Second, phenotype can guide ascertainment. In the most recent exome and targeted resequencing studies of ASD individuals, those with recurrent variants such as in *CHD8* and *DYRK1A* are more similar to one another than the ASD population as a whole[33,179]. Instead of ascertaining on ASD, ascertainment of ASD in addition to another phenotype may enrich for particular variants in phenotypically heterogeneous populations. Such ascertainment would be facilitated by comprehensive electronic medical records (EMR).

Large datasets are amenable to algorithmic discovery, but must be organized in such a way to make this possible. Annotation of both genotype and phenotype is key in this process. For variants, important annotation includes type (missense, loss of function, regulatory, etc.), location, conservation, and more. For phenotype, biological system and severity are important. In addition to these "first tier" annotations, stepping back a level, and looking at meta-annotations is crucial. For example, genes are connected via protein-protein interaction networks and classifying genes in this way may provide statistical power for variant discovery. Such refinement is challenging, but has proven useful in autism[171,180,181], and other neurocognitive disorders[182].

At present, loss of function variants provide the most power for associating particular genes with a disorder. Other types of variation, such as missense and regulatory, are also important in determining clinical outcome. Loss of function variants provide more statistical power because, in most cases, loss of function variants remove a functional copy of a gene. However, not all missense or non-coding variants may affect molecular function. Larger cohorts will enable the identification of which missense and non-coding variants affect a gene, and functional characterization can potentially help identify protein domains and regulatory regions.

At the same time, not all variation in a gene leads to the same phenotype, and different types of variation in the same gene might be associated with distinct clinical sequelae. For example, missense variants clustering in an 11-bp interval of the gene *SETBP1* cause Schinzel-Giedeon syndrome characterized by severe ID and specific craniofacial features[183]. However, loss of function variants elsewhere in the gene and microdeletions show moderate non-syndromic ID without the typical craniofacial features of Schinzel-Giedeon syndrome[184]. Finally, rare variation

has a higher likelihood of pathogenicity, but common variation can play a role, especially in the presence of a known pathogenic variant.

Population based cohorts can refine our study of genetic modifiers in several ways. We will use the 16p11.2 CNV discussed in this thesis as an example. Population-based cohorts will allow unbiased ascertainment of genotype-first cohorts. One might argue that the VIP cohort discussed in this thesis was not collected in a true genotype-first manner. To be included in the cohort each individual was ascertained on the presence of a 16p11.2 CNV, but we only knew if a 16p11.2 CNV was present if the individual had already had some form of genotyping done. Clinical genotyping requires a phenotype that is severe enough to necessitate a clinical microarray. Ascertained individuals also had no large, likely pathogenic CNVs. Therefore, our 16p11.2 cohort represents a subset of the true population of 16p11.2 carriers.

Large population cohorts would allow ascertainment blinded to phenotype and permit understanding of the true breadth of phenotypes associated with the 16p11.2 CNV and a population-based Icelandic cohort of over 100,000 individuals provides a model moving forward[30]. The researchers identified 26 neuropsychiatric CNVs based on the literature and separate the cohort into groups: population controls, controls carrying a neuropsychiatric CNV, controls carrying a non-neuropsychiatric CNV, and individuals with a diagnosis of schizophrenia. The researchers assessed a subset of the cohort for neuropsychiatric metrics including: the adult mathematical history questionnaire (ARHQ), the adult reading history questionnaire (ARHQ), category fluency (CF), global assessment of functioning (GAF), letter fluency (LF), logical memory I and II (LM I and II), perseverative errors (Pers. Errors), performance IQ (P IQ), rapid visual information processing (RVIP), spatial working memory (SWM), verbal IQ (V IQ). A main finding was that the cognitive impairment of controls carrying

a neuropsychiatric CNV fell between that of the individuals with schizophrenia and the other controls (**Figure 5.1**). Furthermore, when restricting to individuals with the 16p11.2 CNV, deletion carriers showed the greatest impairment in the same cognitive domains as the control carriers, which was not the case for the duplication carriers. In particular, the deletion associated with impaired verbal IQ and deficits in verbal letter and category fluency tests, whereas the duplication impairs spatial working memory and executive functions. This study shows the usefulness of a population cohort for exploring the variable expressivity of neuropsychiatric CNVs and allows systematic searching for biochemical foundations of cognitive differences between affected and unaffected carriers of a neurocognitive CNV.

Such an unbiased collection of neuropsychiatric CNV carriers points to ways in which the 16p11.2 VIP has ascertainment bias. First, all initially identified probands have a clinically recognized phenotype. Second, non-carrier parents in the VIP tend to have a higher intelligence quotient than the population average (**Figure 2.3**). One explanation is that individuals who find out about the study via the internet or bring their child to a genetic clinic tend to have higher intelligence. Third, some individuals with a 16p11.2 duplication tend to be severely affected. Based on large CNV case-control studies, the deletion has a higher odds ratio than the duplication, and these severe duplication cases are relatively unexpected[50]. If we ascertain a large 16p11.2 CNV cohort from the population the phenotypes and observed modifiers will likely be more diverse than those we discovered in the VIP and provide deeper insight into the etiology of the phenotypes associated with the 16p11.2 CNV.

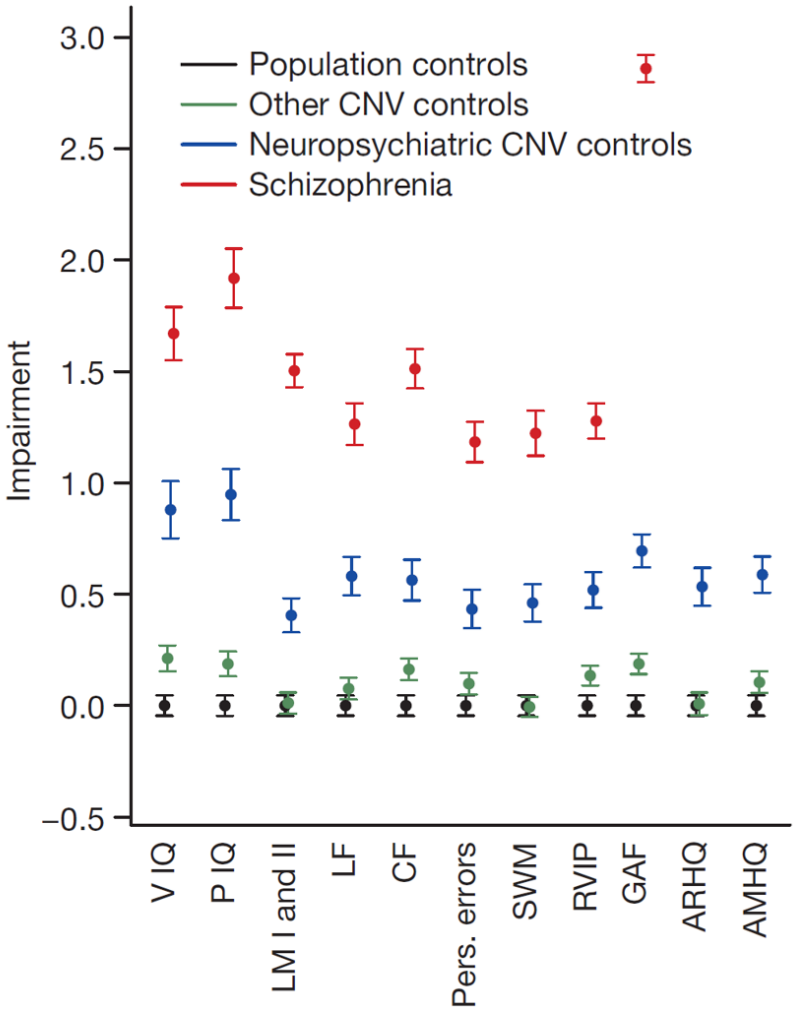

Figure 5.1. Cognitive impairment of control neuropsychiatric CNV carriers and controls. Average standardized cognitive impairment scores between controls carrying a neuropsychiatric CNV (n=465), controls carrying a non-neuropsychiatric CNV (n=465), population controls (475), and schizophrenia patients (n=161). CNVs were ascertained in an Icelandic population cohort of over 100,000 individuals and a subset were worked up for cognitive metrics. 26 CNVs were determined from the literature to be associated with neuropsychiatric disorders and termed "neuropsychiatric CNVs." The population was divided into controls carrying a neurocognitive CNV, controls carrying non-neuropsychiatric CNV, population controls, and patients with a diagnosis of schizophrenia. The scores on the adult reading history questionnaire (ARHQ) and the adult mathematical history questionnaire (AMHQ) separate the neuropsychiatric CNV carriers from the population controls with an effect of 0.50 s.d. ($p=3.1 \times 10^{-6}$) and 0.55 s.d. ($P=2.5 \times 10^{-7}$), respectively. All neuropsychiatric CNV carriers have a cognitive impairment greater than population controls. Metrics assessed include: verbal IQ (V IQ), performance IQ (P IQ), logical memory I and II (LM I and II), letter fluency (LF), category fluency (CF), perseverative errors (Pers. Errors), spatial working memory (SWM), rapid visual information processing (RVIP), global assessment of functioning (GAF), adult mathematical history questionnaire (ARHQ), and the adult reading history questionnaire (ARHQ). (Image adapted from Stefansson *et al.* 2014).

The sequencing of large population cohorts and indeed whole countries is a real possibility and is already being pursued in projects such as the UK10K, which will include exome and/or whole genome sequencing for more than 6,000 individuals with particular disease phenotypes. The proposition of sequencing populations is especially powerful in countries where all medical information is present in a comprehensive database. The Icelandic study[30] shows us that the recurrence rate of the 16p11.2 deletion is 0.058 and duplication 0.067, meaning that with a population size of 100,000, we should have a true "genotype-first" cohort of approximately 58 16p11.2 deletion and 67 16p11.2 duplication carriers, in addition to carriers of a wide variety of other variants. Such large population cohorts allow the systematic study of the relationship between genotype and phenotype. However, as genetic data become ubiquitous, the ethical aspects of genetic data generation, analysis, and sharing must be considered.

Suppose we live in a world where hundreds of thousands of people have had whole genome sequencing performed, and we have found strong correlations between particular genotypes and phenotypes. Several ethical challenges arise. First, who owns the genetic data? If researchers work out the genetics of certain forms of cancers with these data, enabling a new generation of therapeutics, what reciprocation will the study participants receive? If there is a crime for which DNA evidence is available, can the government or another entity screen a genetic database for a match? Do genetic variants count as "pre-existing conditions" or something else that insurance companies can use to modulate premiums? Second, what is the impact for clinical medicine and primary care? If we understand which medications or interventions to prescribe based on genotype, we can tailor therapies for the individual. Most variants have variable expressivity or penetrance associated with them. In the primary care clinic, it is crucial that providers understand and explain to patients the implication of these studies, in particular probabilities behind

genotype-phenotype associations. Just because a variant is present does not mean the patient has a particular disease or disorder. Third, what will be the ramifications for reproductive medicine? Will we allow parents to choose for or against certain traits? If so, which ones? How will this affect the fitness of the population as a whole? While the genotype-phenotype connection will not happen overnight, and will require a great deal of methods development and functional annotation, the advent of personalized medicine and the understanding of molecular mechanism of disease will improve health and well-being for human kind. Like any new technology, these data can steer society towards benefaction and success or towards misery and failure; it is up to us to decide the path to take.

References

1. Mendel, G. (1866). Versuche über Pflanzenhybriden. Verhandlungen Naturforschenden Vereines Brunn 4 3 *44*,.

2. O'Roak, B.J., Vives, L., Fu, W., Egertson, J.D., Stanaway, I.B., Phelps, I.G., Carvill, G., Kumar, A., Lee, C., Ankenman, K., et al. (2012). Multiplex targeted sequencing identifies recurrently mutated genes in autism spectrum disorders. Science *338*, 1619–1622.

3. O'Roak, B.J., Vives, L., Girirajan, S., Karakoc, E., Krumm, N., Coe, B.P., Levy, R., Ko, A., Lee, C., Smith, J.D., et al. (2012). Sporadic autism exomes reveal a highly interconnected protein network of de novo mutations. Nature *485*, 246–250.

4. Sanders, S.J., Murtha, M.T., Gupta, A.R., Murdoch, J.D., Raubeson, M.J., Willsey, A.J., Ercan-Sencicek, A.G., DiLullo, N.M., Parikshak, N.N., Stein, J.L., et al. (2012). De novo mutations revealed by whole-exome sequencing are strongly associated with autism. Nature *485*, 237–241.

5. Neale, B.M., Kou, Y., Liu, L., Ma'ayan, A., Samocha, K.E., Sabo, A., Lin, C.-F., Stevens, C., Wang, L.-S., Makarov, V., et al. (2012). Patterns and rates of exonic de novo mutations in autism spectrum disorders. Nature *485*, 242–245.

6. Julien, P., Miñana, B., Baeza-Centurion, P., Valcárcel, J., and Lehner, B. (2016). The complete local genotype-phenotype landscape for the alternative splicing of a human exon. Nat. Commun. *7*, 11558.

7. Simons Vip Consortium (2012). Simons Variation in Individuals Project (Simons VIP): a genetics-first approach to studying autism spectrum and related neurodevelopmental disorders. Neuron *73*, 1063–1067.

8. Weiss, L.A., Shen, Y., Korn, J.M., Arking, D.E., Miller, D.T., Fossdal, R., Saemundsen, E., Stefansson, H., Ferreira, M.A.R., Green, T., et al. (2008). Association between microdeletion and microduplication at 16p11.2 and autism. N. Engl. J. Med. *358*, 667–675.

9. Kumar, R.A., KaraMohamed, S., Sudi, J., Conrad, D.F., Brune, C., Badner, J.A., Gilliam, T.C., Nowak, N.J., Cook, E.H., Jr, Dobyns, W.B., et al. (2008). Recurrent 16p11.2 microdeletions in autism. Hum. Mol. Genet. *17*, 628–638.

10. de Vries, B.B.A., Pfundt, R., Leisink, M., Koolen, D.A., Vissers, L.E.L.M., Janssen, I.M., Reijmersdal, S. van, Nillesen, W.M., Huys, E.H.L.P.G., Leeuw, N. de, et al. (2005). Diagnostic genome profiling in mental retardation. Am. J. Hum. Genet. *77*, 606–616.

11. Sharp, A.J., Hansen, S., Selzer, R.R., Cheng, Z., Regan, R., Hurst, J.A., Stewart, H., Price, S.M., Blair, E., Hennekam, R.C., et al. (2006). Discovery of previously unidentified genomic disorders from the duplication architecture of the human genome. Nat. Genet. *38*, 1038–1042.

12. Sebat, J., Lakshmi, B., Malhotra, D., Troge, J., Lese-Martin, C., Walsh, T., Yamrom, B., Yoon, S., Krasnitz, A., Kendall, J., et al. (2007). Strong association of de novo copy number mutations with autism. Science *316*, 445–449.

13. Shinawi, M., Liu, P., Kang, S.-H.L., Shen, J., Belmont, J.W., Scott, D.A., Probst, F.J., Craigen, W.J., Graham, B.H., Pursley, A., et al. (2010). Recurrent reciprocal 16p11.2 rearrangements associated with global developmental delay, behavioural problems, dysmorphism, epilepsy, and abnormal head size. J. Med. Genet. *47*, 332–341.

14. Rosenfeld, J.A., Coppinger, J., Bejjani, B.A., Girirajan, S., Eichler, E.E., Shaffer, L.G., and Ballif, B.C. (2010). Speech delays and behavioral problems are the predominant features in individuals with developmental delays and 16p11.2 microdeletions and microduplications. J. Neurodev. Disord. *2*, 26–38.

15. Zufferey, F., Sherr, E.H., Beckmann, N.D., Hanson, E., Maillard, A.M., Hippolyte, L., Macé, A., Ferrari, C., Kutalik, Z., Andrieux, J., et al. (2012). A 600 kb deletion syndrome at 16p11.2 leads to energy imbalance and neuropsychiatric disorders. J. Med. Genet. *49*, 660–668.

16. Walters, R.G., Jacquemont, S., Valsesia, A., de Smith, A.J., Martinet, D., Andersson, J., Falchi, M., Chen, F., Andrieux, J., Lobbens, S., et al. (2010). A new highly penetrant form of obesity due to deletions on chromosome 16p11.2. Nature *463*, 671–675.

17. Girirajan, S., Rosenfeld, J.A., Cooper, G.M., Antonacci, F., Siswara, P., Itsara, A., Vives, L., Walsh, T., McCarthy, S.E., Baker, C., et al. (2010). A recurrent 16p12.1 microdeletion supports a two-hit model for severe developmental delay. Nat. Genet. *42*, 203–209.

18. McCarthy, S.E., Makarov, V., Kirov, G., Addington, A.M., McClellan, J., Yoon, S., Perkins, D.O., Dickel, D.E., Kusenda, M., Krastoshevsky, O., et al. (2009). Microduplications of 16p11.2 are associated with schizophrenia. Nat. Genet. *41*, 1223–1227.

19. Cooper, G.M., Coe, B.P., Girirajan, S., Rosenfeld, J.A., Vu, T.H., Baker, C., Williams, C., Stalker, H., Hamid, R., Hannig, V., et al. (2011). A copy number variation morbidity map of developmental delay. Nat. Genet. *43*, 838–846.

20. Kaminsky, E.B., Kaul, V., Paschall, J., Church, D.M., Bunke, B., Kunig, D., Moreno-De-Luca, D., Moreno-De-Luca, A., Mulle, J.G., Warren, S.T., et al. (2011). An evidence-based approach to establish the functional and clinical significance of copy number variants in intellectual and developmental disabilities. Genet. Med. Off. J. Am. Coll. Med. Genet. *13*, 777–784.

21. Sanders, S.J., Ercan-Sencicek, A.G., Hus, V., Luo, R., Murtha, M.T., Moreno-De-Luca, D., Chu, S.H., Moreau, M.P., Gupta, A.R., Thomson, S.A., et al. (2011). Multiple recurrent de novo CNVs, including duplications of the 7q11.23 Williams syndrome region, are strongly associated with autism. Neuron *70*, 863–885.

22. Chen, R., Shi, L., Hakenberg, J., Naughton, B., Sklar, P., Zhang, J., Zhou, H., Tian, L., Prakash, O., Lemire, M., et al. (2016). Analysis of 589,306 genomes identifies individuals resilient to severe Mendelian childhood diseases. Nat. Biotechnol. *34*, 531–538.

23. Girirajan, S., and Eichler, E.E. (2010). Phenotypic variability and genetic susceptibility to genomic disorders. Hum. Mol. Genet. *19*, R176-187.

24. Girirajan, S., Rosenfeld, J.A., Coe, B.P., Parikh, S., Friedman, N., Goldstein, A., Filipink, R.A., McConnell, J.S., Angle, B., Meschino, W.S., et al. (2012). Phenotypic heterogeneity of genomic disorders and rare copy-number variants. N. Engl. J. Med. *367*, 1321–1331.

25. Bassuk, A.G., Geraghty, E., Wu, S., Mullen, S.A., Berkovic, S.F., Scheffer, I.E., and Mefford, H.C. (2013). Deletions of 16p11.2 and 19p13.2 in a family with intellectual disability and generalized epilepsy. Am. J. Med. Genet. A. *161A*, 1722–1725.

26. Nadeau, J.H. (2001). Modifier genes in mice and humans. Nat. Rev. Genet. *2*, 165–174.

27. Badano, J.L., and Katsanis, N. (2002). Beyond Mendel: an evolving view of human genetic disease transmission. Nat. Rev. Genet. *3*, 779–789.

28. Kajiwara, K., Berson, E.L., and Dryja, T.P. (1994). Digenic retinitis pigmentosa due to mutations at the unlinked peripherin/RDS and ROM1 loci. Science *264*, 1604–1608.

29. Hanson, E., Bernier, R., Porche, K., Jackson, F.I., Goin-Kochel, R.P., Snyder, L.G., Snow, A.V., Wallace, A.S., Campe, K.L., Zhang, Y., et al. (2015). The cognitive and behavioral phenotype of the 16p11.2 deletion in a clinically ascertained population. Biol. Psychiatry *77*, 785–793.

30. Stefansson, H., Meyer-Lindenberg, A., Steinberg, S., Magnusdottir, B., Morgen, K., Arnarsdottir, S., Bjornsdottir, G., Walters, G.B., Jonsdottir, G.A., Doyle, O.M., et al. (2014). CNVs conferring risk of autism or schizophrenia affect cognition in controls. Nature *505*, 361–366.

31. American Psychiatric Association, and American Psychiatric Association (2000). Diagnostic and statistical manual of mental disorders: DSM-IV-TR (Washington, DC: American Psychiatric Association).

32. Stessman, H.A., Bernier, R., and Eichler, E.E. (2014). A genotype-first approach to defining the subtypes of a complex disease. Cell *156*, 872–877.

33. Bernier, R., Golzio, C., Xiong, B., Stessman, H.A., Coe, B.P., Penn, O., Witherspoon, K., Gerdts, J., Baker, C., Vulto-van Silfhout, A.T., et al. (2014). Disruptive CHD8 mutations define a subtype of autism early in development. Cell *158*, 263–276.

34. Golzio, C., Willer, J., Talkowski, M.E., Oh, E.C., Taniguchi, Y., Jacquemont, S., Reymond, A., Sun, M., Sawa, A., Gusella, J.F., et al. (2012). KCTD13 is a major driver of mirrored neuroanatomical phenotypes of the 16p11.2 copy number variant. Nature *485*, 363–367.

35. Blaker-Lee, A., Gupta, S., McCammon, J.M., De Rienzo, G., and Sive, H. (2012). Zebrafish homologs of genes within 16p11.2, a genomic region associated with brain disorders, are active during brain development, and include two deletion dosage sensor genes. Dis. Model. Mech. *5*, 834–851.

36. Horev, G., Ellegood, J., Lerch, J.P., Son, Y.-E.E., Muthuswamy, L., Vogel, H., Krieger, A.M., Buja, A., Henkelman, R.M., Wigler, M., et al. (2011). Dosage-dependent phenotypes in models of 16p11.2 lesions found in autism. Proc. Natl. Acad. Sci. U. S. A. *108*, 17076–17081.

37. Wu, N., Ming, X., Xiao, J., Wu, Z., Chen, X., Shinawi, M., Shen, Y., Yu, G., Liu, J., Xie, H., et al. (2015). TBX6 null variants and a common hypomorphic allele in congenital scoliosis. N. Engl. J. Med. *372*, 341–350.

38. Xander Nuttle, and Giuliana Gianuzzi Emergence of a Homo sapiens-specific gene family and the evolution of autism risk at chromosome 16p11.2. Submitted.

39. Zhang, F., Gu, W., Hurles, M.E., and Lupski, J.R. (2009). Copy number variation in human health, disease, and evolution. Annu. Rev. Genomics Hum. Genet. *10*, 451–481.

40. Fischbach, G.D., and Lord, C. (2010). The Simons Simplex Collection: a resource for identification of autism genetic risk factors. Neuron *68*, 192–195.

41. Weiss, L.A., Shen, Y., Korn, J.M., Arking, D.E., Miller, D.T., Fossdal, R., Saemundsen, E., Stefansson, H., Ferreira, M.A.R., Green, T., et al. (2008). Association between microdeletion and microduplication at 16p11.2 and autism. N. Engl. J. Med. *358*, 667–675.

42. Moreno-De-Luca, A., Evans, D.W., Boomer, K.B., Hanson, E., Bernier, R., Goin-Kochel, R.P., Myers, S.M., Challman, T.D., Moreno-De-Luca, D., Slane, M.M., et al. (2015). The role of parental cognitive, behavioral, and motor profiles in clinical variability in individuals with chromosome 16p11.2 deletions. JAMA Psychiatry *72*, 119–126.

43. Maillard, A.M., Ruef, A., Pizzagalli, F., Migliavacca, E., Hippolyte, L., Adaszewski, S., Dukart, J., Ferrari, C., Conus, P., Männik, K., et al. (2015). The 16p11.2 locus modulates brain structures common to autism, schizophrenia and obesity. Mol. Psychiatry *20*, 140–147.

44. Hanson, E., Bernier, R., Porche, K., Jackson, F.I., Goin-Kochel, R.P., Snyder, L.G., Snow, A.V., Wallace, A.S., Campe, K.L., Zhang, Y., et al. (2014). The Cognitive and Behavioral Phenotype of the 16p11.2 Deletion in a Clinically Ascertained Population. Biol. Psychiatry.

45. Qureshi, A.Y., Mueller, S., Snyder, A.Z., Mukherjee, P., Berman, J.I., Roberts, T.P.L., Nagarajan, S.S., Spiro, J.E., Chung, W.K., Sherr, E.H., et al. (2014). Opposing brain differences in 16p11.2 deletion and duplication carriers. J. Neurosci. Off. J. Soc. Neurosci. *34*, 11199–11211.

46. Steinberg, S., de Jong, S., Mattheisen, M., Costas, J., Demontis, D., Jamain, S., Pietiläinen, O.P.H., Lin, K., Papiol, S., Huttenlocher, J., et al. (2014). Common variant at 16p11.2 conferring risk of psychosis. Mol. Psychiatry *19*, 108–114.

47. Reinthaler, E.M., Lal, D., Lebon, S., Hildebrand, M.S., Dahl, H.-H.M., Regan, B.M., Feucht, M., Steinböck, H., Neophytou, B., Ronen, G.M., et al. (2014). 16p11.2 600 kb Duplications confer risk for typical and atypical Rolandic epilepsy. Hum. Mol. Genet. *23*, 6069–6080.

48. Jacquemont, S., Reymond, A., Zufferey, F., Harewood, L., Walters, R.G., Kutalik, Z., Martinet, D., Shen, Y., Valsesia, A., Beckmann, N.D., et al. (2011). Mirror extreme BMI phenotypes associated with gene dosage at the chromosome 16p11.2 locus. Nature *478*, 97–102.

49. Cooper, G.M., Coe, B.P., Girirajan, S., Rosenfeld, J.A., Vu, T.H., Baker, C., Williams, C., Stalker, H., Hamid, R., Hannig, V., et al. (2011). A copy number variation morbidity map of developmental delay. Nat. Genet. *43*, 838–846.

50. Coe, B.P., Witherspoon, K., Rosenfeld, J.A., van Bon, B.W.M., Vulto-van Silfhout, A.T., Bosco, P., Friend, K.L., Baker, C., Buono, S., Vissers, L.E.L.M., et al. (2014). Refining analyses of copy number variation identifies specific genes associated with developmental delay. Nat. Genet. *46*, 1063–1071.

51. Simons Vip Consortium (2012). Simons Variation in Individuals Project (Simons VIP): a genetics-first approach to studying autism spectrum and related neurodevelopmental disorders. Neuron *73*, 1063–1067.

52. Mullen, E. (1995). Mullen Scales of Early Learning, AGS Edition.

53. Eliot, C. (2007). Differential Abilities Scale, 2nd ed.

54. Wechsler, D. (1999). Wechsler Abbreviated Scale of Intelligence.

55. Sudmant, P.H., Mallick, S., Nelson, B.J., Hormozdiari, F., Krumm, N., Huddleston, J., Coe, B.P., Baker, C., Nordenfelt, S., Bamshad, M., et al. (2015). Global diversity, population stratification, and selection of human copy-number variation. Science *349*, aab3761.

56. Manichaikul, A., Mychaleckyj, J.C., Rich, S.S., Daly, K., Sale, M., and Chen, W.-M. (2010). Robust relationship inference in genome-wide association studies. Bioinforma. Oxf. Engl. *26*, 2867–2873.

57. Girirajan, S., Brkanac, Z., Coe, B.P., Baker, C., Vives, L., Vu, T.H., Shafer, N., Bernier, R., Ferrero, G.B., Silengo, M., et al. (2011). Relative burden of large CNVs on a range of neurodevelopmental phenotypes. PLoS Genet. *7*, e1002334.

58. Brys, G., Hubert, M., and Struyf, A. (2004). A Robust Measure of Skewness. J. Comput. Graph. Stat. *13*, 996–1017.

59. Sanders, S.J., He, X., Willsey, A.J., Ercan-Sencicek, A.G., Samocha, K.E., Cicek, A.E., Murtha, M.T., Bal, V.H., Bishop, S.L., Dong, S., et al. (2015). Insights into Autism Spectrum Disorder Genomic Architecture and Biology from 71 Risk Loci. Neuron *87*, 1215–1233.

60. 1000 Genomes Project Consortium, Abecasis, G.R., Auton, A., Brooks, L.D., DePristo, M.A., Durbin, R.M., Handsaker, R.E., Kang, H.M., Marth, G.T., and McVean, G.A. (2012). An integrated map of genetic variation from 1,092 human genomes. Nature *491*, 56–65.

61. Kong, A., Thorleifsson, G., Gudbjartsson, D.F., Masson, G., Sigurdsson, A., Jonasdottir, A., Walters, G.B., Jonasdottir, A., Gylfason, A., Kristinsson, K.T., et al. (2010). Fine-scale

recombination rate differences between sexes, populations and individuals. Nature *467*, 1099–1103.

62. Xu, D., Shen, W., Guo, R., Xue, Y., Peng, W., Sima, J., Yang, J., Sharov, A., Srikantan, S., Yang, J., et al. (2013). Top3β is an RNA topoisomerase that works with fragile X syndrome protein to promote synapse formation. Nat. Neurosci. *16*, 1238–1247.

63. Stoll, G., Pietiläinen, O.P.H., Linder, B., Suvisaari, J., Brosi, C., Hennah, W., Leppä, V., Torniainen, M., Ripatti, S., Ala-Mello, S., et al. (2013). Deletion of TOP3β, a component of FMRP-containing mRNPs, contributes to neurodevelopmental disorders. Nat. Neurosci. *16*, 1228–1237.

64. Hao, Y., Sekine, K., Kawabata, A., Nakamura, H., Ishioka, T., Ohata, H., Katayama, R., Hashimoto, C., Zhang, X., Noda, T., et al. (2004). Apollon ubiquitinates SMAC and caspase-9, and has an essential cytoprotection function. Nat. Cell Biol. *6*, 849–860.

65. Iossifov, I., O'Roak, B.J., Sanders, S.J., Ronemus, M., Krumm, N., Levy, D., Stessman, H.A., Witherspoon, K.T., Vives, L., Patterson, K.E., et al. (2014). The contribution of de novo coding mutations to autism spectrum disorder. Nature *515*, 216–221.

66. De Rubeis, S., He, X., Goldberg, A.P., Poultney, C.S., Samocha, K., Cicek, A.E., Kou, Y., Liu, L., Fromer, M., Walker, S., et al. (2014). Synaptic, transcriptional and chromatin genes disrupted in autism. Nature *515*, 209–215.

67. Wang, K., Zhang, H., Ma, D., Bucan, M., Glessner, J.T., Abrahams, B.S., Salyakina, D., Imielinski, M., Bradfield, J.P., Sleiman, P.M.A., et al. (2009). Common genetic variants on 5p14.1 associate with autism spectrum disorders. Nature *459*, 528–533.

68. Miyashita, A., Arai, H., Asada, T., Imagawa, M., Matsubara, E., Shoji, M., Higuchi, S., Urakami, K., Kakita, A., Takahashi, H., et al. (2007). Genetic association of CTNNA3 with late-onset Alzheimer's disease in females. Hum. Mol. Genet. *16*, 2854–2869.

69. Hehir-Kwa, J.Y., Rodríguez-Santiago, B., Vissers, L.E., de Leeuw, N., Pfundt, R., Buitelaar, J.K., Pérez-Jurado, L.A., and Veltman, J.A. (2011). De novo copy number variants associated with intellectual disability have a paternal origin and age bias. J. Med. Genet. *48*, 776–778.

70. Kong, A., Steinthorsdottir, V., Masson, G., Thorleifsson, G., Sulem, P., Besenbacher, S., Jonasdottir, A., Sigurdsson, A., Kristinsson, K.T., Jonasdottir, A., et al. (2009). Parental origin of sequence variants associated with complex diseases. Nature *462*, 868–874.

71. Delio, M., Guo, T., McDonald-McGinn, D.M., Zackai, E., Herman, S., Kaminetzky, M., Higgins, A.M., Coleman, K., Chow, C., Jalbrzikowski, M., et al. (2013). Enhanced maternal origin of the 22q11.2 deletion in velocardiofacial and DiGeorge syndromes. Am. J. Hum. Genet. *92*, 439–447.

72. López-Correa, C., Dorschner, M., Brems, H., Lázaro, C., Clementi, M., Upadhyaya, M., Dooijes, D., Moog, U., Kehrer-Sawatzki, H., Rutkowski, J.L., et al. (2001). Recombination hotspot in NF1 microdeletion patients. Hum. Mol. Genet. *10*, 1387–1392.

73. Baran, Y., Subramaniam, M., Biton, A., Tukiainen, T., Tsang, E.K., Rivas, M.A., Pirinen, M., Gutierrez-Arcelus, M., Smith, K.S., Kukurba, K.R., et al. (2015). The landscape of genomic imprinting across diverse adult human tissues. Genome Res. *25*, 927–936.

74. Luedi, P.P., Dietrich, F.S., Weidman, J.R., Bosko, J.M., Jirtle, R.L., and Hartemink, A.J. (2007). Computational and experimental identification of novel human imprinted genes. Genome Res. *17*, 1723–1730.

75. Wang, J., Fan, H.C., Behr, B., and Quake, S.R. (2012). Genome-wide single-cell analysis of recombination activity and de novo mutation rates in human sperm. Cell *150*, 402–412.

76. Krumm, N., Turner, T.N., Baker, C., Vives, L., Mohajeri, K., Witherspoon, K., Raja, A., Coe, B.P., Stessman, H.A., He, Z.-X., et al. (2015). Excess of rare, inherited truncating mutations in autism. Nat. Genet. *47*, 582–588.

77. Jacquemont, S., Coe, B.P., Hersch, M., Duyzend, M.H., Krumm, N., Bergmann, S., Beckmann, J.S., Rosenfeld, J.A., and Eichler, E.E. (2014). A higher mutational burden in females supports a "female protective model" in neurodevelopmental disorders. Am. J. Hum. Genet. *94*, 415–425.

78. Männik, K., Mägi, R., Macé, A., Cole, B., Guyatt, A.L., Shihab, H.A., Maillard, A.M., Alavere, H., Kolk, A., Reigo, A., et al. (2015). Copy number variations and cognitive phenotypes in unselected populations. JAMA *313*, 2044–2054.

79. Iossifov, I., Ronemus, M., Levy, D., Wang, Z., Hakker, I., Rosenbaum, J., Yamrom, B., Lee, Y.-H., Narzisi, G., Leotta, A., et al. (2012). De novo gene disruptions in children on the autistic spectrum. Neuron *74*, 285–299.

80. Dajani, R., Hood, A.M., and Coughtrie, M.W. (1998). A single amino acid, glu146, governs the substrate specificity of a human dopamine sulfotransferase, SULT1A3. Mol. Pharmacol. *54*, 942–948.

81. Dennis, M.Y., Nuttle, X., Sudmant, P.H., Antonacci, F., Graves, T.A., Nefedov, M., Rosenfeld, J.A., Sajjadian, S., Malig, M., Kotkiewicz, H., et al. (2012). Evolution of human-specific neural SRGAP2 genes by incomplete segmental duplication. Cell *149*, 912–922.

82. Zhang, J., Kobert, K., Flouri, T., and Stamatakis, A. (2014). PEAR: a fast and accurate Illumina Paired-End reAd mergeR. Bioinforma. Oxf. Engl. *30*, 614–620.

83. Li, H., and Durbin, R. (2010). Fast and accurate long-read alignment with Burrows-Wheeler transform. Bioinforma. Oxf. Engl. *26*, 589–595.

84. Alamut Software.

85. Kircher, M., Witten, D.M., Jain, P., O'Roak, B.J., Cooper, G.M., and Shendure, J. (2014). A general framework for estimating the relative pathogenicity of human genetic variants. Nat. Genet. *46*, 310–315.

86. Boyle, E.A., O'Roak, B.J., Martin, B.K., Kumar, A., and Shendure, J. (2014). MIPgen: optimized modeling and design of molecular inversion probes for targeted resequencing. Bioinforma. Oxf. Engl. *30*, 2670–2672.

87. Garrison, E. VCFlib.

88. Nuttle, X., Huddleston, J., O'Roak, B.J., Antonacci, F., Fichera, M., Romano, C., Shendure, J., and Eichler, E.E. (2013). Rapid and accurate large-scale genotyping of duplicated genes and discovery of interlocus gene conversions. Nat. Methods *10*, 903–909.

89. Danecek, P., Auton, A., Abecasis, G., Albers, C.A., Banks, E., DePristo, M.A., Handsaker, R.E., Lunter, G., Marth, G.T., Sherry, S.T., et al. (2011). The variant call format and VCFtools. Bioinforma. Oxf. Engl. *27*, 2156–2158.

90. Petrovski, S., Wang, Q., Heinzen, E.L., Allen, A.S., and Goldstein, D.B. (2013). Genic intolerance to functional variation and the interpretation of personal genomes. PLoS Genet. *9*, e1003709.

91. Duyzend, M.H., Nuttle, X., Coe, B.P., Baker, C., Nickerson, D.A., Bernier, R., and Eichler, E.E. (2016). Maternal Modifiers and Parent-of-Origin Bias of the Autism-Associated 16p11.2 CNV. Am. J. Hum. Genet. *98*, 45–57.

92. Christian, S.L., Brune, C.W., Sudi, J., Kumar, R.A., Liu, S., Karamohamed, S., Badner, J.A., Matsui, S., Conroy, J., McQuaid, D., et al. (2008). Novel submicroscopic chromosomal abnormalities detected in autism spectrum disorder. Biol. Psychiatry *63*, 1111–1117.

93. Pinto, D., Pagnamenta, A.T., Klei, L., Anney, R., Merico, D., Regan, R., Conroy, J., Magalhaes, T.R., Correia, C., Abrahams, B.S., et al. (2010). Functional impact of global rare copy number variation in autism spectrum disorders. Nature *466*, 368–372.

94. Girirajan, S., Dennis, M.Y., Baker, C., Malig, M., Coe, B.P., Campbell, C.D., Mark, K., Vu, T.H., Alkan, C., Cheng, Z., et al. (2013). Refinement and discovery of new hotspots of copy-number variation associated with autism spectrum disorder. Am. J. Hum. Genet. *92*, 221–237.

95. Ikeda, M., Tomita, Y., Mouri, A., Koga, M., Okochi, T., Yoshimura, R., Yamanouchi, Y., Kinoshita, Y., Hashimoto, R., Williams, H.J., et al. (2010). Identification of novel candidate genes for treatment response to risperidone and susceptibility for schizophrenia: integrated analysis among pharmacogenomics, mouse expression, and genetic case-control association approaches. Biol. Psychiatry *67*, 263–269.

96. Low, D., and Chen, K.-S. (2010). Genome-wide gene expression profiling of the Angelman syndrome mice with Ube3a mutation. Eur. J. Hum. Genet. EJHG *18*, 1228–1235.

97. Savelieva, K.V., Rajan, I., Baker, K.B., Vogel, P., Jarman, W., Allen, M., and Lanthorn, T.H. (2008). Learning and memory impairment in Eph receptor A6 knockout mice. Neurosci. Lett. *438*, 205–209.

98. Glessner, J.T., Wang, K., Cai, G., Korvatska, O., Kim, C.E., Wood, S., Zhang, H., Estes, A., Brune, C.W., Bradfield, J.P., et al. (2009). Autism genome-wide copy number variation reveals ubiquitin and neuronal genes. Nature *459*, 569–573.

99. Vaags, A.K., Lionel, A.C., Sato, D., Goodenberger, M., Stein, Q.P., Curran, S., Ogilvie, C., Ahn, J.W., Drmic, I., Senman, L., et al. (2012). Rare deletions at the neurexin 3 locus in autism spectrum disorder. Am. J. Hum. Genet. *90*, 133–141.

100. Alazami, A.M., Patel, N., Shamseldin, H.E., Anazi, S., Al-Dosari, M.S., Alzahrani, F., Hijazi, H., Alshammari, M., Aldahmesh, M.A., Salih, M.A., et al. (2015). Accelerating novel candidate gene discovery in neurogenetic disorders via whole-exome sequencing of prescreened multiplex consanguineous families. Cell Rep. *10*, 148–161.

101. Alvarez-Mora, M.I., Calvo Escalona, R., Puig Navarro, O., Madrigal, I., Quintela, I., Amigo, J., Martinez-Elurbe, D., Linder-Lucht, M., Aznar Lain, G., Carracedo, A., et al. (2016). Comprehensive molecular testing in patients with high functioning autism spectrum disorder. Mutat. Res. *784–785*, 46–52.

102. Alazami, A.M., Alzahrani, F., Bohlega, S., and Alkuraya, F.S. (2014). SET binding factor 1 (SBF1) mutation causes Charcot-Marie-tooth disease type 4B3. Neurology *82*, 1665–1666.

103. Nakhro, K., Park, J.-M., Hong, Y.B., Park, J.H., Nam, S.H., Yoon, B.R., Yoo, J.H., Koo, H., Jung, S.-C., Kim, H.-L., et al. (2013). SET binding factor 1 (SBF1) mutation causes Charcot-Marie-Tooth disease type 4B3. Neurology *81*, 165–173.

104. Nava, C., Keren, B., Mignot, C., Rastetter, A., Chantot-Bastaraud, S., Faudet, A., Fonteneau, E., Amiet, C., Laurent, C., Jacquette, A., et al. (2014). Prospective diagnostic analysis of copy number variants using SNP microarrays in individuals with autism spectrum disorders. Eur. J. Hum. Genet. EJHG *22*, 71–78.

105. Veilleux, R.E., Shen, L.Y., and Paz, M.M. (1995). Analysis of the genetic composition of anther-derived potato by randomly amplified polymorphic DNA and simple sequence repeats. Genome Natl. Res. Counc. Can. Génome Cons. Natl. Rech. Can. *38*, 1153–1162.

106. Boyden, E.D., Campos-Xavier, A.B., Kalamajski, S., Cameron, T.L., Suarez, P., Tanackovic, G., Tanackovich, G., Andria, G., Ballhausen, D., Briggs, M.D., et al. (2011). Recurrent dominant mutations affecting two adjacent residues in the motor domain of the monomeric kinesin KIF22 result in skeletal dysplasia and joint laxity. Am. J. Hum. Genet. *89*, 767–772.

107. Valente, P., Castroflorio, E., Rossi, P., Fadda, M., Sterlini, B., Cervigni, R.I., Prestigio, C., Giovedì, S., Onofri, F., Mura, E., et al. (2016). PRRT2 Is a Key Component of the Ca(2+)-Dependent Neurotransmitter Release Machinery. Cell Rep. *15*, 117–131.

108. Maini, I., Iodice, A., Spagnoli, C., Salerno, G.G., Bertani, G., Frattini, D., and Fusco, C. (2016). Expanding phenotype of PRRT2 gene mutations: A new case with epilepsy and benign myoclonus of early infancy. Eur. J. Paediatr. Neurol. EJPN Off. J. Eur. Paediatr. Neurol. Soc. *20*, 454–456.

109. Ebrahimi-Fakhari, D., Saffari, A., Westenberger, A., and Klein, C. (2015). The evolving spectrum of PRRT2-associated paroxysmal diseases. Brain J. Neurol. *138*, 3476–3495.

110. Corominas, R., Yang, X., Lin, G.N., Kang, S., Shen, Y., Ghamsari, L., Broly, M., Rodriguez, M., Tam, S., Trigg, S.A., et al. (2014). Protein interaction network of alternatively spliced isoforms from brain links genetic risk factors for autism. Nat. Commun. *5*, 3650.

111. Navarro, L., Gil-Benso, R., Megías, J., Muñoz-Hidalgo, L., San-Miguel, T., Callaghan, R.C., González-Darder, J.M., López-Ginés, C., and Cerdá-Nicolás, M.J. (2015). Alteration of major vault protein in human glioblastoma and its relation with EGFR and PTEN status. Neuroscience *297*, 243–251.

112. Li, H., Mapolelo, D.T., Randeniya, S., Johnson, M.K., and Outten, C.E. (2012). Human glutaredoxin 3 forms [2Fe-2S]-bridged complexes with human BolA2. Biochemistry (Mosc.) *51*, 1687–1696.

113. Banci, L., Camponeschi, F., Ciofi-Baffoni, S., and Muzzioli, R. (2015). Elucidating the Molecular Function of Human BOLA2 in GRX3-Dependent Anamorsin Maturation Pathway. J. Am. Chem. Soc. *137*, 16133–16143.

114. Nowick, K., Gernat, T., Almaas, E., and Stubbs, L. (2009). Differences in human and chimpanzee gene expression patterns define an evolving network of transcription factors in brain. Proc. Natl. Acad. Sci. U. S. A. *106*, 22358–22363.

115. Fekairi, S., Scaglione, S., Chahwan, C., Taylor, E.R., Tissier, A., Coulon, S., Dong, M.-Q., Ruse, C., Yates, J.R., Russell, P., et al. (2009). Human SLX4 is a Holliday junction resolvase subunit that binds multiple DNA repair/recombination endonucleases. Cell *138*, 78–89.

116. Wyatt, H.D.M., Sarbajna, S., Matos, J., and West, S.C. (2013). Coordinated actions of SLX1-SLX4 and MUS81-EME1 for Holliday junction resolution in human cells. Mol. Cell *52*, 234–247.

117. Muñoz, I.M., Hain, K., Déclais, A.-C., Gardiner, M., Toh, G.W., Sanchez-Pulido, L., Heuckmann, J.M., Toth, R., Macartney, T., Eppink, B., et al. (2009). Coordination of structure-specific nucleases by human SLX4/BTBD12 is required for DNA repair. Mol. Cell *35*, 116–127.

118. Svendsen, J.M., Smogorzewska, A., Sowa, M.E., O'Connell, B.C., Gygi, S.P., Elledge, S.J., and Harper, J.W. (2009). Mammalian BTBD12/SLX4 assembles a Holliday junction resolvase and is required for DNA repair. Cell *138*, 63–77.

119. Fricke, W.M., and Brill, S.J. (2003). Slx1-Slx4 is a second structure-specific endonuclease functionally redundant with Sgs1-Top3. Genes Dev. *17*, 1768–1778.

120. Saito, T.T., Mohideen, F., Meyer, K., Harper, J.W., and Colaiácovo, M.P. (2012). SLX-1 is required for maintaining genomic integrity and promoting meiotic noncrossovers in the Caenorhabditis elegans germline. PLoS Genet. *8*, e1002888.

121. Wan, B., Yin, J., Horvath, K., Sarkar, J., Chen, Y., Wu, J., Wan, K., Lu, J., Gu, P., Yu, E.Y., et al. (2013). SLX4 assembles a telomere maintenance toolkit by bridging multiple endonucleases with telomeres. Cell Rep. *4*, 861–869.

122. Wilson, J.S.J., Tejera, A.M., Castor, D., Toth, R., Blasco, M.A., and Rouse, J. (2013). Localization-dependent and -independent roles of SLX4 in regulating telomeres. Cell Rep. *4*, 853–860.

123. Sarkar, J., Wan, B., Yin, J., Vallabhaneni, H., Horvath, K., Kulikowicz, T., Bohr, V.A., Zhang, Y., Lei, M., and Liu, Y. (2015). SLX4 contributes to telomere preservation and regulated processing of telomeric joint molecule intermediates. Nucleic Acids Res. *43*, 5912–5923.

124. Gaur, V., Wyatt, H.D.M., Komorowska, W., Szczepanowski, R.H., de Sanctis, D., Gorecka, K.M., West, S.C., and Nowotny, M. (2015). Structural and Mechanistic Analysis of the Slx1-Slx4 Endonuclease. Cell Rep.

125. Chauhan, A., and Chauhan, V. (2006). Oxidative stress in autism. Pathophysiol. Off. J. Int. Soc. Pathophysiol. ISP *13*, 171–181.

126. Hildebrandt, M.A.T., Salavaggione, O.E., Martin, Y.N., Flynn, H.C., Jalal, S., Wieben, E.D., and Weinshilboum, R.M. (2004). Human SULT1A3 pharmacogenetics: gene duplication and functional genomic studies. Biochem. Biophys. Res. Commun. *321*, 870–878.

127. Aksoy, I.A., and Weinshilboum, R.M. (1995). Human thermolabile phenol sulfotransferase gene (STM): molecular cloning and structural characterization. Biochem. Biophys. Res. Commun. *208*, 786–795.

128. Brix, L.A., Barnett, A.C., Duggleby, R.G., Leggett, B., and McManus, M.E. (1999). Analysis of the substrate specificity of human sulfotransferases SULT1A1 and SULT1A3: site-directed mutagenesis and kinetic studies. Biochemistry (Mosc.) *38*, 10474–10479.

129. Allali-Hassani, A., Pan, P.W., Dombrovski, L., Najmanovich, R., Tempel, W., Dong, A., Loppnau, P., Martin, F., Thornton, J., Thonton, J., et al. (2007). Structural and chemical profiling of the human cytosolic sulfotransferases. PLoS Biol. *5*, e97.

130. Lu, J.-H., Li, H.-T., Liu, M.-C., Zhang, J.-P., Li, M., An, X.-M., and Chang, W.-R. (2005). Crystal structure of human sulfotransferase SULT1A3 in complex with dopamine and 3'-phosphoadenosine 5'-phosphate. Biochem. Biophys. Res. Commun. *335*, 417–423.

131. Goldstein, D.S., Swoboda, K.J., Miles, J.M., Coppack, S.W., Aneman, A., Holmes, C., Lamensdorf, I., and Eisenhofer, G. (1999). Sources and physiological significance of plasma dopamine sulfate. J. Clin. Endocrinol. Metab. *84*, 2523–2531.

132. Salman, E.D., Kadlubar, S.A., and Falany, C.N. (2009). Expression and localization of cytosolic sulfotransferase (SULT) 1A1 and SULT1A3 in normal human brain. Drug Metab. Dispos. Biol. Fate Chem. *37*, 706–709.

133. Sidharthan, N.P., Minchin, R.F., and Butcher, N.J. (2013). Cytosolic sulfotransferase 1A3 is induced by dopamine and protects neuronal cells from dopamine toxicity: role of D1 receptor-N-methyl-D-aspartate receptor coupling. J. Biol. Chem. *288*, 34364–34374.

134. Riches, Z., Stanley, E.L., Bloomer, J.C., and Coughtrie, M.W.H. (2009). Quantitative evaluation of the expression and activity of five major sulfotransferases (SULTs) in human tissues: the SULT "pie." Drug Metab. Dispos. Biol. Fate Chem. *37*, 2255–2261.

135. Dajani, R., Cleasby, A., Neu, M., Wonacott, A.J., Jhoti, H., Hood, A.M., Modi, S., Hersey, A., Taskinen, J., Cooke, R.M., et al. (1999). X-ray crystal structure of human dopamine sulfotransferase, SULT1A3. Molecular modeling and quantitative structure-activity relationship analysis demonstrate a molecular basis for sulfotransferase substrate specificity. J. Biol. Chem. *274*, 37862–37868.

136. Gamage, N., Barnett, A., Hempel, N., Duggleby, R.G., Windmill, K.F., Martin, J.L., and McManus, M.E. (2006). Human sulfotransferases and their role in chemical metabolism. Toxicol. Sci. Off. J. Soc. Toxicol. *90*, 5–22.

137. Christensen, D.L., Baio, J., Braun, K.V.N., Bilder, D., Charles, J., Constantino, J.N., Daniels, J., Durkin, M.S., Fitzgerald, R.T., Kurzius-Spencer, M., et al. (2016). Prevalence and Characteristics of Autism Spectrum Disorder Among Children Aged 8 Years — Autism and Developmental Disabilities Monitoring Network, 11 Sites, United States, 2012. MMWR Surveill. Summ. *65*, 1–23.

138. American Psychiatric Association (2013). Diagnostic and statistical manual of mental disorders: DSM-5 (Washington, D.C: American Psychiatric Association).

139. Werling, D.M., and Geschwind, D.H. (2015). Recurrence rates provide evidence for sex-differential, familial genetic liability for autism spectrum disorders in multiplex families and twins. Mol. Autism *6*, 27.

140. Hallmayer, J., Cleveland, S., Torres, A., Phillips, J., Cohen, B., Torigoe, T., Miller, J., Fedele, A., Collins, J., Smith, K., et al. (2011). Genetic heritability and shared environmental factors among twin pairs with autism. Arch. Gen. Psychiatry *68*, 1095–1102.

141. O'Roak, B.J., Vives, L., Fu, W., Egertson, J.D., Stanaway, I.B., Phelps, I.G., Carvill, G., Kumar, A., Lee, C., Ankenman, K., et al. (2012). Multiplex targeted sequencing identifies recurrently mutated genes in autism spectrum disorders. Science *338*, 1619–1622.

142. O'Roak, B.J., Deriziotis, P., Lee, C., Vives, L., Schwartz, J.J., Girirajan, S., Karakoc, E., Mackenzie, A.P., Ng, S.B., Baker, C., et al. (2011). Exome sequencing in sporadic autism spectrum disorders identifies severe de novo mutations. Nat. Genet. *43*, 585–589.

143. O'Roak, B.J., Vives, L., Girirajan, S., Karakoc, E., Krumm, N., Coe, B.P., Levy, R., Ko, A., Lee, C., Smith, J.D., et al. (2012). Sporadic autism exomes reveal a highly interconnected protein network of de novo mutations. Nature *485*, 246–250.

144. Hoischen, A., Krumm, N., and Eichler, E.E. (2014). Prioritization of neurodevelopmental disease genes by discovery of new mutations. Nat. Neurosci. *17*, 764–772.

145. Robinson, E.B., St Pourcain, B., Anttila, V., Kosmicki, J.A., Bulik-Sullivan, B., Grove, J., Maller, J., Samocha, K.E., Sanders, S.J., Ripke, S., et al. (2016). Genetic risk for autism spectrum disorders and neuropsychiatric variation in the general population. Nat. Genet.

146. Risi, S., Lord, C., Gotham, K., Corsello, C., Chrysler, C., Szatmari, P., Cook, E.H., Leventhal, B.L., and Pickles, A. (2006). Combining information from multiple sources in the diagnosis of autism spectrum disorders. J. Am. Acad. Child Adolesc. Psychiatry *45*, 1094–1103.

147. Krumm, N., Sudmant, P.H., Ko, A., O'Roak, B.J., Malig, M., Coe, B.P., NHLBI Exome Sequencing Project, Quinlan, A.R., Nickerson, D.A., and Eichler, E.E. (2012). Copy number variation detection and genotyping from exome sequence data. Genome Res. *22*, 1525–1532.

148. Krumm, N., Turner, T.N., Baker, C., Vives, L., Mohajeri, K., Witherspoon, K., Raja, A., Coe, B.P., Stessman, H.A., He, Z.-X., et al. (2015). Excess of rare, inherited truncating mutations in autism. Nat. Genet. *47*, 582–588.

149. Mi, H., Muruganujan, A., Casagrande, J.T., and Thomas, P.D. (2013). Large-scale gene function analysis with the PANTHER classification system. Nat. Protoc. *8*, 1551–1566.

150. Szklarczyk, D., Franceschini, A., Wyder, S., Forslund, K., Heller, D., Huerta-Cepas, J., Simonovic, M., Roth, A., Santos, A., Tsafou, K.P., et al. (2015). STRING v10: protein-protein interaction networks, integrated over the tree of life. Nucleic Acids Res. *43*, D447-452.

151. Kheradmand Kia, S., Verbeek, E., Engelen, E., Schot, R., Poot, R.A., de Coo, I.F.M., Lequin, M.H., Poulton, C.J., Pourfarzad, F., Grosveld, F.G., et al. (2012). RTTN mutations link primary cilia function to organization of the human cerebral cortex. Am. J. Hum. Genet. *91*, 533–540.

152. Shamseldin, H., Alazami, A.M., Manning, M., Hashem, A., Caluseiu, O., Tabarki, B., Esplin, E., Schelley, S., Innes, A.M., Parboosingh, J.S., et al. (2015). RTTN Mutations Cause Primary Microcephaly and Primordial Dwarfism in Humans. Am. J. Hum. Genet. *97*, 862–868.

153. Christopherson, K.S., Ullian, E.M., Stokes, C.C.A., Mullowney, C.E., Hell, J.W., Agah, A., Lawler, J., Mosher, D.F., Bornstein, P., and Barres, B.A. (2005). Thrombospondins are astrocyte-secreted proteins that promote CNS synaptogenesis. Cell *120*, 421–433.

154. Lu, L., Guo, H., Peng, Y., Xun, G., Liu, Y., Xiong, Z., Tian, D., Liu, Y., Li, W., Xu, X., et al. (2014). Common and rare variants of the THBS1 gene associated with the risk for autism. Psychiatr. Genet. *24*, 235–240.

155. Smith, T.S., Southan, C., Ellington, K., Campbell, D., Tew, D.G., and Debouck, C. (2001). Identification, genomic organization, and mRNA expression of LACTB, encoding a serine beta-lactamase-like protein with an amino-terminal transmembrane domain. Genomics *78*, 12–14.

156. Khan, M.A., Rafiq, M.A., Noor, A., Hussain, S., Flores, J.V., Rupp, V., Vincent, A.K., Malli, R., Ali, G., Khan, F.S., et al. (2012). Mutation in NSUN2, which encodes an RNA methyltransferase, causes autosomal-recessive intellectual disability. Am. J. Hum. Genet. *90*, 856–863.

157. Martinez, F.J., Lee, J.H., Lee, J.E., Blanco, S., Nickerson, E., Gabriel, S., Frye, M., Al-Gazali, L., and Gleeson, J.G. (2012). Whole exome sequencing identifies a splicing mutation in NSUN2 as a cause of a Dubowitz-like syndrome. J. Med. Genet. *49*, 380–385.

158. Clark, A.W., Mauro, A., Longenecker, H.E., and Hurlbut, W.P. (1970). Effects of black widow spider venom on the frog neuromuscular junction. Effects on the fine structure of the frog neuromuscular junction. Nature *225*, 703–705.

159. Longenecker, H.E., Hurlbut, W.P., Mauro, A., and Clark, A.W. (1970). Effects of black widow spider venom on the frog neuromuscular junction. Effects on end-plate potential, miniature end-plate potential and nerve terminal spike. Nature *225*, 701–703.

160. Silva, J.-P., and Ushkaryov, Y.A. (2010). The latrophilins, "split-personality" receptors. Adv. Exp. Med. Biol. *706*, 59–75.

161. Bishop, D.F., Henderson, A.S., and Astrin, K.H. (1990). Human delta-aminolevulinate synthase: assignment of the housekeeping gene to 3p21 and the erythroid-specific gene to the X chromosome. Genomics *7*, 207–214.

162. Stessman, H.A.F., Willemsen, M.H., Fenckova, M., Penn, O., Hoischen, A., Xiong, B., Wang, T., Hoekzema, K., Vives, L., Vogel, I., et al. (2016). Disruption of POGZ Is Associated with Intellectual Disability and Autism Spectrum Disorders. Am. J. Hum. Genet. *98*, 541–552.

163. White, J., Beck, C.R., Harel, T., Posey, J.E., Jhangiani, S.N., Tang, S., Farwell, K.D., Powis, Z., Mendelsohn, N.J., Baker, J.A., et al. (2016). POGZ truncating alleles cause syndromic intellectual disability. Genome Med. *8*, 3.

164. Petersen, P.H., Zou, K., Hwang, J.K., Jan, Y.N., and Zhong, W. (2002). Progenitor cell maintenance requires numb and numblike during mouse neurogenesis. Nature *419*, 929–934.

165. Li, H.S., Wang, D., Shen, Q., Schonemann, M.D., Gorski, J.A., Jones, K.R., Temple, S., Jan, L.Y., and Jan, Y.N. (2003). Inactivation of Numb and Numblike in embryonic dorsal forebrain impairs neurogenesis and disrupts cortical morphogenesis. Neuron *40*, 1105–1118.

166. Petersen, P.H., Zou, K., Krauss, S., and Zhong, W. (2004). Continuing role for mouse Numb and Numbl in maintaining progenitor cells during cortical neurogenesis. Nat. Neurosci. *7*, 803–811.

167. Pettem, K.L., Yokomaku, D., Luo, L., Linhoff, M.W., Prasad, T., Connor, S.A., Siddiqui, T.J., Kawabe, H., Chen, F., Zhang, L., et al. (2013). The specific α-neurexin interactor calsyntenin-3 promotes excitatory and inhibitory synapse development. Neuron *80*, 113–128.

168. Anitha, A., Nakamura, K., Thanseem, I., Yamada, K., Iwayama, Y., Toyota, T., Matsuzaki, H., Miyachi, T., Yamada, S., Tsujii, M., et al. (2012). Brain region-specific altered expression and association of mitochondria-related genes in autism. Mol. Autism *3*, 12.

169. Pitts, K.R., McNiven, M.A., and Yoon, Y. (2004). Mitochondria-specific function of the dynamin family protein DLP1 is mediated by its C-terminal domains. J. Biol. Chem. *279*, 50286–50294.

170. Laffin, J.J.S., Raca, G., Jackson, C.A., Strand, E.A., Jakielski, K.J., and Shriberg, L.D. (2012). Novel candidate genes and regions for childhood apraxia of speech identified by array comparative genomic hybridization. Genet. Med. Off. J. Am. Coll. Med. Genet. *14*, 928–936.

171. Hormozdiari, F., Penn, O., Borenstein, E., and Eichler, E.E. (2015). The discovery of integrated gene networks for autism and related disorders. Genome Res. *25*, 142–154.

172. De Rubeis, S., and Bagni, C. (2011). Regulation of molecular pathways in the Fragile X Syndrome: insights into Autism Spectrum Disorders. J. Neurodev. Disord. *3*, 257–269.

173. Richter, J.D., Bassell, G.J., and Klann, E. (2015). Dysregulation and restoration of translational homeostasis in fragile X syndrome. Nat. Rev. Neurosci. *16*, 595–605.

174. Dillon, C., and Goda, Y. (2005). The actin cytoskeleton: integrating form and function at the synapse. Annu. Rev. Neurosci. *28*, 25–55.

175. Fischer, M., Kaech, S., Knutti, D., and Matus, A. (1998). Rapid actin-based plasticity in dendritic spines. Neuron *20*, 847–854.

176. Duffney, L.J., Zhong, P., Wei, J., Matas, E., Cheng, J., Qin, L., Ma, K., Dietz, D.M., Kajiwara, Y., Buxbaum, J.D., et al. (2015). Autism-like Deficits in Shank3-Deficient Mice Are Rescued by Targeting Actin Regulators. Cell Rep. *11*, 1400–1413.

177. Turner, T.N., Hormozdiari, F., Duyzend, M.H., McClymont, S.A., Hook, P.W., Iossifov, I., Raja, A., Baker, C., Hoekzema, K., Stessman, H.A., et al. (2016). Genome Sequencing of Autism-Affected Families Reveals Disruption of Putative Noncoding Regulatory DNA. Am. J. Hum. Genet. *98*, 58–74.

178. de Vries, B.B., White, S.M., Knight, S.J., Regan, R., Homfray, T., Young, I.D., Super, M., McKeown, C., Splitt, M., Quarrell, O.W., et al. (2001). Clinical studies on submicroscopic subtelomeric rearrangements: a checklist. J. Med. Genet. *38*, 145–150.

179. van Bon, B.W.M., Coe, B.P., Bernier, R., Green, C., Gerdts, J., Witherspoon, K., Kleefstra, T., Willemsen, M.H., Kumar, R., Bosco, P., et al. (2015). Disruptive de novo mutations of DYRK1A lead to a syndromic form of autism and ID. Mol. Psychiatry.

180. Willsey, A.J., Sanders, S.J., Li, M., Dong, S., Tebbenkamp, A.T., Muhle, R.A., Reilly, S.K., Lin, L., Fertuzinhos, S., Miller, J.A., et al. (2013). Coexpression networks implicate human midfetal deep cortical projection neurons in the pathogenesis of autism. Cell *155*, 997–1007.

181. Parikshak, N.N., Luo, R., Zhang, A., Won, H., Lowe, J.K., Chandran, V., Horvath, S., and Geschwind, D.H. (2013). Integrative functional genomic analyses implicate specific molecular pathways and circuits in autism. Cell *155*, 1008–1021.

182. Parikshak, N.N., Gandal, M.J., and Geschwind, D.H. (2015). Systems biology and gene networks in neurodevelopmental and neurodegenerative disorders. Nat. Rev. Genet. *16*, 441–458.

183. Hoischen, A., van Bon, B.W.M., Gilissen, C., Arts, P., van Lier, B., Steehouwer, M., de Vries, P., de Reuver, R., Wieskamp, N., Mortier, G., et al. (2010). De novo mutations of SETBP1 cause Schinzel-Giedion syndrome. Nat. Genet. *42*, 483–485.

184. Filges, I., Shimojima, K., Okamoto, N., Röthlisberger, B., Weber, P., Huber, A.R., Nishizawa, T., Datta, A.N., Miny, P., and Yamamoto, T. (2011). Reduced expression by SETBP1 haploinsufficiency causes developmental and expressive language delay indicating a phenotype distinct from Schinzel-Giedion syndrome. J. Med. Genet. *48*, 117–122.

Appendix A. Supplemental Information for Chapter 2

Supplemental Figures

Supplemental Appendix

Supplemental Tables

Supplemental Web Resources

Supplemental References

Supplemental Figures

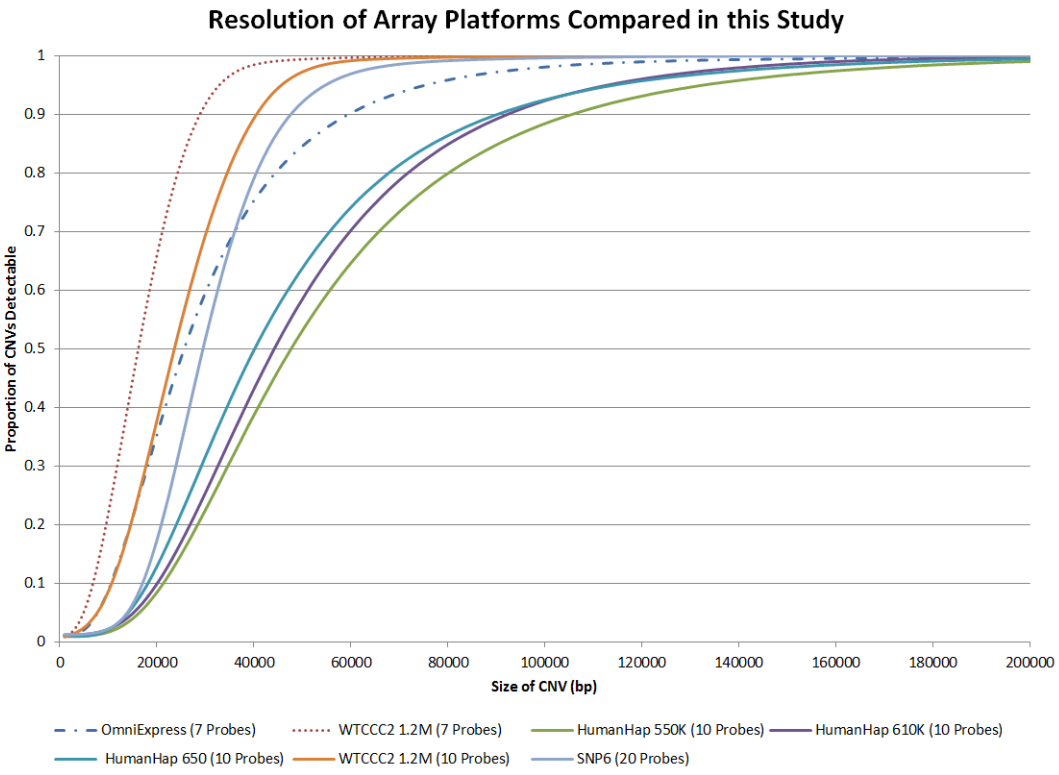

Figure S1: The sensitivity of the SNP microarray platforms used in this study. The number of probes required in each simulated CNV is listed. We used the method for calculating sensitivity by Coe *et al*.[1]

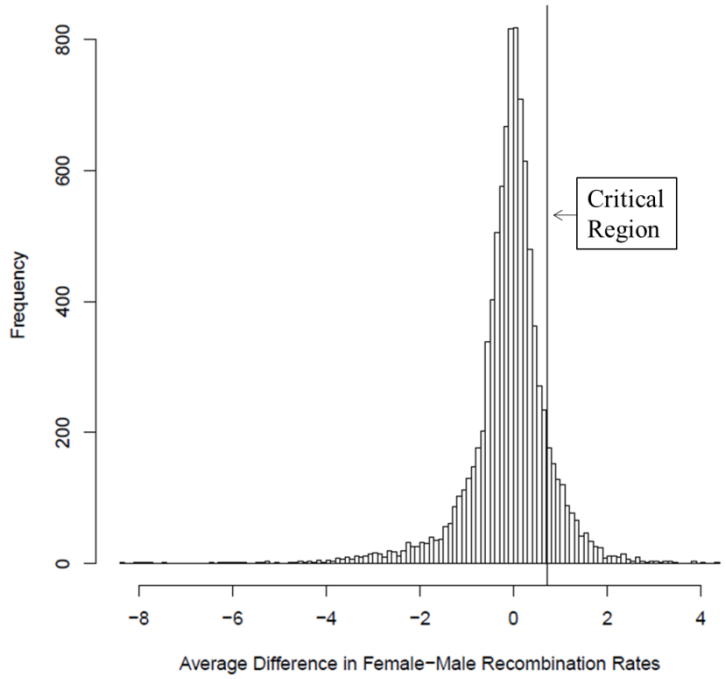

Figure S2: **Average difference in female-male recombination rates for 550 kbp windows genome-wide.** The average difference in female and male recombination rates were calculated for ten thousand 550 kbp windows (the same size as the 16p11.2 critical region), excluding sex chromosomes, regions with segmental duplications, and gaps. The 16p11.2 critical region is in the 87th percentile for the average difference amongst these regions.

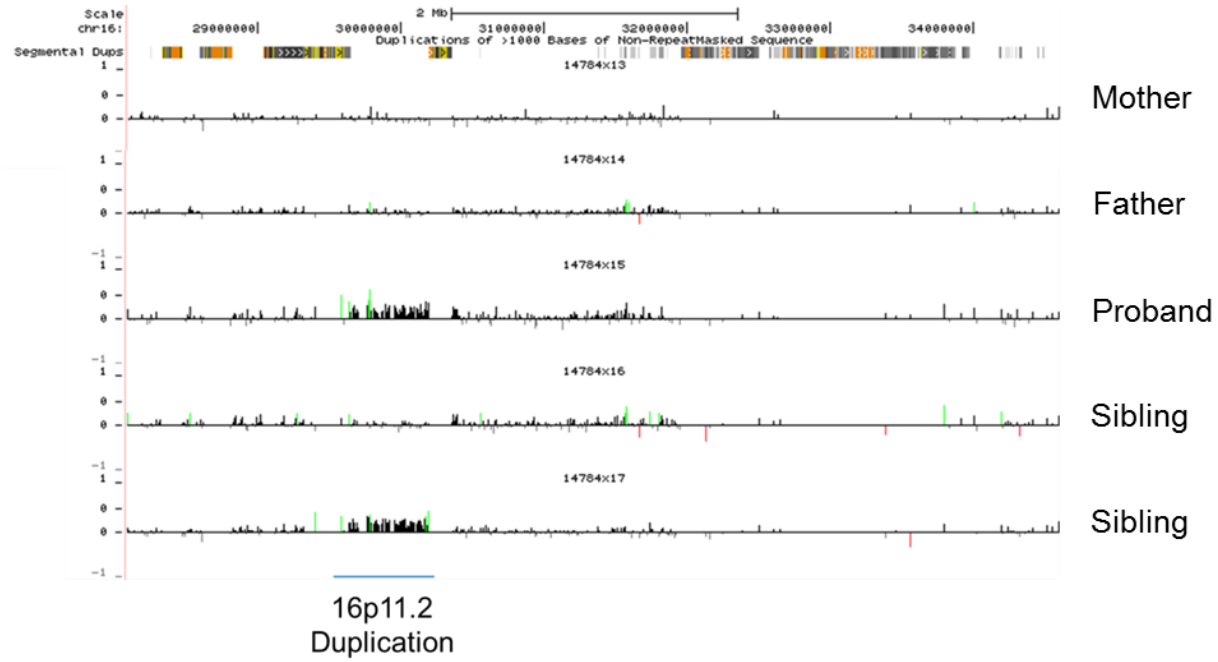

Figure S3: Incorrect inheritance pattern for family 14784. This proband (14784.x15) was labelled as having a de novo duplication, but the sibling (14784.x17), listed as a non-carrier, also carries a duplication. Since the event is not present in the parents (14784.x13, mother; 14784.x14, father), this is likely the result of germline mosaicism.

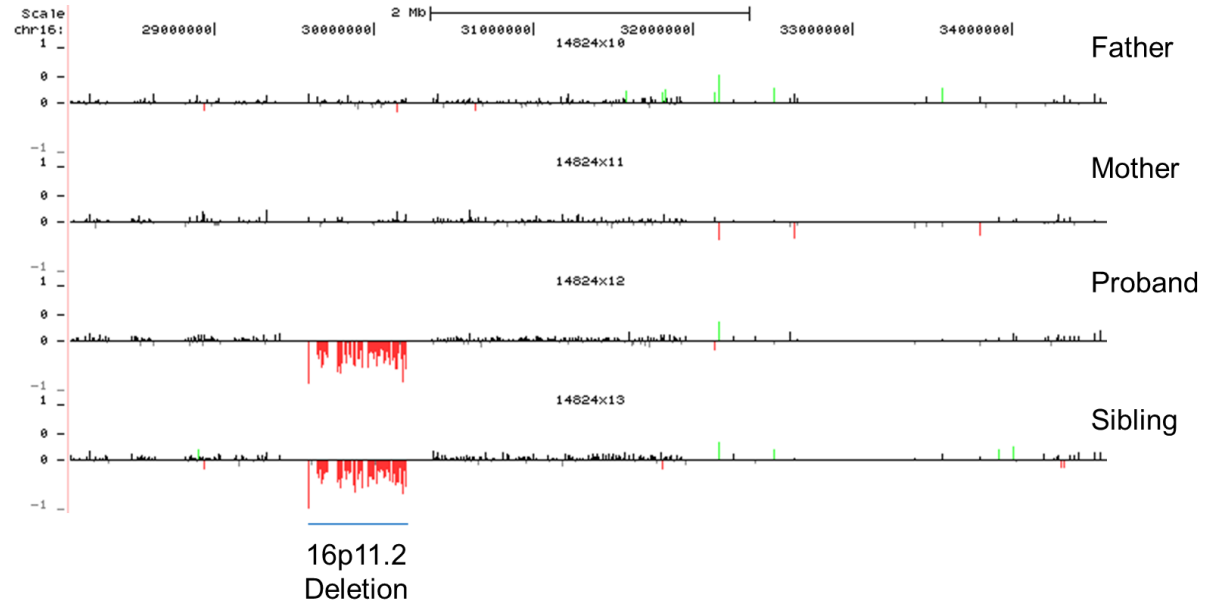

Figure S4: Monozygotic twins in family 14824 with a de novo 16p11.2 deletion.

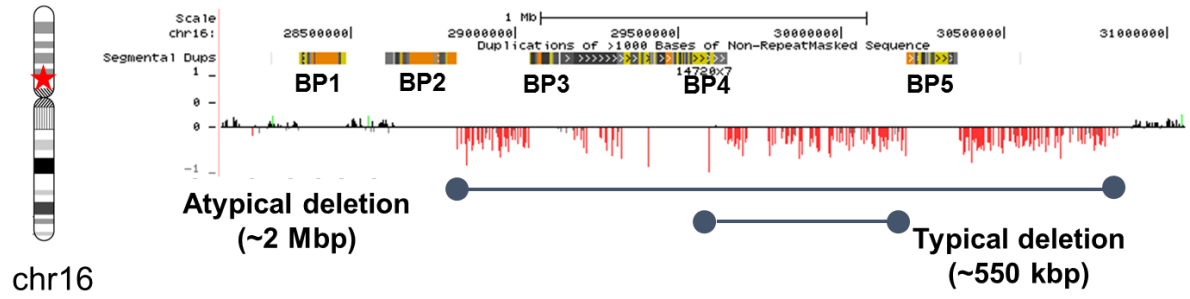

Figure S5: Atypical 16p11.2 deletion. One individual in the cohort (14720.x10) had an atypical de novo 16p11.2 deletion that extends from breakpoint 2 beyond breakpoint 5 with nearly 2 Mbp of genomic DNA deleted.

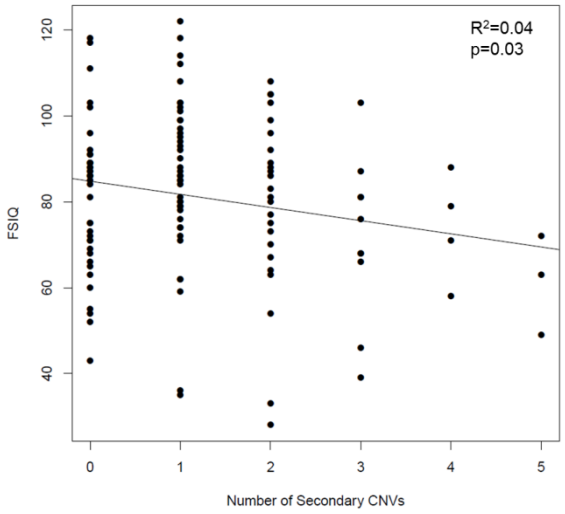

Figure S6: Correlation of FSIQ and the number of secondary CNVs in screened probands. There is a modest, statistically significant correlation between the FSIQ and number of secondary CNVs present in the screened probands (R^2=0.04, p=0.03).

a.

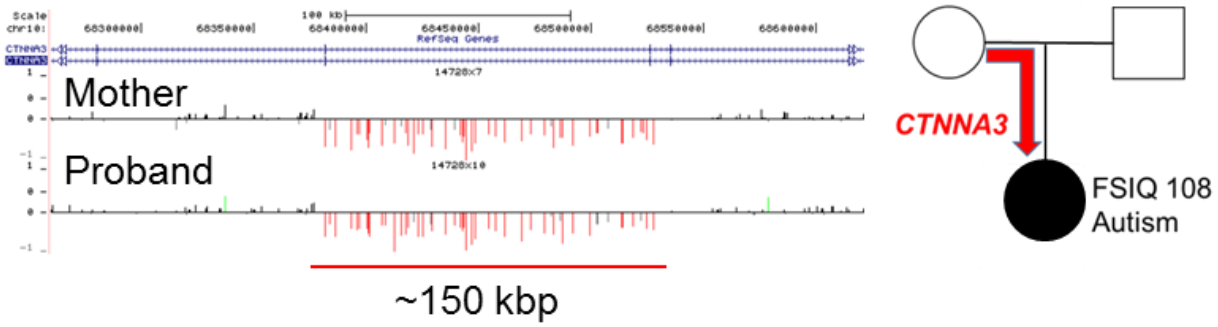

b.

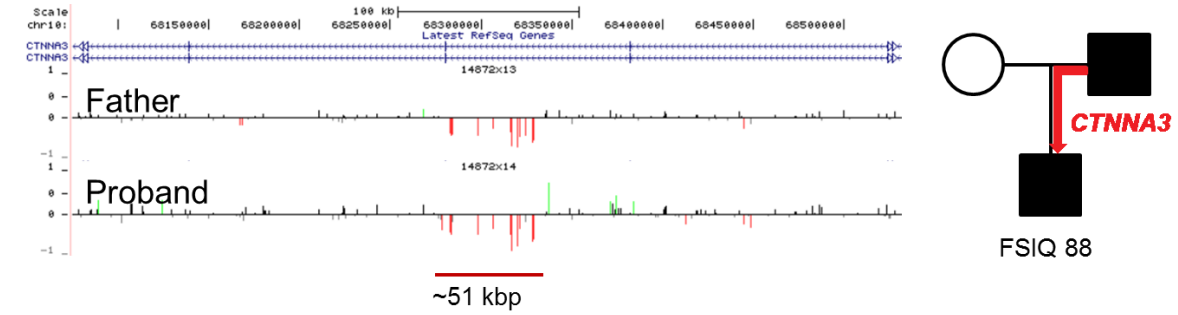

Figure S7: Secondary deletions of *CTNNA3* in 16p11.2 duplication families. We found a recurrent secondary deletion in two 16p11.2 duplication families affecting a gene associated with autism risk variants, αT-catenin, *CTNNA3*. (a) A ~150 kbp deletion involving *CTNNA3* is transmitted from mother to daughter who also carries a 16p11.2 de novo duplication. (b) A ~50 kbp deletion transmitted from father to son. Both father and son carry the 16p11.2 duplication. While both of these CNVs are individually rare, there are a similar number of cases and controls with events across *CTNNA*.[2] However, two large studies have found genetic association between *CTNNA3* and autism[3,4] and rare deletions have been identified in individuals with ASD.[5]

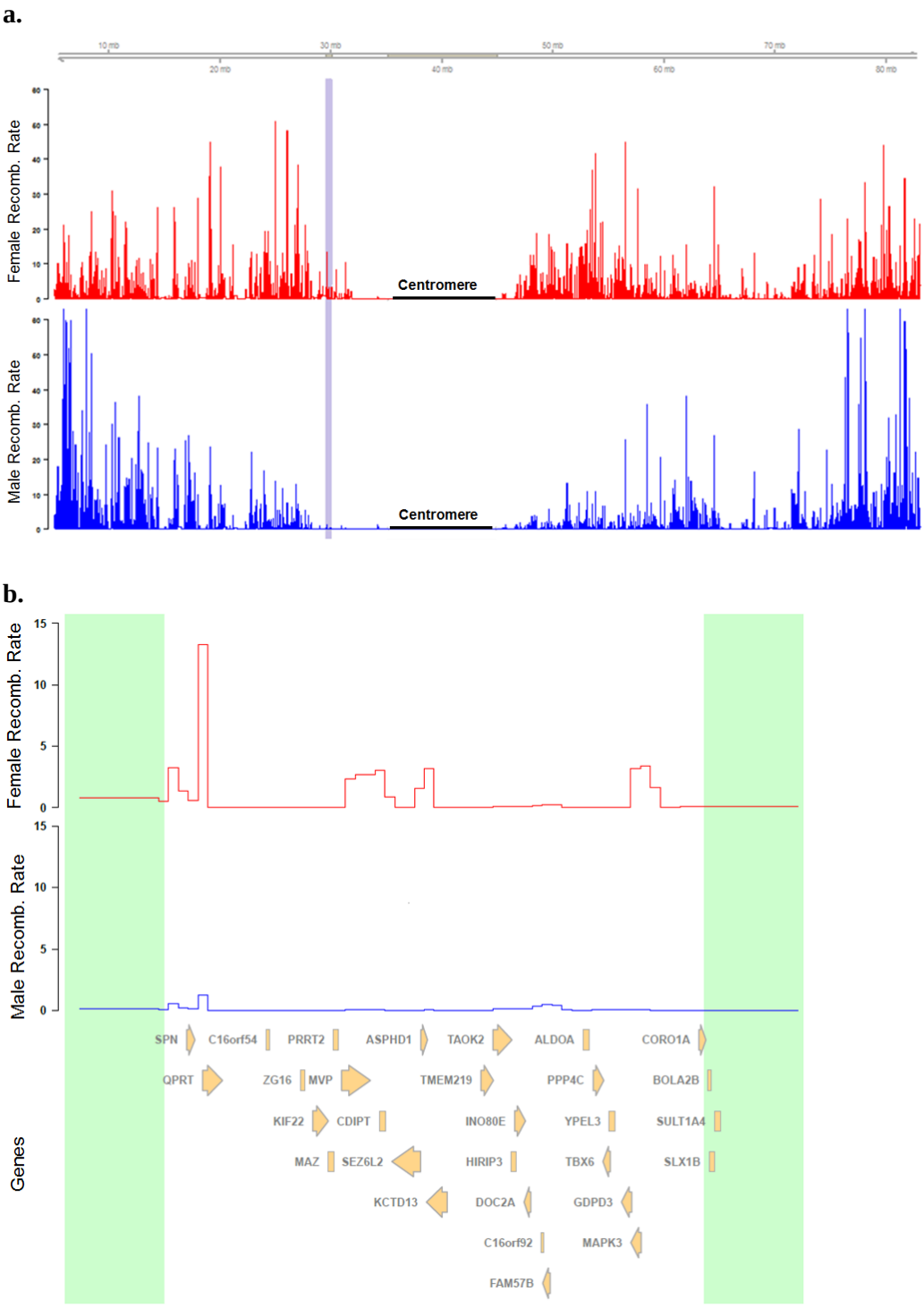

Figure S8: Male and female recombination rates across chromosome 16. a) Not including the telomeres, males have a decreased recombination rate across chromosome 16 compared to females, using data from Kong *et al.*[6]. The lavender bar is the critical region. b) The standardized female recombination rate in females (red) and males (blue) across the 16p11.2 critical region. Note the maternal recombination hotspot in the left-hand most side of the region. (Plotted using the GViz R package[7].)

Supplemental Appendix
This Supplemental Appendix includes the methods for determining the parent-of-origin and mechanism of unequal crossing over of de novo 16p11.2 CNVs.

Method for determining parent-of-origin of de novo 16p11.2 CNVs

De novo 16p11.2 deletions

We used the B-allele frequency data from the SNP microarrays to infer if de novo events originated on the maternal or paternal haplotype. For this analysis, we used data from probes (112, for OmniExpress arrays) falling in the 16p11.2 critical region. In deletion individuals, only one copy of the critical region remains. Therefore, possible SNP genotypes for probes are A or B with corresponding B-allele frequency of 0 or 1. This is tabulated below:

Deletion:		
Affected Haplotype:	*Unaffected Haplotype:*	*B-allele Frequency:*
NA	A	0
NA	B	1

In the case where we had genotype information on both parents (trios), we used the parental genotypes to infer the inheritance of the unaffected haplotype in the proband.

We define the probabilities as follows:
$P(mother|probes)$: Probability of inheritance of the unaffected haplotype from mother given the probes
$P(father|probes)$: Probability of inheritance of the unaffected haplotype from father given the probes
$P(mother)$: Prior probability of inheritance of the unaffected haplotype from mother
$P(probes)$: Posterior probability of the observed probes

By Bayes' theorem,

$$P(mother|probes) = \frac{P(probes \mid mother) * P(mother)}{P(probes)}$$

And similarly for the father,

$$P(father|probes) = \frac{P(probes \mid father) * P(mother)}{P(probes)}$$

Since the prior probability of inheritance of the unaffected haplotype from either parent is 0.5, we have that:

$$P(mother) = \frac{1}{2}$$

and,

$$P(father) = \frac{1}{2}$$

Since the unaffected haplotype must come from either the mother or the father, we also have that,

$$P(mother \mid probes) + P(father \mid probes) = 1$$

Using this relationship, we see that,

$$P(probes) = \frac{P(probes \mid father) + P(probes \mid mother)}{2}$$

To determine the quantity $P(probes \mid mother)$, the probability of observing the set of probes given that the unaffected haplotype comes from the mother, we make the assumption that probe signals are independent and recognize that,

$$P(probes \mid mother) = \prod_{i=1}^{n} P(probe_i \mid mother)$$

where $probe_i$ is the i^{th} probe out of n in the critical region.

To compute $P(probe_i \mid mother)$, we recognize that each site in the unaffected haplotype will have a genotype of either A or B. Since the mother is diploid over the critical region, at each site she has possible genotypes of AA, AB, or BB. Assuming the probability of a genotyping error is 0.001, as suggested by Illumina (see **Supplemental Web Resources**), we build the following probability table:

Mother Genotype at probe *i*	Proband Genotype at probe *i*	P($probe_i$|*mother*)
AA	A	0.999
AB	A	0.5
BB	A	0.001
AA	B	0.001
AB	B	0.5
BB	B	0.999

The approach is identical to compute $P(probes|father)$.

In the cases where we had only one parent available, we estimated the probability of the unobserved parent using the known allele frequencies for that particular probe from the 1000 Genomes Project, when it existed. In these cases, even though we did not have SNP microarray data from the missing parent, in all cases the 16p11.2 CNV was determined to be de novo by clinical microarray or another method. We model the genotype of the missing parent at each probe using the allele frequencies calculated from the 1000 Genomes Project and we only use probes that are present in dbSNP 140 (95 probes). For the missing parent, the probability $P(probe_i|MissingParent)$ now depends on the genotype frequencies. Let a_i be the allele frequency of the A allele at a probe i and b_i be the allele frequency of the B allele at a probe i. Then, assuming the probability of a genotyping error is 0.001, we construct the following probability table:

Missing Parent Genotype at probe *i*	P(Missing Parent Genotype at probe *i*)	Proband Genotype at probe *i*	P($probe_i$|MissingParent)
AA	a_i^2	A	0.999
AB	$2*a_i*b_i$	A	0.5
BB	b_i^2	A	0.001
AA	a_i^2	B	0.001
AB	$2*a_i*b_i$	B	0.5
BB	b_i^2	B	0.999

Then, using Hardy-Weinberg we have:

$$P(probe_i = A|MissingParent) = 0.999 * a_i^2 + 0.5 * 2 * a_i * b_i + 0.001 * b_i^2$$

and

$$P(probe_i = B|MissingParent) = 0.999 * b_i^2 + 0.5 * 2 * a_i * b_i + 0.001 * a_i^2$$

In this way, we calculate the exact probability that the unaffected haplotype was inherited from the mother or father.

In cases where a different version of the same array was run (i.e., Omni1 vs. Omni2), we selected only those probes present on each array in the family.

De novo 16p11.2 duplications

Duplication individuals have three copies of the critical region. The possible SNP genotypes for each probe over the critical region in duplication individuals are AAA, AAB, ABB, and BBB with corresponding B-allele frequencies of 0, 1/3, 2/3, and 1, respectively. Due to the possibilities of either inter or intrachromosomal mechanisms of crossing over, we evaluate the genotypes of both parents and the proband to determine the parent-of-origin. In particular, we compute all possible outcomes of rearrangement given a particular parent-of-origin and mechanism of crossing over (**Table S14**). At each probe *i*, this provides the probabilities of parent-of-origin and, in some cases, mechanism of unequal crossing over. We count the number of partially informative markers (probability >0.5 and <1) and fully informative markers (probability=1) to determine the parent-of-origin of the observed event (**Table S5**).

Genotype			Parent-of-Origin		Mechanism	
Mother	**Father**	**Proband**	**Prob. Mother**	**Prob. Father**	**Prob. Inter**	**Prob. Intra**
AA	AA	AAA	0.50	0.50	0.50	0.50
AA	AA	AAB	NA	NA	NA	NA
AA	AA	ABB	NA	NA	NA	NA
AA	AA	BBB	NA	NA	NA	NA
AA	AB	AAA	0.66	0.33	0.33	0.66
AA	AB	AAB	0.50	0.50	0.50	0.50
AA	AB	ABB	0.00	1.00	0.00	1.00
AA	AB	BBB	NA	NA	NA	NA
AA	BB	AAA	NA	NA	NA	NA
AA	BB	AAB	1.00	0.00	0.50	0.50
AA	BB	ABB	0.00	1.00	0.50	0.50
AA	BB	BBB	NA	NA	NA	NA
AB	AA	AAA	0.33	0.66	0.33	0.66
AB	AA	AAB	0.50	0.50	0.50	0.50
AB	AA	ABB	1.00	0.00	0.00	1.00
AB	AA	BBB	NA	NA	NA	NA
AB	AB	AAA	0.50	0.50	0.00	1.00
AB	AB	AAB	0.50	0.50	0.66	0.33
AB	AB	ABB	0.50	0.50	0.66	0.33
AB	AB	BBB	0.50	0.50	0.00	1.00
AB	BB	AAA	NA	NA	NA	NA
AB	BB	AAB	1.00	0.00	0.00	1.00
AB	BB	ABB	0.50	0.50	0.75	0.25
AB	BB	BBB	0.33	0.66	0.33	0.66
BB	AA	AAA	NA	NA	NA	NA
BB	AA	AAB	0.00	1.00	0.50	0.50
BB	AA	ABB	1.00	0.00	0.50	0.50
BB	AA	BBB	NA	NA	NA	NA
BB	AB	AAA	NA	NA	NA	NA
BB	AB	AAB	0.00	1.00	0.00	1.00
BB	AB	ABB	0.50	0.50	0.75	0.25
BB	AB	BBB	0.66	0.33	0.33	0.66
BB	BB	AAA	NA	NA	NA	NA
BB	BB	AAB	NA	NA	NA	NA
BB	BB	ABB	NA	NA	NA	NA
BB	BB	BBB	0.50	0.50	0.50	0.50

Method for determining mechanism of unequal crossing over of de novo 16p11.2 CNVs

Nonallelic homologous recombination (NAHR) can occur between homologous chromosomes or between or within sister chromatids:

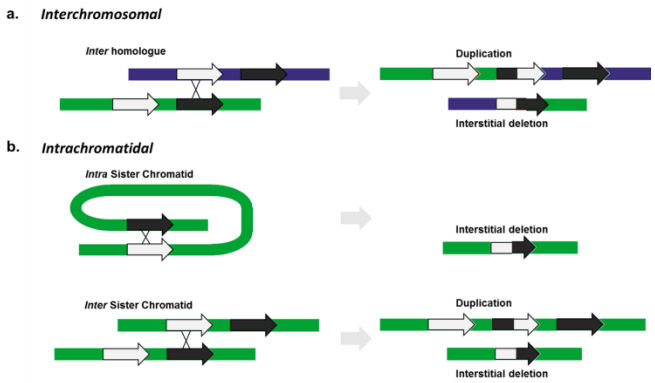

Mechanisms of unequal crossing over. (a) NAHR can occur between homologous chromosomes or (b) between or within sister chromatids.

We used the below method to determine the mechanism of unequal crossover.

Quads:
When possible, we used full quads in order to perfectly phase the parents using the sibling.

(1) *Phase the proband and sibling*

We phased the proband and sibling into maternal and paternal alleles by comparison with the parental genotypes. To determine the mechanism of unequal crossing over, we consider only the haplotype on which the de novo 16p event occurred (maternal or paternal). The possibilities are shown below:

Mother	Father	Child	Maternal Allele	Paternal Allele
AA	AA	AA	A	A
AA	AB	AA	A	A
AA	AB	AB	A	B
AA	BB	AB	A	B
AB	AA	AA	A	A
AB	AA	AB	B	A
AB	AB	AA	A	A
AB	AB	AB	NA	NA
AB	AB	BB	B	B
AB	BB	AB	A	B
AB	BB	BB	B	B
BB	AA	AB	B	A
BB	AB	AB	B	A
BB	AB	BB	B	B
BB	BB	BB	B	B

Only those sites that can distinguish between the two chromosomes in the parent on which the 16p11.2 de novo event originated are informative. For example, if the event occurred on the maternal haplotype, then only heterozygous genotypes in the mother are informative. In total, we considered a total of 314 markers telomeric and 314 markers centromeric of the critical region as possibly informative. For the rest of this discussion, we assume for simplicity that the 16p11.2 de novo CNV occurs on the maternal haplotype.

(2) *Compare the proband and sibling maternal haplotypes*

We assume that no crossing over event has occurred in the 16p11.2 region in the sibling on the haplotype of interest. Therefore, the maternal haplotype present in the sibling should represent perfectly one of the two maternal chromosomes. We determine if the maternal alleles flanking the critical region match the sibling alleles (314 markers on the left, 314 markers on the right). There are four possibilities, shown below:

Left Flank	**Right Flank**	**Conclusion**
Match	Match	Intrachromosomal
Don't Match	Match	Interchromosomal
Match	Don't Match	Interchromosomal
Don't Match	Don't Match	Intrachromosomal

(3) *Calculate a probability that the event occurred by an inter or intrachromosomal mechanism*

We developed a probability model to calculate the probability of an interchromosomal versus an intrachromosomal event given the number of alleles in the left and right flanks (called flank 1 and flank 2 for simplicity) that match the sibling markers. Each marker gets the number 0 if the proband does not match the sibling and 1 if the proband matches the sibling. We notice that the probability of an intrachromosomal event is the probability of the left flank and right flanks of the proband either matching the sibling or both not matching the sibling. We also assume independence of the flanks, so we have that:

$$P(Intrachromosomal|Probes)$$
$$= P\left(((flank1 = 0 \cap flank2 = 0) \cup (flank1 = 1 \ \cap flank2 = 1))|probes\right)$$
$$= P(flank1 = 0|probes)P(flank2 = 0|probes) + P(flank1 = 0|probes)P(flank2 = 0|probes)$$

Similarly, if the flanks do not match each other, than we have an interchromosomal event. That is:

$$P(Interchromosomal|Probes)$$
$$= P\left(((flank\ 1 = 0 \cap flank\ 2 = 1) \cup (flank\ 1 = 0 \ \cap flank\ 2 = 1))|probes\right)$$
$$= P(flank1 = 0|probes)P(flank2 = 1|probes) + P(flank1 = 0|probes)P(flank2 = 1|probes)$$

From this we note that:

$$P(Intrachromosomal|Probes) + P(Interchromosomal|Probes) = 1$$

Using this relationship, we only have to calculate $P(Intrachromosomal|Probes)$. To do so, we must calculate each of the four components that make up this probability. We will show how to do this for the first two components corresponding to flank 1, as the second two follow. Using Bayes' theorem, we have that:

$$P(flank1 = 0|probes) = \frac{P(flank1 = 0) * P(probes|flank1 = 0)}{P(probes)}$$

and also that:

$$P(flank1 = 1|probes) = \frac{P(flank1 = 1) * P(probes|flank1 = 1)}{P(probes)}$$

We assume the probability that proband and sibling match in flank 1 is equal to the probability that they do not match. Therefore,

$P(flank1 = 0) = 0.5$
and,
$P(flank1 = 1) = 0.5$

To calculate *P(probes)* we note that:

$$P(flank1 = 0|probes) + P(flank1 = 1|probes) = 1$$

Expanding this, we have that:

$$P(probes) = \frac{P(probes|flank1 = 0) + P(probes|flank1 = 1)}{2}$$

Finally, we assume independence of individual markers and note that:

$$P(probes|flank1 = 0) = \prod_{probes} P(probe_i|flank1 = 0)$$

and,

$$P(probes|flank1 = 1) = \prod_{probes} P(probe_i|flank1 = 1)$$

To compute the probabilities for the individual probes, we take that the probability of a genotyping error is 0.001. Therefore, we construct the following probability table:

Sibling/Proband Markers	$P(probe_i\|flank1=0)$	$P(probe_i\|flank1=1)$
Don't Match (0)	0.999*0.001*2	$0.999^2*0.001^2$
Match (1)	$0.999^2*0.001^2$	0.999*0.001*2

To determine the accuracy of the assumption that no crossing over events occurred in the sibling, we asked how many crossover events were predicted between the leftmost and rightmost marker in our analysis. Based on the data from Kong *et al.*[1], the genetic distance between the leftmost and rightmost markers in our analysis is 6.20 centimorgans for the female and 0.45 centimorgans for the male, which corresponds to a probability of crossover of 6.2% for the female and 0.45% for the male. Therefore, the number of false positives (an intrachromosomal event being interpreted as an interchromosomal event or vice versa) is 1 in 16 for de novo events originating on the maternal haplotype and 1 in 222 for events originating on the paternal haplotype.

Trios:

In the trio case, we do not have a sibling for phasing the haplotypes of the parent-of-origin. Therefore, we performed statistical phasing of the mothers. The approach was similar to that used for the quads:

(1) *Phase the proband*

We phased the proband into maternal and paternal alleles by comparison with the parental genotypes. As before, we are only concerned with the informative markers that allow us to distinguish between parental haplotypes, i.e., those cases when the parent-of-origin is heterozygous for a particular allele.

(2) *Phase the parent-of-origin haplotypes*

Since a sibling is not present to phase the haplotypes of the parent-of-origin, we instead need to statistically phase the parent-of-origin haplotypes. To do this we used the program Beagle v4.0 (http://faculty.washington.edu/browning/beagle/beagle.html) and used the phased 1000 Genomes Project phase 3 chromosome 16 reference panel for phasing (http://bochet.gcc.biostat.washington.edu/beagle/1000_Genomes_phase3_v5/).
The exact command used is below:

java -Xmx10G -jar beagle.r1399.jar gt=Input.vcf.gz ref=chr16.1kg.phase3.v5.vcf.gz out= phased_data.out impute=false

(3) *Compare the proband to the parent-of-origin*

Next, we compare the proband's haplotype from the parent-of-origin of the 16p11.2 event to one of the haplotypes from the parent-of-origin. As before, the probes will either match or not match in each flank and we use the same probability model as before to compute the probability of an inter or intrachromosomal event.

Duplications

As mentioned above, for duplications certain combinations of maternal, paternal, and proband genotypes are partially or perfectly informative of a mechanism of unequal crossing over. When the flanking marker-based approach did not yield a consistent result, we compared this approach to the approach using probes in the critical region (**Table S5**).

Supplemental Web Resources
Beagle: http://faculty.washington.edu/browning/beagle/beagle.html
cnvPartition Algorithm: http://www.illumina.com/content/dam/illumina-marketing/documents/products/technotes/technote_cnv_plug_ins.pdf
Genotype Rare Variants Tech Note: http://support.illumina.com/content/dam/illumina-marketing/documents/products/technotes/technote_genotyping_rare_variants.pdf

Supplemental References

1. Coe, B.P., Ylstra, B., Carvalho, B., Meijer, G.A., Macaulay, C., and Lam, W.L. (2007). Resolving the resolution of array CGH. Genomics *89*, 647–653.

2. Coe, B.P., Witherspoon, K., Rosenfeld, J.A., van Bon, B.W.M., Vulto-van Silfhout, A.T., Bosco, P., Friend, K.L., Baker, C., Buono, S., Vissers, L.E.L.M., et al. (2014). Refining analyses of copy number variation identifies specific genes associated with developmental delay. Nat. Genet. *46*, 1063–1071.

3. Wang, K., Zhang, H., Ma, D., Bucan, M., Glessner, J.T., Abrahams, B.S., Salyakina, D., Imielinski, M., Bradfield, J.P., Sleiman, P.M.A., et al. (2009). Common genetic variants on 5p14.1 associate with autism spectrum disorders. Nature *459*, 528–533.

4. Miyashita, A., Arai, H., Asada, T., Imagawa, M., Matsubara, E., Shoji, M., Higuchi, S., Urakami, K., Kakita, A., Takahashi, H., et al. (2007). Genetic association of CTNNA3 with late-onset Alzheimer's disease in females. Hum. Mol. Genet. *16*, 2854–2869.

5. O'Roak, B.J., Vives, L., Girirajan, S., Karakoc, E., Krumm, N., Coe, B.P., Levy, R., Ko, A., Lee, C., Smith, J.D., et al. (2012). Sporadic autism exomes reveal a highly interconnected protein network of de novo variants. Nature *485*, 246–250.

6. Kong, A., Thorleifsson, G., Gudbjartsson, D.F., Masson, G., Sigurdsson, A., Jonasdottir, A., Walters, G.B., Jonasdottir, A., Gylfason, A., Kristinsson, K.T., et al. (2010). Fine-scale recombination rate differences between sexes, populations and individuals. Nature *467*, 1099–1103.

7. Hahne,F, Durinck,S., Ivanek,R., Mueller,A., Lianoglou,S., Tan,G., and Parsons,L. Gviz: Plotting data and annotation information along genomic coordinates. R package version 1.12.1.

Appendix B. Supplemental Information for Chapter 3

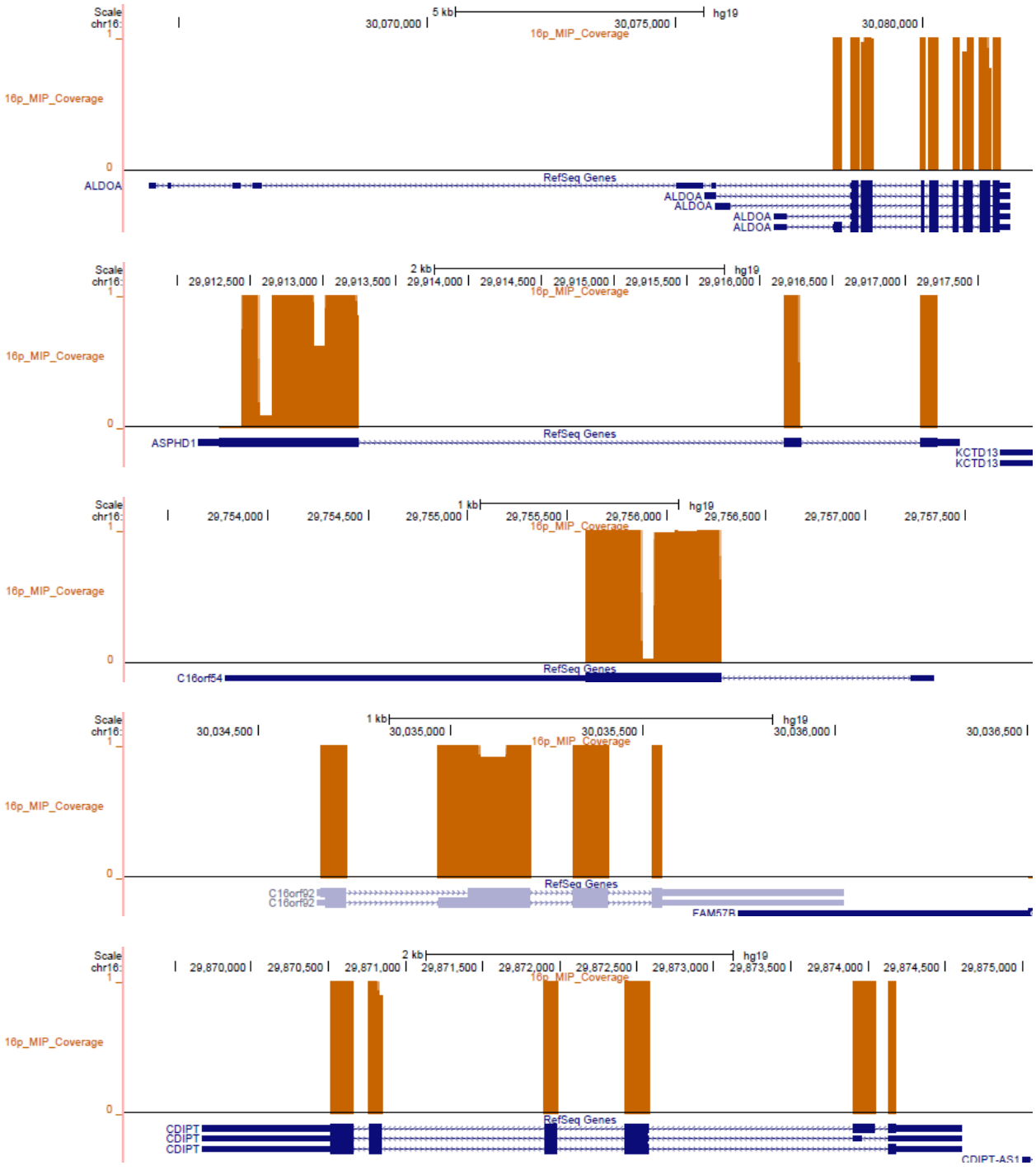

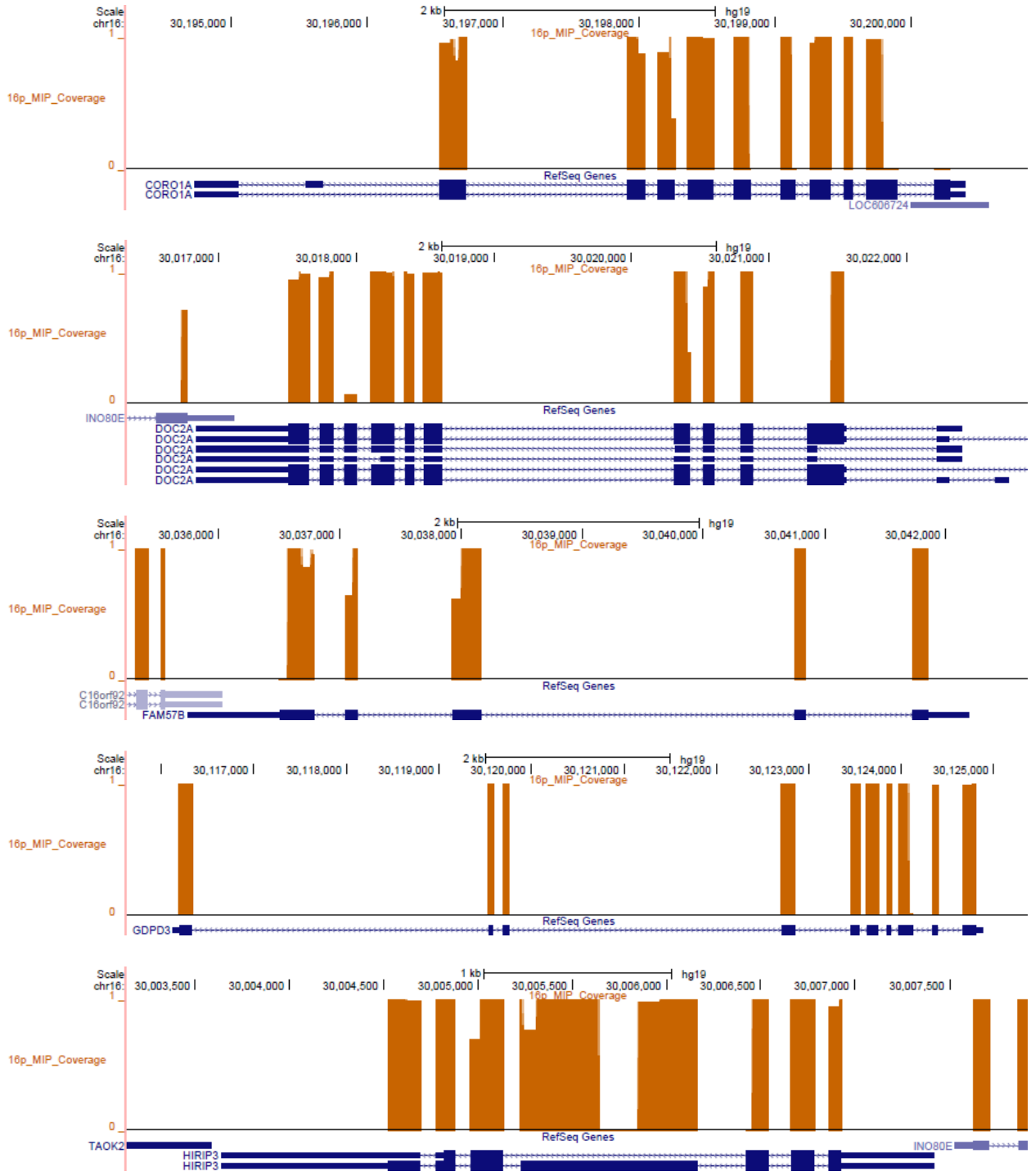
Scale
chr16:
2 kb
hg19
30,195,000
30,196,000
30,197,000
30,198,000
30,199,000
30,200,000
16p_MIP_Coverage
1
0
RefSeq Genes
CORO1A
CORO1A
LOC606724
30,017,000
30,018,000
30,019,000
30,020,000
30,021,000
30,022,000
INO80E
DOC2A
DOC2A
DOC2A
DOC2A
DOC2A
DOC2A
30,036,000
30,037,000
30,038,000
30,039,000
30,040,000
30,041,000
30,042,000
C16orf92
C16orf92
FAM57B
30,117,000
30,118,000
30,119,000
30,120,000
30,121,000
30,122,000
30,123,000
30,124,000
30,125,000
GDPD3
1 kb
30,003,500
30,004,000
30,004,500
30,005,000
30,005,500
30,006,000
30,006,500
30,007,000
30,007,500
TAOK2
HIRIP3
HIRIP3
INO80E

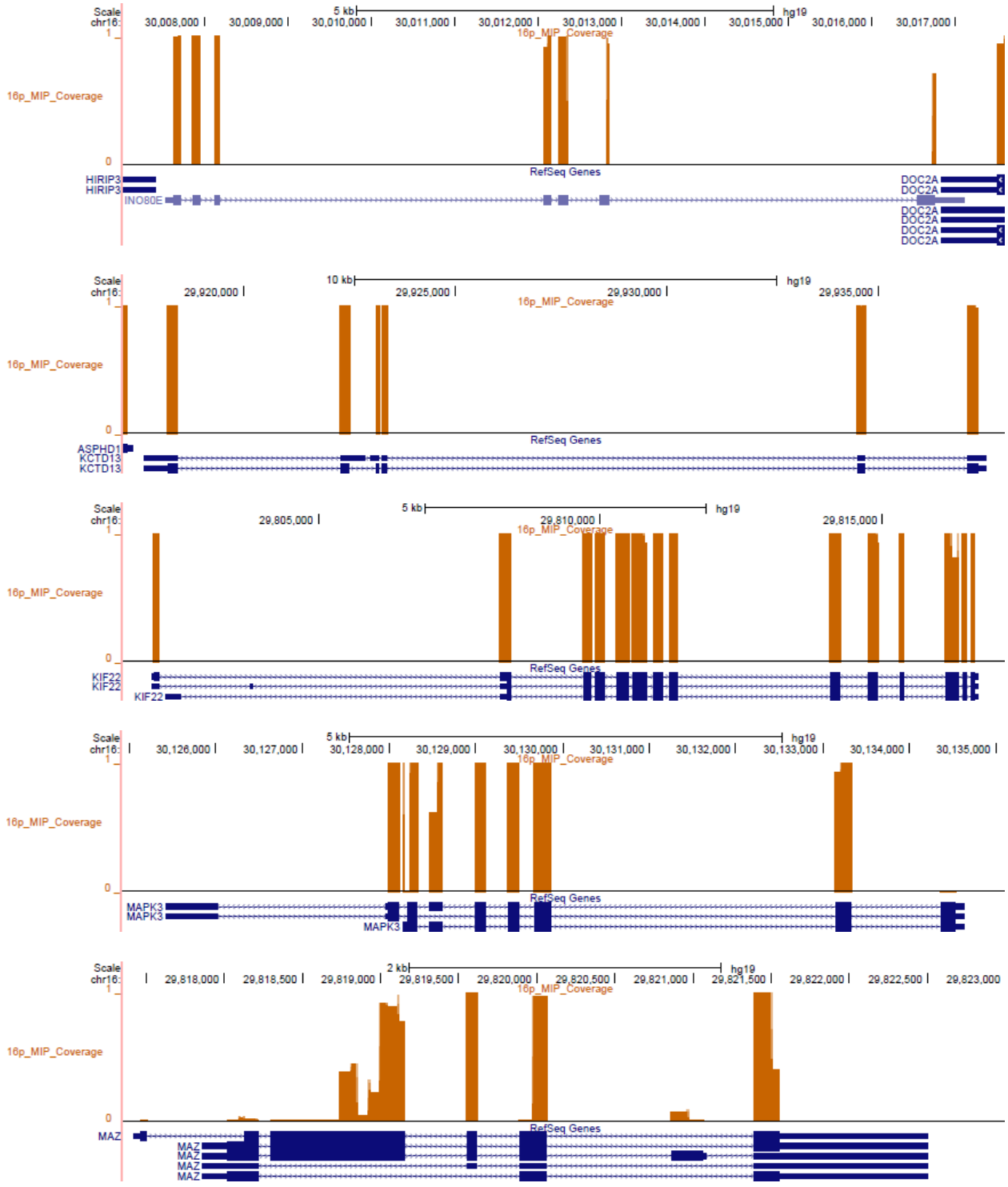
Scale
chr16:
5 kb
hg19
30,008,000
30,009,000
30,010,000
30,011,000
30,012,000
30,013,000
30,014,000
30,015,000
30,016,000
30,017,000
16p_MIP_Coverage
1
0
RefSeq Genes
HIRIP3
HIRIP3
INO80E
DOC2A
DOC2A
DOC2A
DOC2A
DOC2A
DOC2A
10 kb
29,920,000
29,925,000
29,930,000
29,935,000
ASPHD1
KCTD13
KCTD13
29,805,000
29,810,000
29,815,000
KIF22
KIF22
KIF22
30,126,000
30,127,000
30,128,000
30,129,000
30,130,000
30,131,000
30,132,000
30,133,000
30,134,000
30,135,000
MAPK3
MAPK3
MAPK3
2 kb
29,818,000
29,818,500
29,819,000
29,819,500
29,820,000
29,820,500
29,821,000
29,821,500
29,822,000
29,822,500
29,823,000
MAZ
MAZ
MAZ
MAZ
MAZ

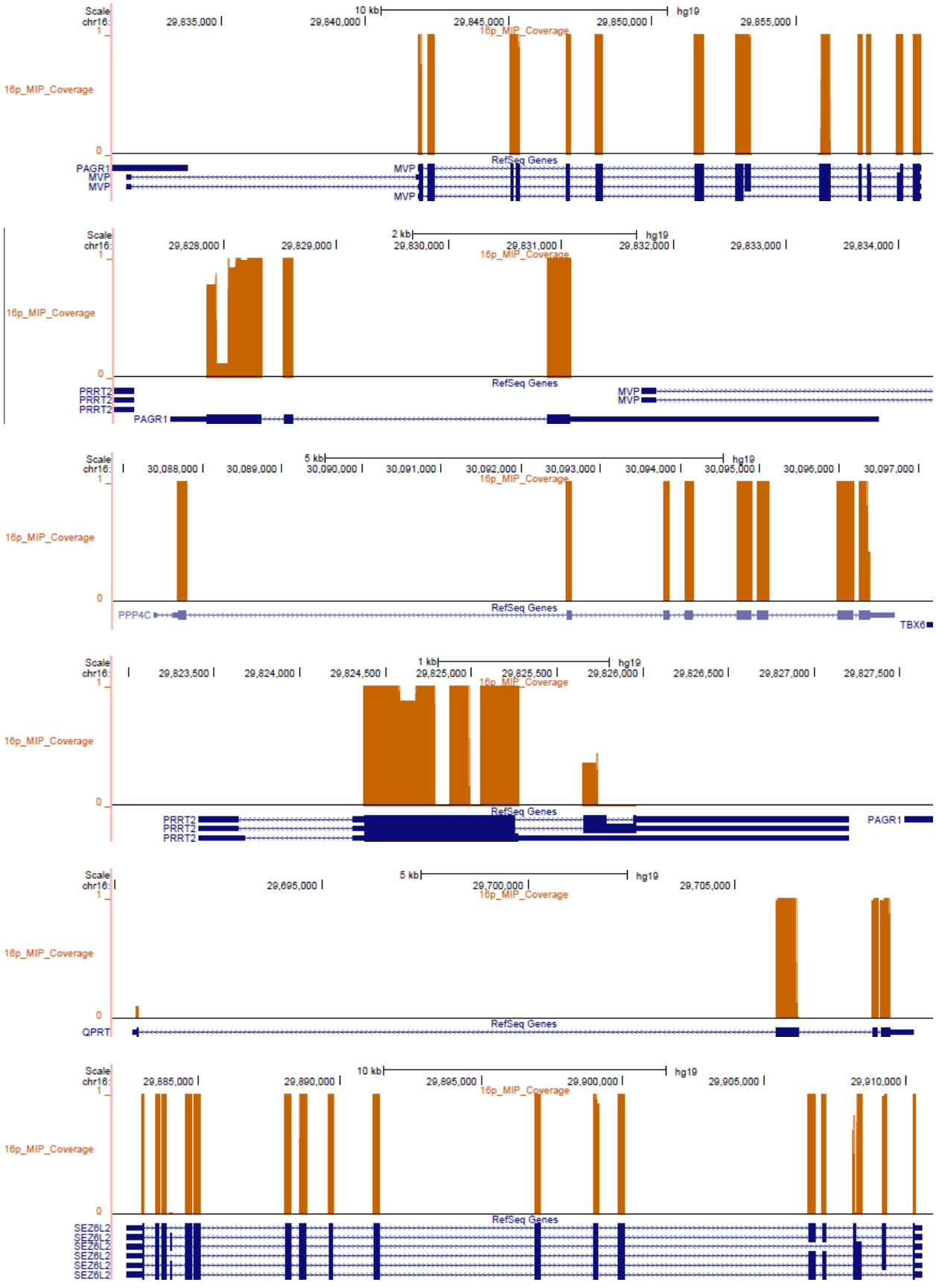
Scale
chr16:
10 kb
hg19
29,835,000
29,840,000
29,845,000
29,850,000
29,855,000
16p_MIP_Coverage
RefSeq Genes
PAGR1
MVP
2 kb
29,828,000
29,829,000
29,830,000
29,831,000
29,832,000
29,833,000
29,834,000
PRRT2
5 kb
30,088,000
30,089,000
30,090,000
30,091,000
30,092,000
30,093,000
30,094,000
30,095,000
30,096,000
30,097,000
PPP4C
TBX6
1 kb
29,823,500
29,824,000
29,824,500
29,825,000
29,825,500
29,826,000
29,826,500
29,827,000
29,827,500
29,695,000
29,700,000
29,705,000
QPRT
29,885,000
29,890,000
29,895,000
29,900,000
29,905,000
29,910,000
SEZ6L2

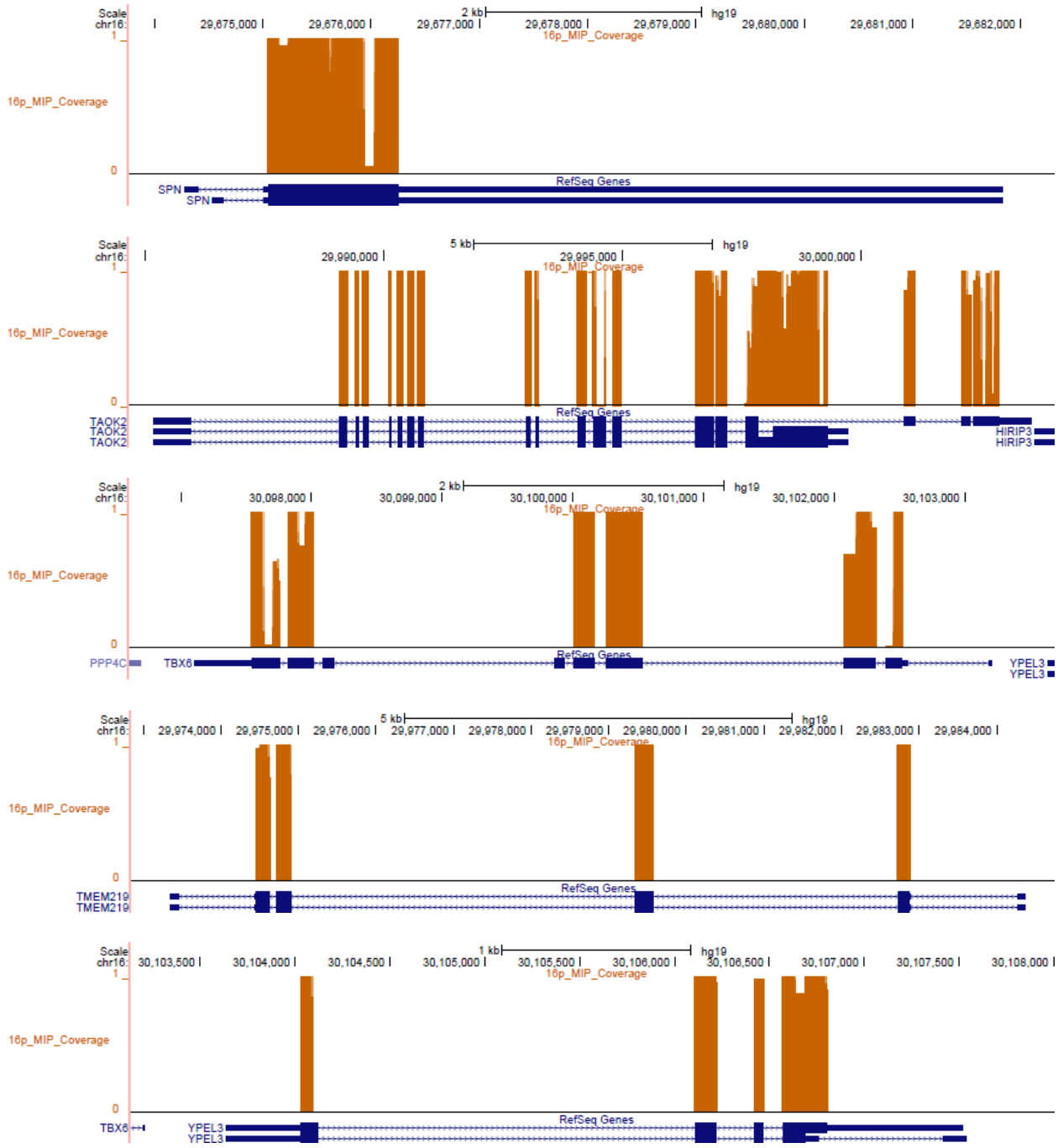
Scale
chr16:
2 kb
hg19
29,675,000
29,676,000
29,677,000
29,678,000
29,679,000
29,680,000
29,681,000
29,682,000
16p_MIP_Coverage
1
0
RefSeq Genes
SPN
SPN
5 kb
29,990,000
29,995,000
30,000,000
TAOK2
TAOK2
TAOK2
HIRIP3
HIRIP3
30,098,000
30,099,000
30,100,000
30,101,000
30,102,000
30,103,000
PPP4C
TBX6
YPEL3
YPEL3
29,974,000
29,975,000
29,976,000
29,977,000
29,978,000
29,979,000
29,980,000
29,981,000
29,982,000
29,983,000
29,984,000
TMEM219
TMEM219
1 kb
30,103,500
30,104,000
30,104,500
30,105,000
30,105,500
30,106,000
30,106,500
30,107,000
30,107,500
30,108,000
TBX6
YPEL3
YPEL3

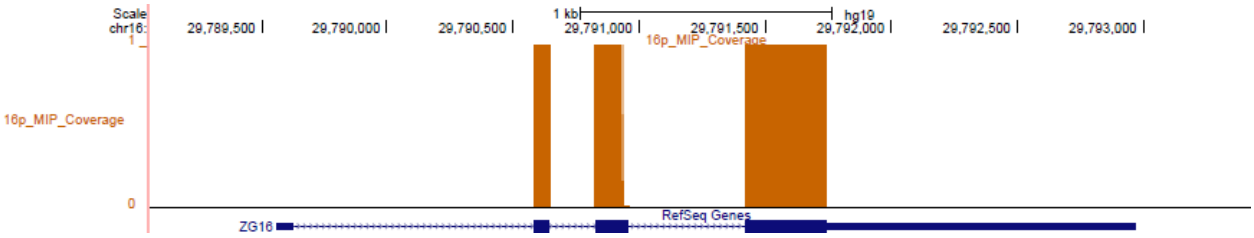

Figure S1. MIP coverage over 27 genes in the critical region. The fraction of samples with quality sequence over each MIP is plotted for each of the 27 unique critical region genes.

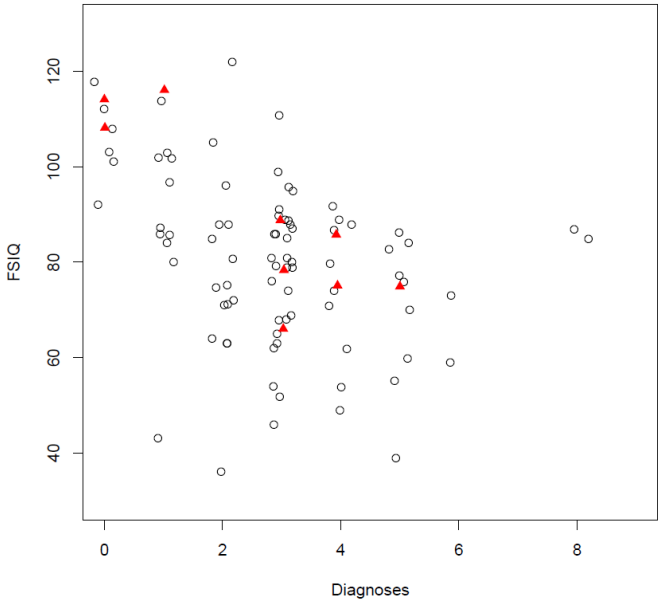

Figure S2. Severity plot for proband with a severe variant in a duplicated gene. Individuals with a severe missense variant in a duplicated gene plotted in red.

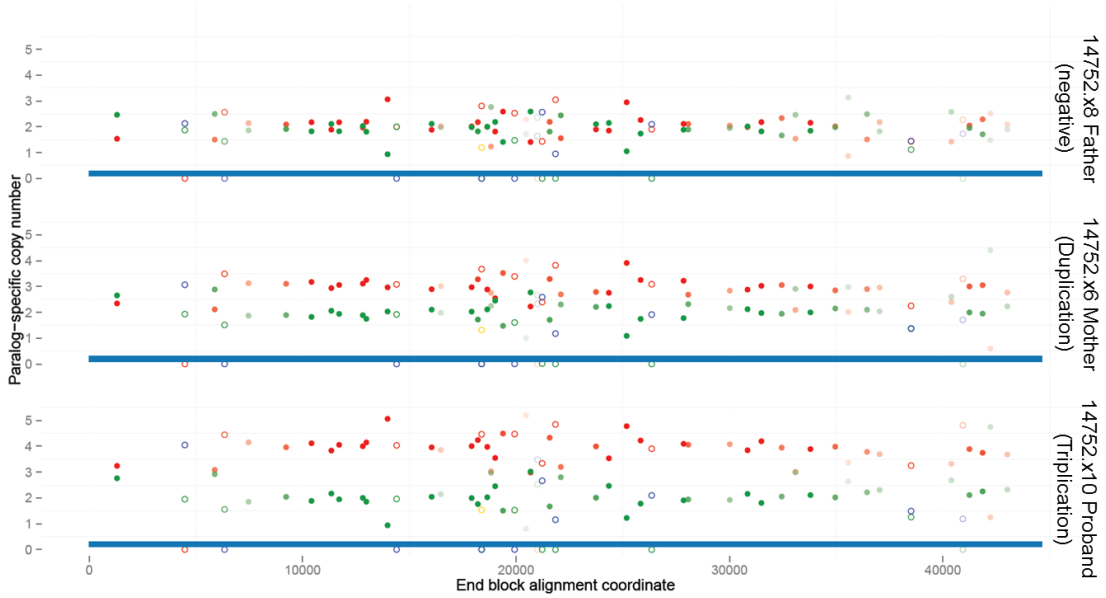

Figure S3. Allele specific MIP copy number estimates. Allele specific copy number estimates are shown for 206 MIPs targeting single nucleotide variants (SNVs) across the 16p11.2 critical region in mother, father, and proband of family 14752. Each point indicates an allele specific copy number estimate, calculated as the product of the allele specific read count frequency for a particular MIP and the aggregate estimated critical region copy number. Allele read count frequencies in the father (14752.x8) cluster around 0, 1/2 and 1, providing strong evidence for a two copy (diploid) state for the critical region. Allele read count frequencies in the mother (14752.x6) cluster around 0, 1/3, 2/3, and 1, providing strong evidence for a three copy state for the critical region. Allele read count frequencies in the proband (14752.x10) cluster around 0, 1/4, 1/2, 3/4, and 1, providing strong evidence for a four copy state for the critical region.

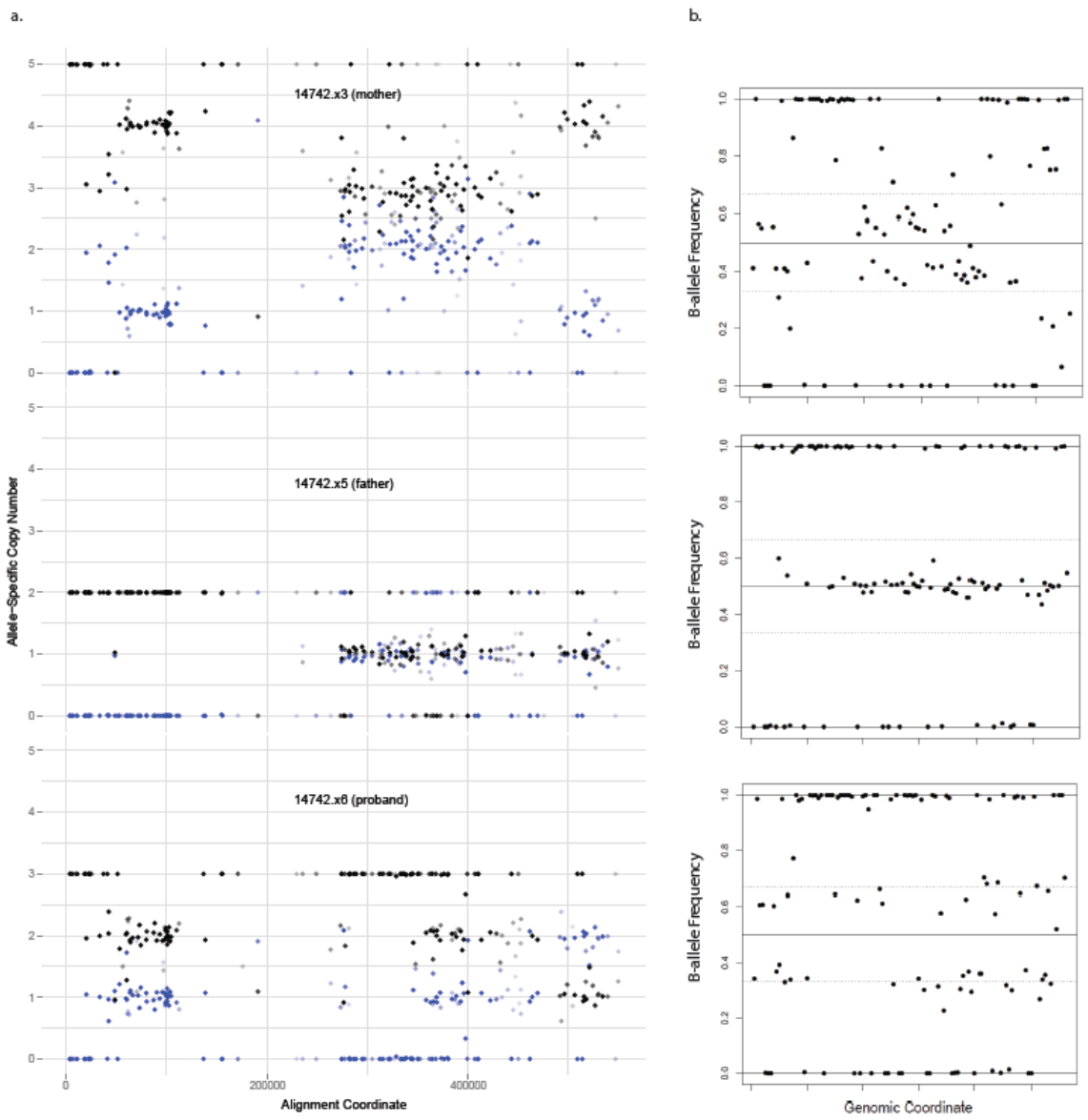

Figure S4. Discovery of an individual with five copies of the 16p11.2 critical region. a) Allele specific copy number estimates are shown for 206 MIPs targeting single nucleotide variants (SNVs) across the 16p11.2 critical region in mother, father, and proband of family 14742. Each point indicates an allele specific copy number estimate, calculated as the product of the allele specific read count frequency for a particular MIP and the aggregate estimated critical region copy number. Allele read count frequencies in the mother (14742.x3) cluster around 0, 1/5, 2/5, 3/5, 4/5, and 1, providing strong evidence for a five copy state for the critical region in this individual. b) The corresponding B-allele frequency plots from the SNP microarray.

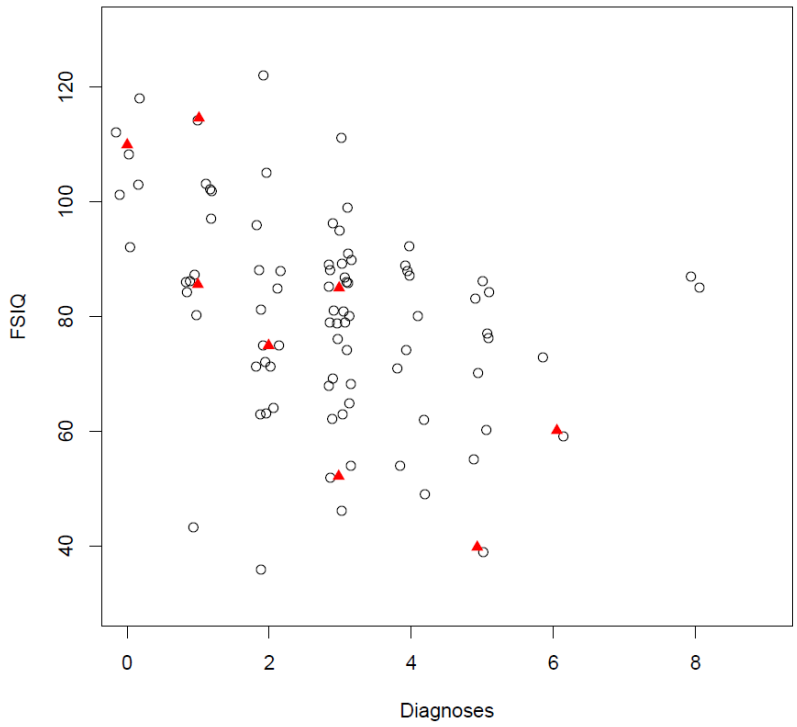

Figure S5. Severity plot of 13 probands with severe exonic variants in SFARI genes. Individuals with severe exonic variants are plotted as red triangles.

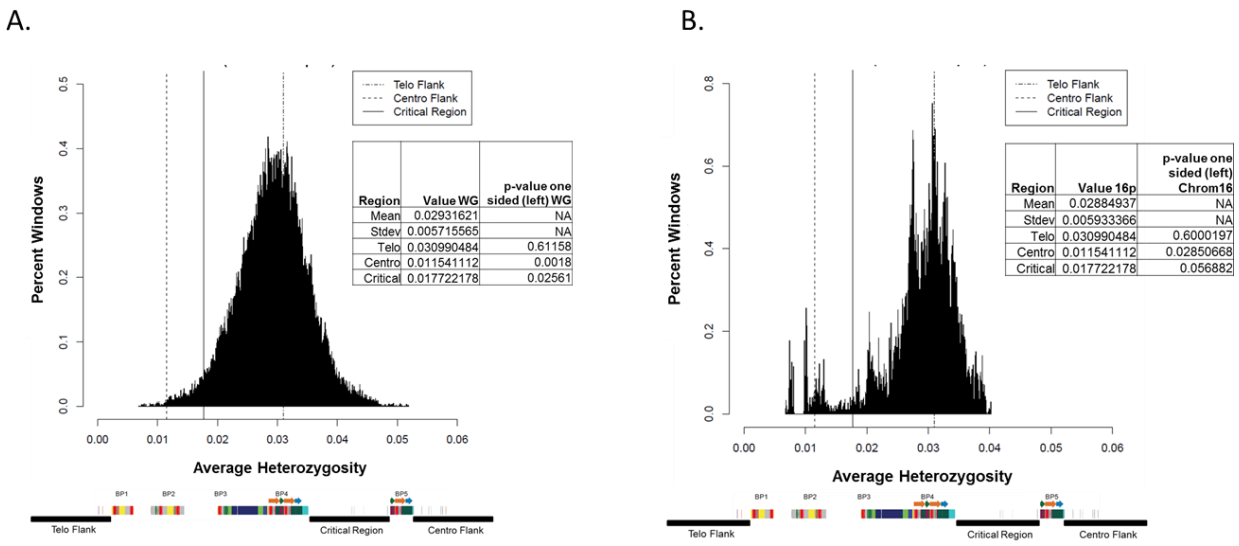

Figure S6. Distribution of average heterozygosity across 500kbp windows. A. The genome-wide distribution of average heterozygosity for 550kbp regions from 2500 individuals from the 1000 genomes phase 3 release sampled 100,000 times. Lines indicate the average heterozygosities of the 550kbp telomeric flank, centromeric flank and critical region. The critical region lies in the bottom 2.5 percentile of the distribution. B. The chromosome 16 distribution of average heterozygosity for 550kbp regions from 2500 individuals from the 1000 genomes phase 3 release sampled 30,000 times. Lines indicate the average heterozygosities of the 550kbp telomeric flank, centromeric flank and critical region. The critical region lies in the bottom 5.6 percentile of the distribution.

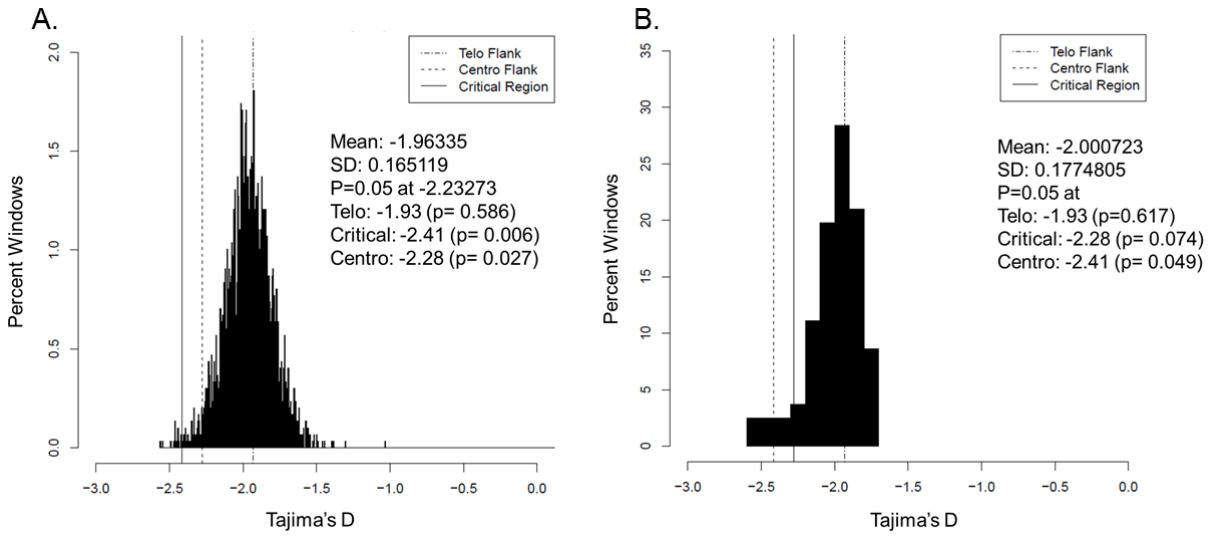

Figure S7. Distribution of Tajima's D across 500kbp windows. a. The Tajima's D value for 550 kbp regions from 2500 individuals from the 1000 genomes phase 3 release sampled 100,000 times. Lines indicate the Tajima's D values of the 550 kbp telomeric flank, centromeric flank and critical region. The critical region lies in the bottom 1 percentile of the distribution. b. The chromosome 16 distribution of Tajima's D for 550kbp regions from the 2500 individuals from the 1000 genomes phase 3 release sampled 30,000 times. Lines indicate the Tajima's D values of the 550kbp telomeric flank, centromeric flank, and critical region. The critical region lies in the bottom 7.4 percentile of the distribution.

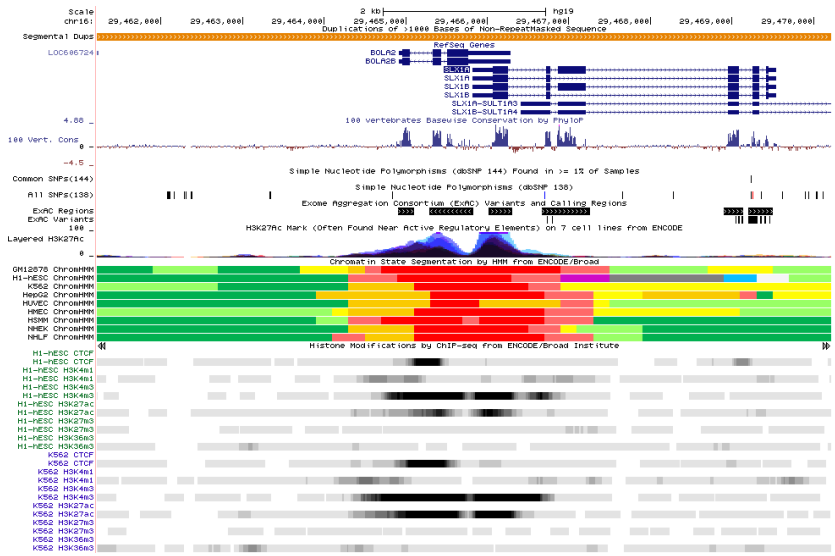

Figure S8. The genomic structure of *BOLA2* and *SLX1A*. BOLA2 and SLX1A are transcribed in opposite directions from the same promoter. Promoter signatures from chromatin state segmentation are represented in red.

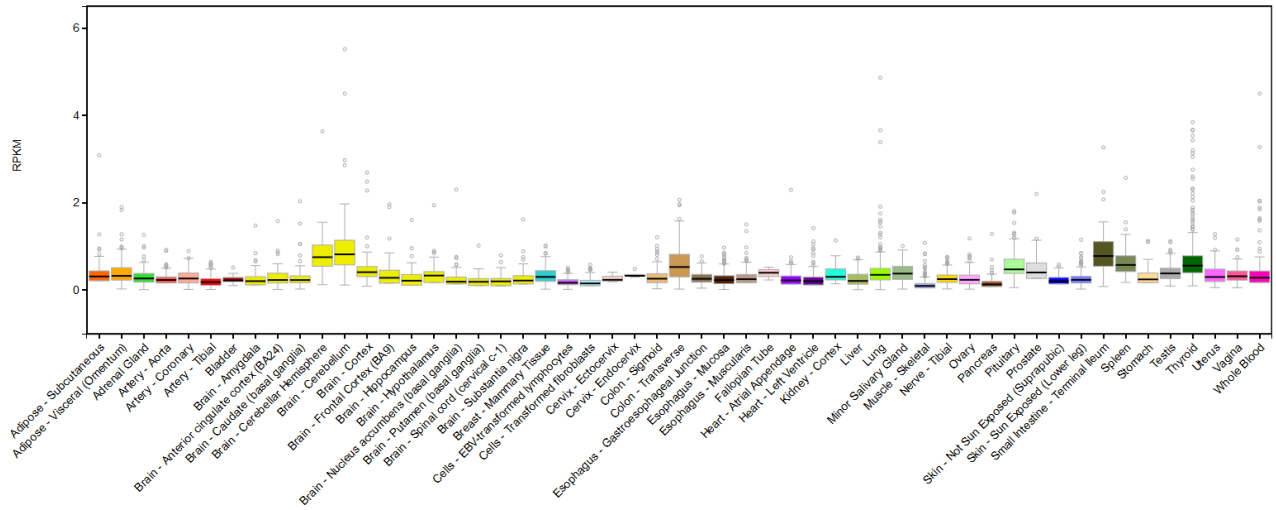

Figure S9. SULT1A3 tissue expression from the GTeX database.